1990

QCD corrections to properties of technipions in technicolor theories

David H. Slaven
Iowa State University

INFORMATION TO USERS

The most advanced technology has been used to photograph and reproduce this manuscript from the microfilm master. UMI films the text directly from the original or copy submitted. Thus, some thesis and dissertation copies are in typewriter face, while others may be from any type of computer printer.

The quality of this reproduction is dependent upon the quality of the copy submitted. Broken or indistinct print, colored or poor quality illustrations and photographs, print bleedthrough, substandard margins, and improper alignment can adversely affect reproduction.

In the unlikely event that the author did not send UMI a complete manuscript and there are missing pages, these will be noted. Also, if unauthorized copyright material had to be removed, a note will indicate the deletion.

Oversize materials (e.g., maps, drawings, charts) are reproduced by sectioning the original, beginning at the upper left-hand corner and continuing from left to right in equal sections with small overlaps. Each original is also photographed in one exposure and is included in reduced form at the back of the book.

Photographs included in the original manuscript have been reproduced xerographically in this copy. Higher quality 6" x 9" black and white photographic prints are available for any photographs or illustrations appearing in this copy for an additional charge. Contact UMI directly to order.

UMI

University Microfilms International
A Bell & Howell Information Company
300 North Zeeb Road, Ann Arbor, MI 48106-1346 USA
313/761-4700 800/521-0600

Order Number 9101377

QCD corrections to properties of technipions in technicolor theories

Slaven, David H., Ph.D.

Iowa State University, 1990

U·M·I
300 N. Zeeb Rd.
Ann Arbor, MI 48106

QCD corrections to properties of technipions in technicolor theories

by

David H. Slaven

A Dissertation Submitted to the
Graduate Faculty in Partial Fulfillment of the
Requirements for the Degree of
DOCTOR OF PHILOSOPHY

Department: Physics
Major: High Energy Physics

Approved:

Signature was redacted for privacy.
In Charge of Major Work

Signature was redacted for privacy.
For the Major Department

Signature was redacted for privacy.
For the Graduate College

Iowa State University
Ames, Iowa
1990

TABLE OF CONTENTS

LIST OF TABLES

LIST OF FIGURES

DEDICATION

This dissertation is dedicated to Mom, Dad, Pat and Chris, and to everyone that I've ever drank a beer or hit a softball with.

1. INTRODUCTION

Theoretical high energy physics is currently suffering from a demoralizing curse. That is, it has a complete working model. In fact, this working model has been in place for about fifteen years, and shows no obvious signs of weakening. QCD has been accepted as the only contender for a theory of strong interactions since the mid-1970s, and its position has continually become more secure. The rest of the standard model, the electroweak model of Glashow, Salam, and Weinberg is even older, dating back to 1967. The experimental verification of this part of the model has been impressive, and there are no anomalous data requiring theorists to amend the model. It's no wonder, therefore, that experimenters and theorists alike are crying out for new physics. But so far their call has gone unanswered.

There are, of course, a few loose ends to the standard model. First of all, there is the t quark. This particle is an indispensable element of the standard model, both aesthetically (so that the third family of fermions is identical to the first two) and mathematically (so that triangle anomalies are canceled and the theory is renormalizable). But it has yet to be discovered. We have a lower bound of about 89 GeV, and a theoretical upper bound of about 200 GeV. Within this range, however, there are no constraints on the t quark, and so the fact that it has not been discovered yet doesn't alarm anyone.

Then there is the Higgs particle. The Higgs is a remnant of the symmetry breaking of the standard model, required to give mass to the weak interaction gauge bosons, the $W^{\pm}$ and Z^0. It is a scalar particle, the only one in the entire model. There are very few constraints on the mass of the Higgs, and so once again, the fact that it has not been discovered yet is not very disconcerting.

Finally, there is the inability to calculate many quantities in low energy QCD with any confidence, since the strength of the coupling constant α_s bars us from perturbative calculations. A great deal of work has been done to improve this situation through current algebra, effective Lagrangians, and lattice gauge theory calculations. But progress in low energy QCD is slow.

Although there are these uncertainties in the standard model, there has been no evidence to contradict it, nor has there been any experimental indications of what might improve or replace it. But in spite of all the strengths of the standard model, high energy physicists are generally dissatisfied with the model as a complete theory of the universe. There are several complaints with the model, but most of them can be summed up by saying that, while the standard model provides a remarkable *description* of high energy physics, it provides no *explanations.*

For example, there is no explanation in the standard model for the relatively complicated gauge group, $SU(3)_c \times SU(2)_L \times U(1)_Y$. Then there is the tantalizing spectrum of fermions. We have three generations of fermions, each alike in all things except mass. The masses of particles steadily increase from one generation to the next. The standard model can easily incorporate this structure, but offers no reason for it. Next, there is the abundance of parameters in the standard model, 19 of them to be precise. And this is only in the simplest version of the model! The standard

model gives no insight into the values of any of these parameters.

Finally, there is that most mysterious area of the standard model, the electroweak symmetry breaking. The standard model Lagrangian contains an $SU(2)_L \times U(1)_Y$ gauge symmetry, which we need to break in order to give mass to the weak gauge bosons. In the standard model, this symmetry breaking is accomplished by the Higgs mechanism. This mechanism, while pleasing in some ways, and certainly effective in implementing the model, is somewhat of a sore thumb. It is a lone pair of scalar fields in a theory of fermions and vector bosons. Its sole purpose is to couple to these fermions and vector bosons, and destroy the gauge symmetry that was so carefully installed in the model initially. Finally, it is the most experimentally elusive particle in the standard model, primarily because its mass is completely arbitrary, and because its coupling to other particles is proportional to their masses. We are only able to perform experiments with a few light particles, and the couplings of these particles to the Higgs are miniscule. We have yet to create the experiment that is able to observe any aspect of the Higgs, and so we have no experimental knowledge of either the mass or the couplings of the Higgs.

This is where our work enters the picture. Because the Higgs mechanism is not well liked for a variety of reasons, people have searched for alternative methods of breaking the symmetry of the standard model. One such alternative is called technicolor, and it is this possibility that we shall be exploring in this work.

Technicolor is based on a phenomenon observed in QCD known as chiral symmetry breaking. QCD is a theory with a running coupling constant. In particular, the coupling is relatively weak at high energies, and becomes very strong at low energies. Once the strength of the coupling surpasses a certain level, it becomes ener-

getically favorable for the vacuum to spontaneously produce quark–anti-quark pairs. Mathematically speaking, the quantity $\bar{\psi}\psi$ has a non-zero expectation value in the vacuum state: $\langle 0|\bar{\psi}\psi|0\rangle \neq 0$. Chiral symmetry is a symmetry in which the Lagrangian remains invariant under separate transformations of the left-handed and the right-handed components of its fermions. Decomposing $\bar{\psi}\psi$ into its left- and right-handed components gives us $\bar{\psi}_L\psi_R + \bar{\psi}_R\psi_L$. This quantity is not invariant under a chiral transformation, but is invariant only under that subgroup of the chiral symmetry in which the left-handed and right-handed transformations are equal.

The end result of this, then, is that we start with a theory with chiral symmetry, but we find that the vacuum state does not respect that symmetry. This is exactly what is meant by spontaneous symmetry breaking. The crucial point to all this is that we have a gauge symmetry, $SU(2)_L$ that we need broken. This $SU(2)_L$ can be identified as a subset of the chiral symmetry of the QCD Lagrangian, and so this vacuum expectation value that we've discovered will in fact break electroweak symmetry! We could use this symmetry breaking to give mass to the W's and Z in the standard model, but unfortunately the masses would be on the order of the pion decay constant, $f_\pi = 93$ MeV. This is much too small for the masses of the electroweak gauge bosons, which are both near 100 GeV.

And so in 1979 Susskind and Weinberg proposed a new interaction, called technicolor, which would be similar to QCD, but at a scale $\mathcal{O}(100\text{ GeV})$, not $\mathcal{O}(100\text{ MeV})$. This interaction can be used to give mass to the electroweak gauge bosons. There are many ways that one can implement technicolor to give mass to these gauge bosons. The most common ones predict, among other things, a whole slew of pseudoscalars analogous to the pions and kaons of QCD. These particles are referred to generically

as technipions, and they will be the focus of our work. In particular, we shall devote most of our energy to the study of one particular technipion, which is often denoted $P^{0\prime}$.

The standard model and technicolor are described in Chapter 2. In Chapter 3, we describe our method for studying technipions. The method we've chosen is the effective Lagrangian technique, which has had some success in low energy QCD. Since technicolor is by design very similar to QCD, it is only natural that we can us a technique from QCD to work for us in technicolor. There are some differences, however. Most notably, the technipion spectrum is rather different from the QCD light pseudoscalar spectrum, since the spectra of fermions in the two theories (QCD and technicolor) are different. Second, in QCD we were required to gauge an Abelian subgroup (QED) of the chiral symmetry in our effective low energy Lagrangian. Low energy technicolor, on the other hand, is at the scale of high energy QCD. Hence, we must deal with QCD in its fundamental form, as a theory of colored fermions (both ordinary quarks, and the new techniquarks) and gluons. As a result, we must gauge a non-Abelian subgroup of the chiral symmetry of technicolor. This will lead us to additional complications.

The processes we'll be examining will mostly consist of decays of the $P^{0\prime}$. One of these decays involves three gluons in the final state. Calculations involving many gluons are known to be very complicated, due to the presence of unphysical polarization states in the mathematical formalism. In QED, these unphysical states are not a problem, since they don't couple to any particles in the theory, due to the Ward–Takahashi identity. In QCD, however, we do not have this identity, and so the unphysical polarization states must in general be tediously subtracted out at the

end of the calculation. But we do have an identity similar to the Ward–Takahashi identity, known as the Slavnov–Taylor identity. In Chapter 4, we use this identity to develop a technique to simplify multi-gluon calculations, and in fact we use our technique later in our $P^{0\prime}$ decay calculations.

Chapter 5 contains our first work on the decay modes of the $P^{0\prime}$ in which we calculate three body decays which are simply QCD corrections to two body decays. In the past, researchers in technicolor ignored higher order decays of technipions, assuming that the lowest order decays would dominate. We set out to test this by calculating three body decays, and in fact we'll see that they are significant, if not dominant. We also examine the possibility of producing $P^{0\prime}$'s at high transverse momentum at hadron colliders and find that they should be plentiful.

There are other corrections to the $P^{0\prime}$ decay modes which are of the same order in α_s, the QCD coupling constant, as the three body decays of Chapter 5. These are interference terms between the tree level two body Feynman diagrams and one loop diagrams of these same decays. In principle, we should consider these along with the three body decays. In practice, it was not clear at the beginning whether this would even be possible.

The main obstacle in doing loop calculations in almost any process is the presence of divergences. These divergences are of two types: ultraviolet and infrared. Ultraviolet divergences are normally disposed of through a program called renormalization. Not every theory is renormalizable, however, and in fact our theory, with its technipion effective Lagrangian, is not. Therefore, it is not clear that we can dispose of the ultraviolet divergences so that we can actually reach a sensible answer. The problem of infrared divergences is resolved differently. Infrared divergences have a

physical interpretation. They arise because of the degeneracy of certain final states of our processes. For example, the decay $P^{0\prime} \rightarrow ggg$ in which one of the gluons carries virtually no energy is degenerate with the decay $P^{0\prime} \rightarrow gg$. This degeneracy is reflected in the infrared divergences, and when we consider all degenerate final states, all infrared divergences must vanish.

As a result, one of our goals in our work with the $P^{0\prime}$ is simply to learn whether such a calculation is possible, and to learn what path we have to take and what paths are excluded in order to reach a sensible result.

Chapter 6 contains a review of renormalization, along with a presentation of what choices we are forced to make in the renormalization in order to reach a final answer which is free of divergences and correct. In fact, through the judicious choice of methods of regularizing divergences and performing our renormalization, we are able to arrive at a final answer. The results of our calculation are given in Chapter 7. Chapter 8 consists of a short summary of our work.

There are also two appendices. The first of these is just a roll call of Feynman rules used in our calculations. The second of these is devoted to all the phase space integrals that we had to perform. Although the details of such a calculation can be very boring, the details of these integrals are intricate, and they include enough trickiness so as to merit inclusion. For now, however, we can begin with a review of the standard model of high energy physics.

2. THE STANDARD MODEL AND TECHNICOLOR

2.1. The Standard Model

The standard model [1] is a spontaneously broken non-Abelian gauge field theory, [2] based on the Lie group $SU(3)_c \times SU(2)_L \times U(1)_Y$. To see what this means, we'll construct it from scratch, beginning with the simplest part, $SU(3)_c$, better known as quantum chromodynamics, or QCD. We start with three quarks, denoted by the colors red, green, and blue. (The three here is unrelated to the number of light quark flavors.) We write a Lagrangian which is symmetric under an $SU(3)$ transformation among the fermions:

$$\mathcal{L} = i\bar{q}\,\partial\!\!\!/ q. \tag{2.1}$$

Here $q = (q^r, q^g, q^b)^T$, $\partial\!\!\!/ = \partial_\mu \gamma^\mu I$, I is a three by three identity matrix, and T denotes the transpose. This is symmetric under the transformation $q \to Uq$ where U is an element of $SU(3)_c$. U must be independent of the space-time coordinates for this symmetry to hold, and so we say that this symmetry is a "global" one. We can expand the symmetry to a "local" one by introducing a covariant derivative. This is called "gauging" the theory. We define

$$D_\mu = \partial_\mu + igT^a G_\mu^a. \tag{2.2}$$

T^a are the generator matrices for the group $SU(3)_c$, g is the gauge coupling constant, and G^a_μ are the gauge fields, called "gluons" for $SU(3)_c$. The generators T^a satisfy the commutation relations

$$[T^a, T^b] = if^{abc}T^c \tag{2.3}$$

where f^{abc} are the structure constants for $SU(3)_c$. The existence of nonzero commutators is what gives the theory its "non-Abelian" label. We will normalize the generators, T^a, so that $\mathrm{Tr}(T^aT^b) = \frac{1}{2}\delta^{ab}$.

The Lagrangian

$$\mathcal{L}_F = i\bar{q}\not{D}q \tag{2.4}$$

is invariant under the transformation

$$\begin{aligned} &q(x) \to U(x)q(x) \qquad\qquad \bar{q}(x) \to \bar{q}(x)U^\dagger(x) \\ &G_\mu(x) \to U(x)G_\mu(x)U(x)^{-1} - \tfrac{i}{g}U(x)(\partial_\mu U(x)^{-1}), \end{aligned} \tag{2.5}$$

where

$$U(x) = \exp(ig\theta^a(x)T^a), \tag{2.6}$$

and

$$G_\mu = G^a_\mu T^a. \tag{2.7}$$

We now have a Lagrangian describing fermions and vector bosons having an $SU(3)_c$ gauge symmetry. We need to write a kinetic energy term in our Lagrangian for the gluons. A gauge invariant term which contains the necessary kinetic energy term for the gluons is

$$\mathcal{L}_G = -\frac{1}{4}G^{a\mu\nu}G^a_{\mu\nu} \tag{2.8}$$

where

$$G^a_{\mu\nu} = \partial_\mu G^a_\nu - \partial_\nu G^a_\mu - gf^{abc}G^b_\mu G^c_\nu. \tag{2.9}$$

This term also contains interactions between three or four gluons.

There are complications when one quantizes QCD. These arise from the fact that each gluon apparently has four degrees of freedom ($\mu = 0, ..., 3$), while in fact there are only two degrees of freedom due to the gauge symmetry . The extra states can effectively be canceled [3] by adding a gauge fixing term and a Fadeev-Popov ghost term to the Lagrangian:

$$\mathcal{L}_{GF} = -\frac{1}{2\xi}(\partial^\mu G^a_\mu)^2 \tag{2.10}$$

and

$$\mathcal{L}_{FP} = (\partial^\mu c^a)^\dagger(\partial_\mu c^a + g f^{abc} c^b G^c_\mu). \tag{2.11}$$

ξ is called the gauge parameter, and can be set arbitrarily. c and $c^\dagger$ are ghost fields which arise from the quantization of the gluon fields. They are Lorentz scalars which are governed by Fermi statistics. They are unphysical, but must be considered, for example, in processes involving gluon loops. These two terms, along with $\mathcal{L}_F$ and $\mathcal{L}_G$ describe QCD with one massless quark (which comes in three colors).

The full-blown standard model is QCD combined with the Glashow-Salam-Weinberg [4] electroweak model. It is based on the gauge group $SU(3)_c \times SU(2)_L \times U(1)_Y$ and it contains the fermions shown in Table 2.1. The top row contains the left-handed quarks. They all come in three colors, and thus transform by the fundamental representation of $SU(3)_c$. They also form doublets under the group $SU(2)_L$. The second row contains the right-handed quarks, which behave similarly to the left-handed ones, except they are $SU(2)_L$ singlets. The six different quarks are said to be different "flavors." The primes on the d, s, and b quarks will be explained later. The third and fourth rows contain the leptons, which are like the quarks except they lack color (i.e., they are $SU(3)_c$ singlets). There are also no right-handed neutrinos as far

Table 2.1. The fermion spectrum of the standard model. Each column is one generation

$\begin{pmatrix} u \\ d' \end{pmatrix}_L^{r,g,b}$	$\begin{pmatrix} c \\ s' \end{pmatrix}_L^{r,g,b}$	$\begin{pmatrix} t \\ b' \end{pmatrix}_L^{r,g,b}$
$u_R^{r,g,b}$ $d_R'^{r,g,b}$	$c_R^{r,g,b}$ $s_R'^{r,g,b}$	$t_R^{r,g,b}$ $b_R'^{r,g,b}$
$\begin{pmatrix} \nu_e \\ e^- \end{pmatrix}_L$	$\begin{pmatrix} \nu_\mu \\ \mu^- \end{pmatrix}_L$	$\begin{pmatrix} \nu_\tau \\ \tau^- \end{pmatrix}_L$
e_R^-	μ_R^-	τ_R^-

as we know, although we could easily include these as well. An important feature of the standard model is that the roster above has three columns. These are referred to as generations or families. Each succeeding generation differs from the first only in mass. There may be more generations as well, although experiments at LEP have shown that if there are, then the neutrinos must be heavier than half the Z mass. We must also list the $U(1)_Y$ quantum numbers of these fermions. $U(1)_Y$ is an Abelian group, and the fermions which transform under it have an additive quantum number, Y (hypercharge), like electric charge. The left-handed quarks have $Y = 1/3$; u_R, c_R, and t_R have $Y = 4/3$; d_R, s_R, and b_R have $Y = -2/3$; the left-handed leptons have $Y = -1$; and the right-handed leptons have $Y = -2$. If right-handed neutrinos exist, they are expected to have $Y = 0$ and be $SU(2)_L$ singlets. The t quark has not been observed, but is widely believed to exist because of the generation structure and from theoretical constraints.

In addition to the eight gluons from QCD, we have three gauge bosons associ-

ated with $SU(2)_L$ and one associated with $U(1)_Y$. Here is where we start to run into problems. The gauge symmetry requires that these gauge bosons all be massless. Weak interaction phenomena require that three of these bosons have masses around 100 GeV. However, the gauge symmetry is necessary for the theory to be renormalizable. That is, without the symmetry, we have divergences in the theory which cannot be removed by adding a finite number of counterterms to the Lagrangian. (We will discuss renormalization later.) Hence our Lagrangian must be gauge invariant, while at low energy the symmetry must appear badly broken. This can be achieved by introducing an $SU(2)_L$ doublet of scalar fields which can be used to spontaneously break the gauge symmetry and give mass to the gauge bosons. This is the Higgs [5] mechanism, and the scalar fields are known as Higgs fields.

Consider the added term

$$\mathcal{L}_H = (D_\mu \Phi)^\dagger (D^\mu \Phi) - V(\Phi) \tag{2.12}$$

$$V(\Phi) = -\mu^2 \Phi^\dagger \Phi + \lambda (\Phi^\dagger \Phi)^2. \tag{2.13}$$

where D_μ is a covariant derivative

$$D_\mu \Phi = \left(\partial_\mu + i g W_\mu^i \frac{\sigma^i}{2} + i g' B_\mu \frac{Y}{2} \right) \Phi \tag{2.14}$$

and Φ is an $SU(2)_L$ doublet of complex scalar fields,

$$\begin{pmatrix} \phi^+ \\ \phi^0 \end{pmatrix}. \tag{2.15}$$

Φ has hypercharge $Y = 1$, g and g' are the $SU(2)_L$ and $U(1)_Y$ coupling constants, W^i and B are the gauge bosons for these groups, and σ^i are the Pauli spin matrices,

the generators of $SU(2)_L$. If μ^2 is positive, then we find that the minimum of the potential V is not $\langle\Phi\rangle_0 = 0$, but rather

$$\langle\Phi\rangle_0 = \begin{pmatrix} 0 \\ \frac{v}{\sqrt{2}} \end{pmatrix}. \tag{2.16}$$

where $v = (\mu^2/\lambda)^{1/2}$. (This choice is not unique. We could change v by a phase, or put it at the top of the doublet, or have both components of the doublet non-zero. Any choice, however, ultimately leads to the same consequences.)

The crucial consequence of this is that the "physical" field is not Φ, but

$$\Phi' = \begin{pmatrix} \phi^+ \\ \phi^0 - \frac{v}{\sqrt{2}} \end{pmatrix}. \tag{2.17}$$

We must remember that what we observe as physical fields are deviations from the lowest energy state, the vacuum. Hence we take the physical fields to be the ones with vacuum expectation value = 0. Since the vacuum is $\langle\Phi\rangle_0$, instead of 0, we take the physical field to be $\Phi - \langle\Phi\rangle_0$. We can rewrite Φ as

$$\Phi(x) = e^{i\zeta^i(x)\sigma^i/v} \begin{pmatrix} 0 \\ \frac{v+H(x)}{\sqrt{2}} \end{pmatrix} \tag{2.18}$$

where our four scalar fields (recall that Φ is complex, so each element of the doublet contains two fields) are ζ^i and H. The exponential is exactly in the form of an $SU(2)_L$ gauge transformation, and so we can transform it away. In this "unitary" gauge we see that we have only one physical scalar field, and it is this field H that is referred to as the Higgs particle.

To see the consequence of this, we take the Lagrangian and plug in our new

expression for Φ,

$$\Phi(x) = \begin{pmatrix} 0 \\ \frac{v+H(x)}{\sqrt{2}} \end{pmatrix}. \tag{2.19}$$

When we do this, we see two important things. First, we find that the field H has mass $m_H = \sqrt{2}\mu$. Second, and more importantly, we find that the gauge bosons for $SU(2)_L$ and $U(1)_Y$ acquire mass as well. If we define

$$W^{\pm} = (W^1 \mp iW^2)/\sqrt{2} \tag{2.20}$$

and

$$\begin{aligned} Z &= \cos\theta_W W^3 - \sin\theta_W B \\ A &= \sin\theta_W W^3 + \cos\theta_W B \end{aligned} \tag{2.21}$$

where $\tan\theta_W = g'/g$, then the new fields have masses

$$\begin{aligned} M_W^2 &= g^2v^2/4 \\ M_Z^2 &= (g^2 + g'^2)v^2/4 \\ M_A^2 &= 0 \end{aligned} \tag{2.22}$$

Experiments have found $M_W = 80$ GeV, $M_Z = 91.2$ GeV, and $\sin^2\theta_W = .23$. v is related to the Fermi constant by

$$\frac{G_F}{\sqrt{2}} = \frac{g^2}{8M_W^2} = \frac{1}{2v^2}. \tag{2.23}$$

A convenient and important parameter which is not too difficult to measure is the ρ parameter

$$\rho = \frac{M_W^2}{M_Z^2 \cos^2\theta_W} \tag{2.24}$$

which is 1 in the standard model (ignoring radiative corrections).

The disappearance of three scalar particles and the appearance of gauge boson masses are not a coincidence. This is what is actually referred to as the Higgs mechanism. An important thing to notice is that the number of degrees of freedom do not change. Before spontaneous symmetry breaking, we have four scalars, each with one degree of freedom, and three gauge bosons, each with two degrees of freedom. (A massive vector particle will have three spin states, but a massless particle with gauge symmetry has only two.) This gives us a total of ten. After symmetry breaking we have one scalar, and three massive vector bosons. The massive vector bosons have three degrees of freedom each, and so the total is still ten. We say that the three Higgs bosons are "eaten" by the $W^{\pm}$ and Z, and it is this which gives them mass.

The fact that the gauge boson A_μ is still massless indicates that we have not broken the symmetry $SU(2)_L \times U(1)_Y$ completely. There is one generator for which there still exists a local symmetry. That generator is the linear combination

$$Q \equiv \frac{\sigma^3}{2} + \frac{Y}{2}. \tag{2.25}$$

So we're left with a $U(1)$ gauge symmetry in which a particle's charge is given by its "weak isospin" ($+1/2$ for the top element of an $SU(2)_L$ doublet, $-1/2$ for the bottom element, and 0 for a singlet) plus half its hypercharge. This remaining symmetry is exactly quantum electrodynamics (QED), and the charge is just electric charge. Hence we've broken the symmetry of the standard model

$$SU(3)_c \times SU(2)_L \times U(1)_Y \longrightarrow SU(3)_c \times U(1)_{EM}, \tag{2.26}$$

where $U(1)_{EM}$ is QED. The fermions in our theory now have electric charges $Q_u = +2/3, Q_d = -1/3, Q_e = -1$, and $Q_{\nu_e} = 0$ with the other generations following similarly.

At this point, the fermions in our theory are still massless. A mass term in the Lagrangian involves a left-handed fermion and a right-handed fermion. But the left-handed fermions are in $SU(2)_L$ doublets while the right-handed fermions are $SU(2)_L$ singlets. Hence any fermion mass terms would violate the gauge symmetry on which the standard model is based, and would therefore render the theory non-renormalizable. We can, however, give the fermions mass through Yukawa couplings between the Higgs and fermions. Consider the gauge invariant term

$$C(\ \bar{\nu}_e \quad \bar{e}\ )_L \Phi e_R = C\bar{e}_L \left(\frac{H+v}{\sqrt{2}}\right) e_R \tag{2.27}$$

where the equal sign holds in unitary gauge. We will continue to work in unitary gauge. If we choose $C = \sqrt{2}m_e/v$, then the term proportional to v in (2.27) will give the electron a mass m_e. We can give masses to the other charged leptons similarly.

Giving masses to quarks is a trickier business. The mass eigenstates are not equal to the $SU(2)_L \times U(1)_Y$ eigenstates. Instead the mass eigenstates are mixtures of the weak interaction eigenstates. Hence instead of having a separate mass term for each generation as we can do in the lepton sector, we will have a mass matrix. First we must introduce the conjugate doublet to the Higgs doublet we had before. This would have been necessary earlier if we had needed to give mass to the neutrinos. We define

$$\tilde{\Phi} \equiv i\sigma_2 \Phi^* = \begin{pmatrix} \frac{H(x)+v}{\sqrt{2}} \\ 0 \end{pmatrix}. \tag{2.28}$$

Using this, we can write mass terms for all the quarks. We will write $q_{L\alpha}, u_{R\alpha}$, and $d'_{R\alpha}$ to denote the left-handed quark doublet, right-handed charge 2/3 quark, and right-handed charge $-1/3$ quark respectively of the α generation. ($\alpha = 1, 2, 3.$) Then

we can write our quark mass terms

$$\mathcal{L}_{\text{qmass}} = \sum_{\alpha,\beta=1}^{3} \left(\frac{1}{v} \bar{q}_{L\alpha} \Phi M_{\alpha\beta} d'_{R\beta} + \frac{1}{v} \bar{q}_{L\alpha} \tilde{\Phi} \tilde{M}_{\alpha\beta} u_{R\beta} + \text{c.c.} \right) \tag{2.29}$$

where M and $\tilde{M}$ are 3×3 matrices and c.c. denotes complex conjugation. The first term gives mass to the charge $-1/3$ quarks and couples them to the physical Higgs, and the second term does the same for the charge $2/3$ quarks.

Without loss of generality, we can choose $\tilde{M}$ to be diagonal. This amounts to a rearranging of generations in the original roster of fermions, which we are free to do since the generations all behave the same. We can diagonalize M with the matrix A so that AMA^{-1} is diagonal. Then we can redefine our quarks as

$$\begin{pmatrix} d \\ s \\ b \end{pmatrix} = A \begin{pmatrix} d' \\ s' \\ b' \end{pmatrix}. \tag{2.30}$$

The unprimed quarks are our mass eigenstates. We must see how these behave in electroweak interactions.

We can write the interactions between quarks and $SU(2)_L$ gauge bosons

$$\mathcal{L} = -g J^{i\mu} W^i_\mu \tag{2.31}$$

where

$$J^{i\mu} = \bar{q}_\alpha \gamma^\mu \left(\frac{1-\gamma^5}{2} \right) \frac{\sigma^i}{2} q_\alpha. \tag{2.32}$$

We can extract the W^1 and W^2 terms from this, and substitute $W^\pm$. We get

$$\frac{-g}{\sqrt{2}} (J^-_\mu W^{+\mu} + J^+_\mu W^{-\mu}) \tag{2.33}$$

where

$$J_\mu^- = \overline{u}\gamma_\mu \left(\frac{1-\gamma^5}{2}\right) d' \tag{2.34}$$

and J_μ^+ is its Hermitian conjugate. We've suppressed the generation index in $J^\pm$. We can express this current in terms of the mass eigenstates,

$$J_\mu^- = \overline{u}\gamma_\mu \left(\frac{1-\gamma^5}{2}\right) A^{-1} d. \tag{2.35}$$

Now we see that the effect of mixing on the charged current interactions is that the $W^\pm$ can couple with quark pairs of different generations. This coupling is governed by the matrix A which diagonalizes the mass matrix for the lower quarks (d, s, and b). The matrix A^{-1} (usually denoted by V, as I'll refer to it hereafter, or U) is called the Cabibbo-Kobayashi-Maskawa [6] matrix. It is unitary, and experiment shows that the off-diagonal elements are much smaller than the diagonal ones.

This leaves us only with the neutral current sector of the quark interactions to consider. Without going into too much detail, we will just note that the neutral current sector is unaffected by generation mixing. The neutral currents before generation mixing are flavor diagonal. That is, each term contains only one kind of quark. Hence a typical term looks like

$$J_\mu \propto \overline{d'}\mathcal{O}_\mu d' \tag{2.36}$$

where again d' is the vector $(d', s', b')^T$ and $\mathcal{O}$ is some operator which is flavor independent. Rewriting this in terms of the mass eigenstates, we see that this is

$$J_\mu \propto \overline{d}V^{-1}\mathcal{O}_\mu V d. \tag{2.37}$$

Since $\mathcal{O}$ is flavor independent, we can commute $\mathcal{O}$ with V, and since $V^{-1}V = I$ the resultant current is still flavor independent. This is not a trivial fact. When the

electroweak model was first presented there were only three flavors of quarks: u, d, and s. It was thought that s was an $SU(2)_L$ singlet. A problem arose when d and s were allowed to mix. Because d and s didn't possess the same electroweak quantum numbers, neutral currents were not flavor independent. As a result, in neutral current operators such as the one above, one could not commute $\mathcal{O}$ with V, and so the current was not flavor diagonal when written with the mass eigenstates. Glashow, Iliopoulos, and Maiani [7] eliminated this problem by adding the then unobserved c quark to the standard model in an $SU(2)_L$ doublet with s.

These are the rudiments of the standard model. It has met with much success. More than fifteen years after its inception it can still accommodate all of the experimental data that we have today (at least as far as we can calculate physical observables from the model). The general belief, however, is that the standard model is not the whole story of the workings of the universe. There are several unattractive features of the standard model, and as a result, physicists are constantly looking for what physics lies beyond the standard model [8].

2.2. Problems and Extensions of the Standard Model

The complaints with the standard model can probably be best summed up by saying that the standard model describes very well, but it doesn't explain. That is, while it accommodates all the data very well and has made many predictions which have since been verified, such as the weak neutral current, and the W and Z bosons (all unknown when the standard model was conceived), it does not have the look of a truly fundamental theory, and leaves several questions unanswered.

Perhaps the greatest irritation is the arbitrariness of the standard model. First,

let's look at the number of arbitrary parameters. There are the three gauge couplings. Next come the two arbitrary parameters in the Higgs sector, its mass and its self-coupling. Then there are the masses of nine fermions (twelve if the neutrinos have mass). There are also four arbitrary parameters in the Cabibbo–Kobayashi–Maskawa matrix. Finally, there is the strong CP violating parameter, a quantity which is observed to be very close to 0 for no apparent reason. I won't discuss this, since it will not be relevant to my work. But including it in our parameter count increases the total to at least 19, more if we have massive neutrinos or a fourth generation.

The number of generations is another unexplained mystery. There seems to be no reason why there should be three rather than one or four or sixty. The standard model has nothing to say about this, but offers us only the tantalizing trends that each generation is heavier than the previous one, the quarks are heavier than their corresponding leptons, and the neutrinos are very light if not massless.

The Higgs sector is even more mysterious. Although the "minimal" standard model has only two parameters in this sector, we can easily envision an only slightly extended version with many more representations (constrained mainly by the ρ parameter). Furthermore, the Higgs has been experimentally invisible. Not only have we not seen it, but experimental constraints on it are virtually nonexistent. While it certainly appears that we have an $SU(2)_L \times U(1)_Y$ symmetry broken to $U(1)_{EM}$, we have hardly a glimpse of the mechanism of this breaking. This leaves open the question of whether there may be other possible mechanisms for this symmetry breaking.

On a broader scale, the choice of representations for the fermions is not specified within the general framework of non-Abelian gauge theories. The only apparent constraint is that no part of the gauge symmetry can be anomalous. An anomaly is a

violation in a quantum theory of a symmetry which would hold exactly in the corresponding classical theory. We will see an example of this later on. Although anomalies are often unpleasant to deal with, they are generally harmless. The standard model, however, relies on its gauge symmetry for renormalizability. An anomalous breaking of this gauge symmetry would be very bad. There are in fact anomalies in the gauge symmetry of the standard model, but we can cause them to cancel through a judicious choice of fermion representations. It turns out that we need only to make sure that the sum of the charges of all the fermions in each generation is zero. The fermions observed in one generation consist of three colors of charge $2/3$ quarks, three colors of charge $-1/3$ quark, one neutral lepton, and one charge -1 lepton, a collection which satisfies our constraint.

Even broader, there is no theoretical indication of why the gauge symmetry of the universe should be the relatively complicated group $SU(3)_c \times SU(2)_L \times U(1)_Y$. There is also the problem of incorporating a quantum theory of gravity into the scheme. If we really want to stretch our minds, we could question whether nature is really described by a non-Abelian gauge theory, whether it is described by quantum field theory, or even whether is is describable by mathematics.

We won't be that ambitious; instead, we'll lead up to technicolor through a discussion of grand unified theories (GUTs). GUTs are basically an attempt to simplify the gauge group. In a grand unified theory, we attempt to embed the gauge symmetry of the standard model in a larger symmetry. In the simplest example [9] of a GUT, the standard model symmetry is embedded in the group $SU(5)$. The symmetry breaking then proceeds as

$$SU(5) \longrightarrow SU(3)_c \times SU(2)_L \times U(1)_Y \longrightarrow SU(3)_c \times U(1)_{EM}. \qquad (2.38)$$

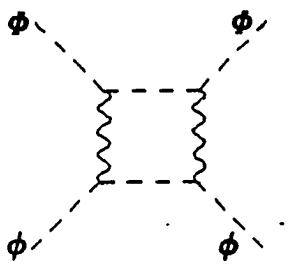

Figure 2.1. A box diagram in a typical GUT which relates scalar fields responsible for symmetry breaking at different scales

The symmetry breaking is accomplished at two vastly different energy scales, the higher one being around 10^{14} GeV, and the lower one being at its usual scale of 250 GeV. In both cases it is accomplished via the Higgs mechanism.

While the ever increasing lower limit on the proton lifetime has pushed $SU(5)$ out of the limelight, other GUTs remain, such as $SO(10)$ and the very popular E_6. One obvious question that comes to mind with a grand unified theory is why a unified theory would contain two (or more in many cases) mass scales so far apart. This question is termed the "hierarchy problem." Upon closer examination of the simplest GUTs, another, related problem appears. When we examine one loop box diagrams, such as those in Figure 2.1, we find that the interactions between the heavy Higgs particles (those that come with the symmetry breaking of the GUT) and the light ones (coming with the symmetry breaking of the standard model) will renormalize the scales of the two Higgs sectors. In particular, the heavy scale will remain roughly the same while the lower scale will be raised to about the same level as the higher one. We can avoid this, but only by imposing very careful relationships on the parameters of the Higgs sectors, out to about 26 decimal places. Furthermore, this adjustment must be remade at every order in perturbative calculations. This is referred to as the

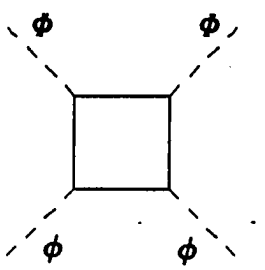

Figure 2.2. A box diagram which supplements that of Figure 2.1 in a supersymmetric GUT

"fine tuning" problem, although it is often included in the hierarchy problem.

One answer to the fine tuning problem is supersymmetry (SUSY). In supersymmetric theories, every fermion has a supersymmetric bosonic partner, and *vice versa.* The consequence of this, relevant to the fine tuning problem, is that the box diagram, Figure 2.1, has a partner, Figure 2.2 in which the box is a fermion loop instead of a boson loop. Since fermion loops in perturbation theory come with an overall minus sign, the fermion loop diagram cancels parts of the boson loop diagram. In particular, a part that is quadratically divergent and leads to the merging of scales is canceled. In any realistic theory, supersymmetry is only an approximate symmetry. If the symmetry were exact, then all particles would have the same mass as their supersymmetric partners. Since we have not yet observed any supersymmetric pair of particles, this is clearly not the case. Using supersymmetry as a solution to the fine tuning problem, however, places constraints on the masses of supersymmetric particles and on the degree of supersymmetry breaking. Supersymmetry alone does not present any solution to the hierarchy.

There are many theories besides supersymmetry and GUTS which try to address one or more of the problems of the standard model. We won't say much more about

these two. The class of theories that we'll be addressing here is technicolor theories.

2.3. Technicolor

Technicolor [10, 11] is a theory based on a non-Abelian gauge theory, like QCD. While QCD was introduced in Section 2.1, we did not go into the details of its phenomonology. The primary tool of high energy physicists for investigating phenomenology is perturbation theory. Even in the most perturbative theories, however, perturbation theory can only tell us so much. In QCD, the situation is worse than in most cases. This is because perturbative calculations are performed around one or more coupling constants, which are assumed to be small. In low energy QCD this is not the case.

We can, however, use perturbation theory to investigate the behavior of the coupling "constant" as a function of the energy scale of the interaction we're interested in. To do this, we must use the renormalization group approach. We will not go into this, since all we require is the result.

The result we find [12] is that the dependence of the coupling constant on the scale is described by the β function, through the renormalization group equation

$$\frac{dg}{d\log(Q^2/\mu^2)} = \beta \tag{2.39}$$

where Q^2 is the momentum scale of interest, and μ^2 is some reference scale. We can calculate β to one loop, and the result is

$$\beta = \frac{g^3}{16\pi^2}\left[-\frac{11}{3}N + \frac{2}{3}n_F + \frac{1}{6}n_S\right] \tag{2.40}$$

for an $SU(N)$ theory with n_F fermions and n_S scalars, all in the fundamental representation. In the case of QCD, we have 6 colored fermions, no colored scalars, and

$N = 3$. By plugging in these numbers, we see that in the standard model even extended well beyond three generations, β is negative. This means that the strength of the coupling decreases with increasing energy and increases with decreasing energy. To be precise, we can write the coupling constant in QCD as

$$\alpha_s(Q^2) = \frac{4\pi}{\left(11 - \frac{2}{3}n_F\right)\log(Q^2/\Lambda^2)}, \tag{2.41}$$

where Λ is a mass scale which replaces the coupling constant g as a fundamental quantity in the theory. The terms "asymptotic freedom" and "infrared slavery" are used to describe the fact that the coupling gets very weak at high energies and so strong at low energies that we do not observe quarks or gluons except in colorless ($SU(3)_C$ singlet) bound states. The result is that at high energies the coupling is small enough that we can use perturbation theory, while at low energies the coupling is too strong, in agreement with our experience with the strong interaction.

The behavior of QCD at low energies is much more complicated than just a large coupling constant. To see what goes on at low energies, we must go back and reexamine the symmetries of QCD. We have six flavors of quarks which, with respect to QCD, are completely identical except in mass. We will restrict ourselves to the lightest three quarks, since they are nearly massless ($m_u \approx 6$ MeV, $m_d \approx 10$ MeV, and $m_s \approx 200$ MeV). Massless quarks contain more symmetry than massive ones. In particular, these three flavors of quarks are symmetric (ignoring their masses) under a global transformation of the form

$$\begin{aligned} q_L &\to U_L q_L \\ q_R &\to U_R q_R \end{aligned} \tag{2.42}$$

where $q_L = (u,d,s)_L^T$, $q_R = (u,d,s)_R^T$, and (U_L, U_R) is an element of $SU(3)_L \times$

$SU(3)_R$. This type of symmetry, in which left and right handed fields transform independently, is called "chiral symmetry. "

But this symmetry is spontaneously broken. In particular, we can look at the vacuum expectation value $\langle 0|\bar{q}q|0\rangle$. The quantity $\bar{q}q$ is not invariant under the full chiral symmetry. Instead, we can define vector and axial vector transformations, V and A respectively, by

$$\begin{aligned} q &\rightarrow Vq, \quad V = e^{i\alpha^i T^i} \\ q &\rightarrow Aq, \quad A = e^{i\beta^i T^i \gamma^5} \end{aligned} \tag{2.43}$$

If the quantity $\langle 0|\bar{q}q|0\rangle$ is 0, then our theory is still invariant under the transformations (2.43) which are equivalent to (2.42). This quantity has been calculated in various manners, however, and it is well established [13] that for sufficiently strong coupling (particularly, $g^2 C_2(r)/4\pi \gtrsim \pi/3$),

$$\langle 0|\bar{q}q|0\rangle \neq 0. \tag{2.44}$$

But, as mentioned before, the coupling constant in QCD in fact gets very strong at low energies. Hence $\langle 0|\bar{q}q|0\rangle$ is 0 at high energies and nonzero at lower energies. Since the vacuum is still invariant under the vector transformation, V, $SU(3)_V$ is still a good symmetry. Since the vacuum is no longer symmetric under $SU(3)_A$, this symmetry is broken at low energies.

Goldstone's theorem tells us that anytime we have spontaneous symmetry breaking of a continuous symmetry, we find a massless boson [14], called a Nambu–Goldstone boson, for each broken generator of the symmetry. In the case of three flavor QCD, we have $SU(3)_L \times SU(3)_R \rightarrow SU(3)_V$, and so the broken generators are the generators of the broken $SU(3)$. There are eight of these, and so we expect eight massless bosons. In fact, we don't have eight massless bosons. The reason

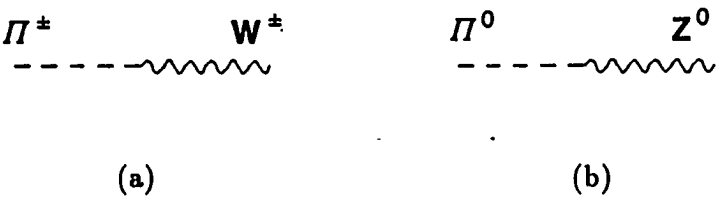

Figure 2.3. Couplings between technipions and electroweak gauge bosons

for this is that the symmetry that was broken was not an exact symmetry, since the quarks are in fact massive. We do, however, have eight relatively light bosons, $\pi^{\pm}, \pi^0, K^{\pm}, K_L^0, K_S^0$, and η. Such bosons, light bosons arising from a spontaneously broken approximate symmetry, are called pseudo-Nambu–Goldstone bosons.

Part of the symmetry that this condensate breaks is the $SU(2)_L \times U(1)_Y$ gauge symmetry for which we introduced the Higgs sector. It would appear that we don't need any mechanism beyond this condensate in order to break the electroweak symmetry. This breaking, however, leads to W and Z masses about three orders of magnitude too small. We should notice a key feature of this type of symmetry breaking, called dynamical symmetry breaking. If we assume that the standard model is part of a grander theory which only reveals its fuller symmetry at much higher energies, the two symmetry breaking scales will remain far apart without any care on our part. We see that this type of symmetry breaking can naturally provide a hierarchy with no need for fine tuning. For this reason, dynamical symmetry breaking is an attractive mechanism.

If we wish to use this mode of symmetry breaking in the electroweak sector of the standard model, we must postulate a new interaction, which we call technicolor.

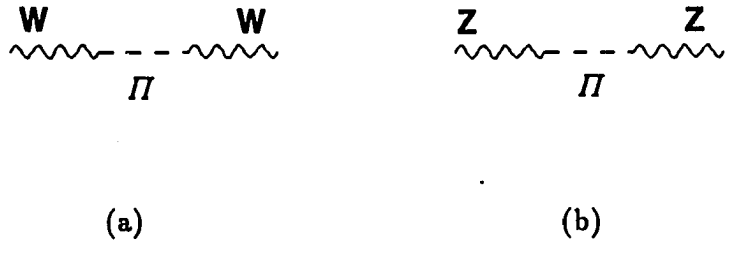

Figure 2.4. Electroweak gauge boson propagator corrections due to the presence of technipions

Roughly speaking, this is just a scaled-up version of QCD. To see what scale we need for technicolor, we calculate the masses of the W and Z bosons in such a theory. These masses are related to the coupling of the technipions, the technicolor analogue of the ordinary pions and kaons, to the W and Z. We start by defining the technipion decay constant, F_π, by

$$\langle 0|J_5^{\mu i}(0)|\Pi^j(p)\rangle = F_\pi p^\mu \delta^{ij}. \tag{2.45}$$

Here, Π^j are the technipions, J_5^i are the axial currents, and the QCD analogue of F_π, f_π is around 93 MeV. The current which couples to the $SU(2)_L$ gauge bosons is a linear combination of the vector and axial vector currents, $J_L^\mu = (J^\mu - J_5^\mu)/2$, and (2.45) tells us how this current couples to the technipions. Hence we know how the technipions couple to the electroweak gauge bosons. In particular, the couplings are given in Figure 2.3.

Using these couplings, we can calculate the corrections to the gauge boson propagators. The propagator is of the form

$$\frac{g^{\mu\nu} - k^\mu k^\nu/k^2}{k^2(1+\Pi(k^2))}, \tag{2.46}$$

where $\Pi(k^2)$ represents the corrections. The vacuum polarizations, $\Pi(k^2)$, are computed from the diagrams in Figure 2.4. The result is that $\Pi(k^2)$ contains a pole. From (2.46) we see that a pole in Π will shift the pole in the propagator away from zero. The result is that the $W^{\pm}$ obtain a mass

$$M_W = \frac{1}{2} g F_\pi. \tag{2.47}$$

As before, we obtain a mass matrix between the W^3 and B bosons, which can be diagonalized just as before. The masses of the photon and Z boson, which are related to the W^3 and B by the same angle θ_W as before, are

$$\begin{aligned} M_A^2 &= 0 \\ M_Z^2 &= \tfrac{1}{4}(g^2 + g'^2) F_\pi^2, \end{aligned} \tag{2.48}$$

where g and g' are once again the $SU(2)_L$ and $U(1)_Y$ couplings, respectively. We can see that the ρ parameter, defined earlier, $M_W^2/(M_Z^2 \cos^2 \theta_W)$ is still 1. The masses of the W and Z are reproduced if we take $F_\pi = v$ where v is the vacuum expectation value of the standard model Higgs, about 250 GeV. Hence we see that technicolor can be used to generate gauge boson masses consistent with the standard model. The masses in (2.47) and (2.48) assume just one $SU(2)_L$ doublet of left-handed techniquarks along with a right handed singlet for each of them. If we have more doublets, then each one contributes to the vacuum polarization of the gauge bosons, and the resulting masses are larger. To reproduce the correct masses for an arbitrary number of doublets, N_D, we have

$$F_\pi = \frac{v}{\sqrt{N_D}}. \tag{2.49}$$

While there are many ways to arrange technifermions in a technicolor model, there are two main ideas. We can either have just one colorless doublet of technifermions,

or since all other fermions seem to come in families, we can have one family of technifermions, with two flavors of techniquarks, each coming in three colors of course, and two technileptons. The former has the advantage of simplicity, while the latter may be more useful in giving masses to the ordinary fermions. The chiral symmetry of the first theory is $SU(2)_L \times SU(2)_R \rightarrow SU(2)_V$ where the symmetry breaking is provided by the technifermion condensate, of course. There are three broken generators, which would mean three Nambu–Goldstone bosons. These are eaten by the $W^{\pm}$ and Z, just as three Higgs bosons are in the standard model. Therefore there are no technipions in such a theory. In the second case, the chiral symmetry is $SU(8)_L \times SU(8)_R \rightarrow SU(8)_V$. In this case, there are 63 Nambu–Goldstone bosons, three of which are eaten, leaving 60 technipions. We will have to worry about giving mass to these in such a model. This will be addressed later.

Hence we've accomplished with technicolor half of what the Higgs sector does in the standard model. We've shown that we can give the correct masses to the electroweak bosons. What we need to do now is to give masses to fermions. Here is where technicolor runs into problems.

2.4. Fermion Masses and Extended Technicolor

In the standard model, we gave masses to fermions through Yukawa couplings with the Higgs. Here we have no fundamental scalars, and so we must find some other way. We have already said, however, that the technipions play a role that is analogous to the Higgs fields in giving the gauge bosons masses. Hence it is reasonable to suggest that we can give mass to fermions through Yukawa couplings to technipions. The technipions, of course, are composite. In terms of its fundamental constituents,

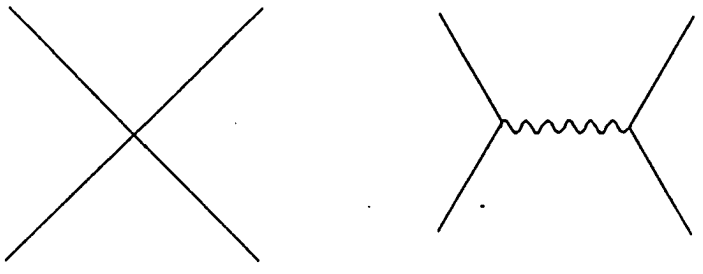

(a) (b)

Figure 2.5. A four-fermion vertex in Fermi's weak interaction theory, (a), and the corresponding vertex in electroweak theory, (b)

a technipion-ordinary fermion Yukawa coupling looks like

$$\overline{\Psi}\Psi\overline{\psi}\psi \tag{2.50}$$

where Ψ is a technifermion, and ψ is an ordinary fermion. Since $\langle 0|\overline{\Psi}\Psi|0\rangle$ is non-zero, (2.50) will give an ordinary fermion mass at low energies.

This term, unfortunately, is a dimension six operator, and is therefore non-renormalizable. We have a precedent for this. The original theory of weak interactions, due to Fermi, was also a non-renormalizable theory consisting of four-fermion couplings. This theory was remedied by the introduction by Weinberg, Salam, and Glashow of the weak gauge bosons, by which the non-renormalizable interactions of Figure 2.5a became the renormalizable interactions of Figure 2.5b. At low energies, the W boson propagator, $i(-g^{\mu\nu} + k^\mu k^\nu/M_W^2)/(k^2 - M_W^2)$ becomes approximately $ig^{\mu\nu}/M_W^2$ since $k^2 \ll M_W^2$. This gives a theory at low energies that approximates a four-fermion theory, with a weak coupling $\sim g^2/M_W^2$.

Just as Weinberg et al. introduced a new gauge interaction to generate the ob-

served weak interactions, so will we introduce a new interaction [15], which we will call extended technicolor (ETC), to give us the four-fermion couplings we need to give ordinary fermions mass. This can in general give us three types of four-fermion interactions,

$$\overline{\Psi}\Psi\overline{\psi}\psi, \tag{2.51}$$

$$\overline{\Psi}\Psi\overline{\Psi}\Psi, \tag{2.52}$$

and

$$\overline{\psi}\psi\overline{\psi}\psi. \tag{2.53}$$

The first of these gives us the ordinary fermion masses we want. The second term gives masses to the technifermions, or equivalently, the technipions. The final term leads to interactions between ordinary fermions mediated by ETC gauge bosons. A problem arises because of the observed flavor mixing between the ordinary fermions, described by the CKM matrix, which must be reproduced by (2.51). This means that (2.51) cannot be flavor diagonal. The three terms must be related, however, since ETC is assumed to have some Lie group symmetry. Therefore we get flavor changing in the ordinary fermion sector from (2.53). While flavor changing is okay in charged current interactions, (2.53) will in general produce flavor changing neutral currents [16] as well. In addition, (2.51) can cause flavor changing neutral currents in the ordinary fermion sector via technipion exchange. We need to see how big these are expected to be.

In general, we expect flavor changing neutral currents (FCNC) from ETC gauge bosons (as in Figure 2.6) to be proportional to g_{etc}^2/M_{etc}^2 where g_{etc} is the ETC coupling constant, and M_{etc} is the mass of the gauge boson exchanged in the process.

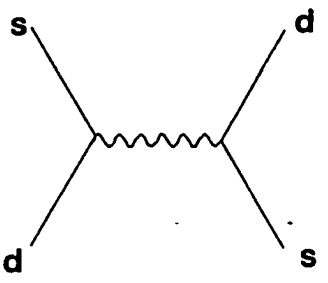

Figure 2.6. An ETC vertex leading to flavor changing neutral current interactions

(This could in general depend on which fermions are involved.) We would also expect these transitions to show some indication of the mixings of the CKM matrix. Hence we expect the relevant coupling constants to be approximately equal to these mixing elements. Hence, for a neutral current process involving a d to s transition ($\Delta S = 2$) we find

$$\mathcal{L}_{sd} \approx \left[(\overline{s}_L\gamma^\mu d_L)^2, (\overline{s}_L\gamma^\mu d_L)(\overline{s}_R\gamma^\mu d_R), (\overline{s}_R\gamma^\mu d_R)^2\right] \frac{\theta^2}{v_{d,s}^2}. \tag{2.54}$$

$(v_{d,s}^2)^{-1}$ is g_{etc}^2/M_{etc}^2, and in particular, M is taken to be the mass of some particular gauge boson which couples to u and d. θ^2 for this transition is expected to be equal to the Cabibbo angle, $\sim 1/20$. Constraining the FCNCs in this model to be no larger than the standard model FCNCs from box diagrams, we obtain the constraint

$$v_{d,s}^2 \gtrsim 5 \times 10^4 \text{ TeV}^2. \tag{2.55}$$

It seems, then, that by making the ETC scale sufficiently large, we can make the FCNCs sufficiently small.

There is a limit, however, on how large we can make the ETC scale. We still need to supply masses to the ordinary fermions. We can constrain the ETC scale from the fact that we need to generate fermion masses $\sim$ 1 GeV from the same ETC gauge

(a) (b)

Figure 2.7. An ETC vertex leading to mass for an ordinary fermion (a) and the effective vertex in the limit of infinite ETC gauge boson mass

bosons that give these FCNCs. The masses come from diagrams such as in Figure 2.7a. When we let the ETC boson mass get large, the effective diagram becomes Figure 2.7b, where the $\times$ on the technifermion line represents the condensate. From this we can estimate the fermion mass as

$$m_f = \frac{g_{ETC}^2}{2M_{ETC}^2}\langle 0|\sum \overline{\Psi}\Psi|0\rangle. \tag{2.56}$$

Since technicolor is just a scaled-up version of QCD (naïvely, anyway) we can estimate the technicolor condensate by looking at the dependence of the QCD condensate on f_π and N_c, where N_c is the number of colors. The result is

$$\langle 0|\overline{\Psi}\Psi|0\rangle = \langle 0|\bar{q}q|0\rangle \left(\frac{F_\pi}{f_\pi}\right)^3 \left(\frac{3}{N}\right)^{1/2} \tag{2.57}$$

where N is the number of technicolors, and the condensates are summed over the number of technicolors or colors, as appropriate. The QCD condensate can be estimated from partially conserved axial vector current (PCAC) theory,

$$\frac{1}{2}(m_u + m_d)\langle 0|\bar{u}u + \bar{d}d|0\rangle = f_\pi^2 m_\pi^2. \tag{2.58}$$

The result is that $\langle 0|\bar{q}q|0\rangle = .011$ GeV^3 and $\langle 0|\overline{\Psi}\Psi|0\rangle = .020$ TeV^3 for a one family model with $N = 3$. In order to obtain fermion masses around 1 GeV we must therefore have

$$v_{d,s}^2 \approx 1200 \text{ TeV}^2. \tag{2.59}$$

Comparing this with the constraint (2.55), we see a clear conflict.

Although the flavor changing neutral current problem is not addressed in this work, we'll discuss it briefly here. This problem still has not been resolved to most people's satisfaction. In particular, there are several things that one would like a good technicolor theory to do:

1. It should break the electroweak symmetry, giving the correct masses to the W and Z bosons.

2. It should be renormalizable.

3. It should give correct fermion masses.

4. It should give sufficiently large technipion masses.

5. It should have no fundamental scalars.

6. It should have no flavor changing neutral currents at tree level nor any other troublesome phenomonology.

There is, for now, no technicolor theory that meets all these criteria. There are, for example, models that meet most of the criteria, but have fundamental scalars at some higher scale. Nor is it difficult to construct non-renormalizable theories which meet all the other requirements. But if one sticks to renormalizable theories with no

scalars, then one is left with the flavor changing neutral current vs. fermion mass tug of war.

There are two main directions from which people are attempting to handle this problem. One is by attempting to formulate a theory containing a symmetry analogous to the GIM mechanism which prohibits FCNCs at tree level. This has been attempted both in an ETC model [17] and a composite technicolor [18] model, and it has not been fully successful in either case.

The other popular options are to attempt to find some mechanism by which the condensate of (2.56) takes on a much higher value than that obtained from scaling up QCD. By raising the condensate, one can then raise the ETC scale to a high enough level that the FCNCs will be sufficiently suppressed. Such an enhancement has been shown to come about in three different ways: from a slowly running [19] technicolor coupling, in a technicolor theory with an ultraviolet fixed point [20], or from four fermion interactions [21] arising, for example, in ETC. The slowly running coupling theory will probably not lead to a large enough enhancement unless the coupling runs *very* slowly. Finding such a theory will be a tough problem. The fixed point theory, which provides the condensate enhancement by the same mechanism as the slowly running coupling theory, will provide sufficient enhancement. The proponents of this mechanism claim to have shown the existence of such a theory, but their arguments are not totally convincing. In particular, they make some approximations in demonstrating the fixed point, and it is not clear that the fixed point exists outside their approximations. The four fermion interactions appear to be able, under the proper conditions, to provide a sufficient condensate enhancement. Whether such conditions (which mainly concern the value of the ETC coupling constant) are actually

met in a realistic ETC model remains to be seen. Hence while the first of these options appears not to be very promising, the latter two options leave much room for work.

We will not be dealing with the flavor changing neutral current problem here. Rather, we will look at some properties of some of the neutral technipions in a one family model. That is, we will be looking at the low energy consequences of such a model. This is not a straightforward task, since at low energies the technicolor coupling is very strong. Perturbation theory alone will not describe anything accurately. But we have QCD as a guide. There are several approaches to examining low energy QCD. The one which we'll use is the effective Lagrangian technique.

3. TECHNIPIONS: AN EFFECTIVE LAGRANGIAN AND MASSES

3.1. A Lagrangian with Global Chiral Symmetry

The techniques for extracting the low-energy consequences of technicolor theories are mostly generalizations of techniques for low energy QCD. In this case, we will construct an effective Lagrangian, which will consist of the pseudo-Nambu-Goldstone bosons (technipions) of the theory. We begin by writing the simplest expression we can, which is consistent with the symmetries of the fundamental theory (in this case, technicolor.) A technicolor theory with N flavors of technifermions possesses an $SU(N)_L \times SU(N)_R \times U(1)$ chiral symmetry which at low energies is broken dynamically to an $SU(N)_V \times U(1)$ vector symmetry. The simplest Lagrangian which reflects this is

$$\mathcal{L} = \frac{F_\pi^2}{4}\mathrm{Tr}(\partial_\mu U)(\partial^\mu U^\dagger), \tag{3.1}$$

where

$$U = \exp\left(\frac{2i}{F_\pi}\phi^i\Lambda^i\right). \tag{3.2}$$

Here, ϕ^i are the technipion fields ($i = 1, \ldots, N^2-1$) and Λ^i are the generator matrices for $SU(N)$. The generators are normalized so that

$$\mathrm{Tr}(\Lambda^i, \Lambda^j) = \frac{1}{2}\delta^{ij}. \tag{3.3}$$

F_π is the technipion decay constant.

This Lagrangian is symmetric under the transformation $U \to AUB^\dagger$ where A and B are elements of $SU(N)_L$ and $SU(N)_R$, respectively. We can obtain the low energy limit of this by expanding U. The lowest order term is $\frac{1}{2}(\partial_\mu \phi^i)(\partial^\mu \phi^i)$ which is invariant under $SU(N)_V$, the subgroup of $SU(N)_L \times SU(N)_R$ in which $A = B$. We can verify that the constant F_π is indeed the technipion decay constant by deriving the lowest order Nöether currents of (3.1). The left- and right-handed currents are

$$\begin{aligned} J_L^{i\mu} &= \tfrac{iF_\pi^2}{4}\mathrm{Tr}\left[(\partial^\mu U^\dagger)\Lambda^i U - U^\dagger \Lambda^i (\partial^\mu U)\right] \\ J_R^{i\mu} &= \tfrac{iF_\pi^2}{4}\mathrm{Tr}\left[(\partial^\mu U)\Lambda^i U^\dagger - U\Lambda^i (\partial^\mu U^\dagger)\right]. \end{aligned} \tag{3.4}$$

The vector and axial vector currents are linear combinations of these,

$$J_{V,A}^\mu = J_R^\mu \pm J_L^\mu. \tag{3.5}$$

We can expand U and $U^\dagger$ and obtain these currents to lowest non-vanishing order in $1/F_\pi$. This gives

$$\begin{aligned} J_V^{i\mu} &= 2i\mathrm{Tr}\left[(\partial^\mu \phi)\Lambda^i \phi - \phi \Lambda^i (\partial^\mu \phi)\right] \\ J_A^{i\mu} &= -F_\pi (\partial^\mu \phi^i). \end{aligned} \tag{3.6}$$

Here ϕ is $\phi^i \Lambda^i$. Since the technipions are pseudoscalars, we can see that $J_V^{i\mu}$ is a vector (it has an even number of pseudoscalars) while $J_A^{i\mu}$ is an axial vector.

The definition of F_π involves the matrix element of the axial vector current between the vacuum and a one pion state. The vector current matrix element is 0, again because of the even number of technipion fields it contains. We can compute the axial vector matrix element from (3.6). We get

$$\langle 0|J_A^{i\mu}(0)|\phi^j(p)\rangle = iF_\pi p^\mu \delta^{ij}. \tag{3.7}$$

This is exactly the definition of F_π, and so we see that we were correct in identifying the constant in (3.1) as F_π. Thus (3.1) is an acceptable start for our effective

Lagrangian.

Since there are no techniquark mass terms to *explicitly* break chiral symmetry (unlike in QCD), the symmetry that's spontaneously broken is an exact one, and so the Nambu–Goldstone bosons remain massless. We will not add mass terms at this stage. Once we gauge the standard model symmetry, the Nambu–Goldstone bosons will acquire mass from strong and electroweak interactions. Before we gauge the Lagrangian, however, we must add another part to it. The Lagrangian (3.1) does not allow for a transition from an even number of technipions to an odd number, or vice versa. But we will be interested in, for example, $P^{0\prime} \to gg$, which involves such a transition. The Lagrangian describing such transitions is due to Wess and Zumino [22], and to Witten [23]. Its source is the Adler–Bell–Jackiw [24] anomaly.

To describe the Adler–Bell–Jackiw anomaly, we start with a Lagrangian containing fermions with a global chiral symmetry which may be explicitly broken by fermion mass terms. In particular,

$$\mathcal{L} = \overline{\psi}(i\,\partial\!\!\!/ - m)\psi \tag{3.8}$$

contains an $SU(N)_L \times SU(N)_R$ chiral symmetry in the limit $m \to 0$. This approximate symmetry leads to the classical identities

$$\partial_\mu J^\mu = 0 \tag{3.9}$$

and

$$\partial_\mu J_5^\mu = 2imJ_5, \tag{3.10}$$

where $J^\mu = \bar{\psi}\gamma^\mu\psi$, $J_5^\mu = \bar{\psi}\gamma^\mu\gamma_5\psi$, and $J_5 = \bar{\psi}\gamma_5\psi$. By applying these identities and others to Green functions such as $\langle 0|T(J^\mu(x)J^\nu(y)J_5^\lambda(z))|0\rangle$ we can obtain Ward–

(a) (b)

Figure 3.1. Triangle diagrams leading to the Adler–Bell–Jackiw anomaly

Takahashi [25] identities. The main ones that we shall be concerned with here involve

$$T^{\mu\nu\lambda}(k_1,k_2,q) = i\int d^4x_1 d^4x_2 \langle 0|T(J^\mu(x_1)J^\nu(x_2)J_5^\lambda(0))|0\rangle e^{ik_1x_1+ik_2x_2} \qquad (3.11)$$

and

$$T^{\mu\nu}(k_1,k_2,q) = i\int d^4x_1 d^4x_2 \langle 0|T(J^\mu(x_1)J^\nu(x_2)J_5(0))|0\rangle e^{ik_1x_1+ik_2x_2}. \qquad (3.12)$$

They are

$$k_1^\mu T_{\mu\nu\lambda} = k_2^\nu T_{\mu\nu\lambda} = 0 \qquad (3.13)$$

and

$$q^\lambda T_{\mu\nu\lambda} = 2mT_{\mu\nu}. \qquad (3.14)$$

We can calculate these perturbatively. The relevant Feynman diagrams are shown in Figure 3.1. Here is where problems begin to arise. The diagrams have a superficial linear divergence. That is, they contain linearly divergent terms, but these terms will cancel each other leaving a finite result. The leftover finite part, however, depends on the definition of the loop momenta. In the first diagram, for example, we can assign the momenta (clockwise from upper left) $(l-k_1, l, l+k_2)$,

or $(l, l+k_1, l+k_1+k_2)$, or any number of other ways. These different momentum assignments are related by a shift in the integration variable l. Because of the linear divergence, such a shift in the integration variable changes the value of the integral. Hence we have an ambiguity[1] in our calculation of $T^{\mu\nu\lambda}$.

We could hope to resolve this ambiguity by appealing to the Ward–Takahashi identities to choose some convention as the correct one. It turns out, however, that there is no momentum assignment that is consistent with *both* of the Ward–Takahashi identities, (3.13) and (3.14). Hence one or both of these identities are violated. Such violations of classical conservation laws in a quantized theory are called anomalies, and this particular type (arising from fermion triangle diagrams) is called an Adler–Bell–Jackiw anomaly. It turns out that such anomalies are present only in calculations of Green functions involving the axial vector current, J_5^μ. Therefore it is customary to label the momenta in such a way that the vector Ward–Takahashi identity (3.13) is preserved while the axial vector one (3.14) is not. The new Ward–Takahashi identities read

$$k_1^\mu T_{\mu\nu\lambda} = k_2^\nu T_{\mu\nu\lambda} = 0 \tag{3.15}$$

and

$$q^\lambda T_{\mu\nu\lambda} = 2mT_{\mu\nu} - \frac{1}{2\pi^2}\epsilon_{\mu\nu\rho\sigma}k_1^\rho k_2^\sigma. \tag{3.16}$$

Wess and Zumino [22] used these anomalous Ward–Takahashi identities as the starting point for deriving a Lagrangian for the strongly interacting pseudoscalars of QCD (π's, K's, and η's). The resulting Lagrangian contains interactions between five

[1] In dimensional regularization (discussed in Chapter 6) a shift in the integration variable is allowed, but there is an ambiguity in the definition of γ_5 in an arbitrary number of dimensions. In the end we have the same freedom to choose which Ward–Takahashi identities to keep and which to give up.

pseudoscalars, and between one or three pseudoscalars and photons.

Witten [23] derived the same Lagrangian years later from a very different point of view. Witten argued that the Lagrangian (3.1) actually contains more symmetry than the underlying theory, QCD. An additional symmetry is $U \leftrightarrow U^\dagger$, which is equivalent to $\phi^i \leftrightarrow -\phi^i$. This symmetry conserves the quantity $(-1)^{N_B}$ where N_B is the number of bosons. Witten set out to construct a Lagrangian that violated this symmetry while preserving all the symmetries of QCD. It turns out that such a Lagrangian cannot be constructed in closed form in four dimensions. Witten constructed his Lagrangian in a five dimensional space with four dimensional Minkowski space as its boundary. The coefficient of this Lagrangian is determined up to an arbitrary integer by topological arguments, and this integer can be shown to equal the number of colors in the underlying theory, N in $SU(N)$. The result for the action is

$$\Gamma(U) = -\frac{iN}{240\pi^2}\int d\Sigma^{ijklm}\mathrm{Tr}\left[U^\dagger\frac{\partial U}{\partial y^i}U^\dagger\frac{\partial U}{\partial y^j}U^\dagger\frac{\partial U}{\partial y^k}U^\dagger\frac{\partial U}{\partial y^l}U^\dagger\frac{\partial U}{\partial y^m}\right], \qquad (3.17)$$

where $d\Sigma^{ijklm}$ is the hypersphere measure in the five-dimensional space. Expanding U to lowest order gives

$$\mathcal{L} = \frac{2N}{15\pi^2 F_\pi^5}\epsilon^{\mu\nu\alpha\beta}\mathrm{Tr}(\phi\,\partial_\mu\phi\,\partial_\nu\phi\,\partial_\alpha\phi\,\partial_\beta\phi). \qquad (3.18)$$

If we were interested in constructing an effective Lagrangian for only the technipions, we might quit here. However, we are interested mainly in describing the interactions between technipions and gluons and between technipions and ordinary fermions. The $SU(N)_L \times SU(N)_R$ symmetry contains $SU(3)_V$ as a subgroup. This is exactly the symmetry of QCD. In order to describe the interactions between technipions and gluons, we must gauge this subgroup.

3.2. Gauging the Effective Lagrangian

The ordinary (non-anomalous) part of the Lagrangian can be gauged in a straightforward manner. We select the subgroup of the chiral symmetry group that we want to gauge, and introduce a covariant derivative to replace the ordinary derivative. The covariant derivative contains new vector fields, which are our gauge fields, and we define the transformation properties of this field so that the new Lagrangian is invariant under a local gauge transformation. A gauge transformation is described by a collection of space-time dependant parameters, and generator matrices. We can write these as

$$\varepsilon_{L,R} = \varepsilon^{\sigma}(x)\Lambda^{\sigma}_{L,R} \tag{3.19}$$

where $\varepsilon^{\sigma}_{L,R}$ are arbitrary infinitesimal functions, Λ^{σ} are linear combinations of the Λ^{i}'s, and σ runs from 1 to the number of generators we wish to gauge, $2N^2 - 2$ at most. The left-handed generators are assumed to commute with the right-handed generators. Many of the Λ^{σ}'s can be 0 for L or R. We can also define

$$G_{L,R\mu} = \sum_{\sigma} g_{\sigma} G^{\sigma}_{\mu} \Lambda^{\sigma}_{L,R}. \tag{3.20}$$

The subscript on g reflects the fact that we are free to gauge several subgroups which may have different coupling constants. G^{σ}_{μ} are the gauge fields. Notice that the same gauge fields occur in both G_L and G_R.

Our locally invariant Lagrangian will be

$$\mathcal{L} = \frac{F_{\pi}^2}{4}\mathrm{Tr}(D_{\mu}U)(D^{\mu}U)^{\dagger}, \tag{3.21}$$

where

$$\begin{aligned} D_{\mu}U &= \partial_{\mu}U + iG_{L\mu}U - iUG_{R\mu} \\ (D_{\mu}U)^{\dagger} &= \partial_{\mu}U^{\dagger} - iU^{\dagger}G_{L\mu} + iG_{R\mu}U^{\dagger}. \end{aligned} \tag{3.22}$$

We must define the transformation properties of the gauge fields such that the Lagrangian is invariant under a local gauge transformation. Under such a transformation, $U \rightarrow AUB^{\dagger}$, where A and B are elements of $SU(N)_L$ and $SU(N)_R$ respectively, are space-time dependant, and take on the form

$$e^{i\epsilon_{L,R}(x)} \tag{3.23}$$

By making an infinitesimal gauge transformation, one can show that G_μ^σ must transform as

$$G_\mu^\sigma \rightarrow G_\mu^\sigma - \frac{1}{g_\sigma}\partial_\mu \epsilon^\sigma + f^{\sigma\tau\rho}\epsilon^\tau G_\mu^\rho. \tag{3.24}$$

Next we'll see what this means in the case where we gauge the QCD subgroup for the one family technicolor model. First we'll describe the technipion spectrum of the one family model. In this model, we have eight technifermions,

$$(U^r, U^g, U^b, N, D^r, D^g, D^b, L). \tag{3.25}$$

The U and D techniquarks fall into $SU(3)_c$ triplets, while N and L are $SU(3)_c$ singlets. The chiral symmetry is $SU(N)_L \times SU(N)_R$. Hence the generators of $SU(3)_c$ (a subset of the generators of $SU(8)_L \times SU(8)_R$) look like

$$\left(\begin{array}{c|c|cc} T^a & & & \\ \hline & 0 & & \\ \hline & & T^a & \\ \hline & & & 0 \end{array}\right) \tag{3.26}$$

where T^a are the $SU(3)$ generator matrices. We'll continue to use letters in the middle of the alphabet $(i, j, k, ...)$ for $SU(8)$ Lie algebra indices, and letters at the beginning $(a, b, c, ...)$ for $SU(3)$ indices. When necessary, we'll use Greek indices with $SU(2)$

Table 3.1. The technipion spectrum in a one family technicolor model

$P_8^{\pm}, P_8^0$	$\bar{Q}\gamma_5 T^a \sigma^\alpha Q$	$(8,3)$
$P_8^{0'}$	$\bar{Q}\gamma_5 T^a Q$	$(8,1)$
P_3^α	$\bar{Q}\gamma_5 \sigma^\alpha L$	$(\bar{3},3)$
$\bar{P}_3^\alpha$	$\bar{L}\gamma_5 \sigma^\alpha Q$	$(3,3)$
P_3	$\bar{Q}\gamma_5 L$	$(\bar{3},1)$
$\bar{P}_3$	$\bar{L}\gamma_5 Q$	$(3,1)$
$\Pi^{\pm,0}$	$\bar{Q}\gamma_5 \sigma^\alpha Q + \bar{L}\gamma_5 \sigma^\alpha L$	$(1,3)$
$P^{\pm,0}$	$\bar{Q}\gamma_5 \sigma^\alpha Q - 3\bar{L}\gamma_5 \sigma^\alpha L$	$(1,3)$
$P^{0'}$	$\bar{Q}\gamma_5 Q - 3\bar{L}\gamma_5 L$	$(1,1)$

generators. The 63 pseudo-Nambu–Goldstone bosons can be grouped according to their $SU(3)_c \times SU(2)_L \times U(1)_Y$ representations. The result is displayed in Table 3.1.

The left column of Table 3.1 contains the names we'll be using for the technipions. The middle column gives the techniquark composition of the technipions, with

$$Q = \begin{pmatrix} U \\ D \end{pmatrix}^{r,g,b} \qquad \text{and} \qquad L = \begin{pmatrix} N \\ E \end{pmatrix}. \tag{3.27}$$

The final column gives the dimension of the representations that each technipion falls into under $SU(3)_c$ and $SU(2)_L$, respectively. One can count these and see that there are 63 of them. The ones denoted $\Pi^{\pm,0}$ are eaten by the $W^\pm$ and Z, and will not be a part of the spectrum in the end.

Now we're ready to gauge the $SU(3)_c$ subgroup of this theory. The subgroup we wish to gauge is a vector subgroup, which is a subgroup of $SU(8)_L \times SU(8)_R$ in which the left and right handed transformations are the same. That is,

$$U \to AUA^\dagger, \qquad U^\dagger \to AU^\dagger A^\dagger. \tag{3.28}$$

In terms of Equations (3.19) and (3.20), which define $\varepsilon_{L,R}$ and $G^{\mu}_{L,R}$, the QCD subgroup corresponds to choosing $\Lambda^a_L = \Lambda^a_R$, with a running from 1 to 8 and Λ^a taking on the form of (3.26). We use a as our superscript now, since these generators are $SU(3)$ generators. There is only one coupling constant, which is just the strong coupling constant, which we will continue to denote g. For the vector case, $G_{L\mu} = G_{R\mu}$ and we can rewrite the covariant derivative

$$\begin{aligned} D_\mu U &= \partial_\mu U + ig[G_\mu, U] \\ D_\mu U^\dagger &= \partial_\mu U^\dagger - ig[U^\dagger, G_\mu], \end{aligned} \tag{3.29}$$

where $G_\mu = G^a_\mu \Lambda^a$.

The normalization of the generators in (3.26) and (3.29) is not the same as we originally defined it in (3.3). This is necessary in (3.29) so that g here is the same as the strong coupling constant defined in Chapter 2. The correct normalization is obtained by deriving the transformation properties of the gluon fields and comparing them to the gluon fields obtained from gauging the $SU(3)_c$ quark symmetry as in Chapter 2. The effective technipion Lagrangian with QCD is just (3.21) with the covariant derivative of (3.29).

The fact that the gauge fields in our covariant derivative occur only in commutators is significant. Setting $U = U^\dagger = I$ in our covariant derivatives (i.e., extracting the lowest order term) yields 0, since the generators in G_μ all commute with the identity matrix, I. This is a consequence of the vector nature of the subgroup we gauged. That is, it arose because $\Lambda^a_L = \Lambda^a_R$. If this had not been the case, then setting $U = I$ in (3.29) would leave a term containing only G_μ, with the coefficient proportional to the coupling constant. Evaluating our effective Lagrangian (3.21) with $U = I$ would then yield an easily calculable mass for the gauge bosons. This should be expected.

The technicolor condensate leaves only the vector symmetry intact. If we had gauged some non-vector symmetry, we would expect the symmetry to be broken, resulting in massive gauge bosons. This is exactly what happens to the $SU(2)_L \times U(1)_Y$ electroweak symmetry.

Gauging the anomalous part of the Lagrangian is not as straightforward a task. This is because it is not given in a closed four-dimensional form, and so we cannot substitute a covariant derivative with a four-dimensional vector field for the ordinary five-vector derivative. Instead, one can gauge (3.17) by making a gauge transformation, adding terms that will cancel the new terms generated by the transformation, and repeating the process until, if one is lucky, the process closes and a gauge invariant form is reached. One is, in fact, lucky in this case. If we gauge the entire chiral symmetry [23, 26], the result is that the action (3.17) must be replaced by

$$\tilde{\Gamma}(U, G_L, G_R) = \Gamma(U) + \frac{N}{48\pi^2} \int d^4x \epsilon_{\mu\nu\alpha\beta} Z^{\mu\nu\alpha\beta}, \tag{3.30}$$

where

$$\begin{aligned}
Z^{\mu\nu\alpha\beta} = & -\mathrm{Tr}\left[G_L^\mu U_L^\nu U_L^\alpha U_L^\beta + (L \to R)\right] \\
& + i\mathrm{Tr}\left\{\left[(\partial^\mu G_L^\nu G_L^\alpha + G_L^\mu \partial^\nu G_L^\alpha)\right] U_L^\beta + (L \to R)\right\} \\
& - i\mathrm{Tr}\left[(\partial^\mu G_L^\nu)(\partial^\alpha U) G_R^\beta U^\dagger - (\partial^\mu G_R^\nu)(\partial^\alpha U^\dagger) G_L^\beta U\right] \\
& - i\mathrm{Tr}\left[G_R^\mu U^\dagger G_L^\nu U U_R^\alpha U_R^\beta - G_L^\mu U G_R^\nu U^\dagger U_L^\alpha U_L^\beta\right] \\
& - \frac{i}{2}\mathrm{Tr}\left[G_L^\mu U_L^\nu G_L^\alpha U_L^\beta - (L \to R)\right] \\
& - \mathrm{Tr}\left[G_L^\mu G_L^\nu G_L^\alpha U_L^\beta + (L \to R)\right] \\
& - \mathrm{Tr}\left\{\left[(\partial^\mu G_R^\nu) G_R^\alpha + G_R^\mu (\partial^\nu G_R^\alpha)\right] U^\dagger G_L^\beta U\right. \\
& \quad \left. - \left[(\partial^\mu G_L^\nu) G_L^\alpha + G_L^\mu (\partial^\nu G_L^\alpha)\right] U G_R^\beta U^\dagger\right\}
\end{aligned} \tag{3.31}$$

$$
\begin{aligned}
&-\mathrm{Tr}\left(G_L^\mu U G_R^\nu U^\dagger G_L^\alpha U_L^\beta + G_R^\mu U^\dagger G_L^\nu U G_R^\alpha U_R^\beta\right) \\
&-i\mathrm{Tr}\left(G_R^\mu G_R^\nu G_R^\alpha U^\dagger G_L^\beta U - G_L^\mu G_L^\nu G_L^\alpha U G_R^\beta U^\dagger\right. \\
&\quad \left.+\frac{1}{2} G_R^\mu U^\dagger G_L^\nu U G_R^\alpha U^\dagger G_L^\beta U\right) \\
&+ir\mathrm{Tr}\left\{\left[(\partial^\mu G_L^\nu + iG_L^\mu G_L^\nu\right] U \left[(\partial^\alpha G_R^\beta + iG_R^\alpha G_R^\beta\right] U^\dagger\right\}.
\end{aligned}
$$

$U_L^\mu = (\partial^\mu U)U^\dagger$, and $U_R^\mu = U^\dagger(\partial^\mu U)$. r is a constant which is undetermined by gauge invariance alone. We require parity conservation, however, and this constrains r to be 0.

Making a gauge transformation on the Wess–Zumino–Witten action gives

$$
\begin{aligned}
\delta\tilde{\Gamma} = -\frac{N}{24\pi^2}\int d^4x \epsilon_{\mu\nu\alpha\beta}\mathrm{Tr}\left\{\varepsilon_L\left[(\partial^\mu A_L^\nu)(\partial^\alpha A_L^\beta)\right.\right. \\
\left.\left.-\frac{i}{2}\partial^\mu(A_L^\nu A_L^\alpha A_L^\beta)\right]\right\} - (L \to R). \qquad (3.32)
\end{aligned}
$$

Our Lagrangian is not invariant unless this vanishes. It does, in fact, vanish provided

$$
\mathrm{Tr}(\Lambda_L^\sigma)^3 = \mathrm{Tr}(\Lambda_R^\sigma)^3. \qquad (3.33)
$$

But this is just the normal condition for canceling anomalies in the underlying (quark) theory. Hence the Lagrangian (3.30) is invariant under a local gauge transformation, provided the symmetry we gauge is not anomalous. Vector theories such as QCD are not anomalous, so (3.30) is invariant under a QCD gauge transformation. For QCD we choose $G_{L\mu}$ and $G_{R\mu}$ just as we did when we gauged the ordinary part of the Lagrangian.

At this point we've constructed almost all the Lagrangian we need for our purpose. We can now extract the interaction terms we need. In particular, we need terms involving the technipions $P^{0'}$ and $P_8^{0'}$. We will not derive them here, but they

are contained in Appendix A. Instead, we will now turn our attention to the question of technipion masses.

3.3. Technipion Masses

We have not included mass terms for the technipions. If they were true Nambu–Goldstone bosons, they would, in fact, be massless. But the chiral symmetry which is broken by the technifermion condensate is not an exact symmetry. There are three ways in which the symmetry is explicitly broken, and each one contributes mass to some or all of the technipions. First, we have gauged the QCD subgroup of $SU(8) \times SU(8)$. This will lead to masses for the colored technipions. Second, we have also gauged (although we haven't shown it here) the electroweak subgroup. This will lead to masses for charged technipions. Finally, we assume that there is some sort of extended technicolor theory. This will contribute to masses for all the technipions.

The calculation of masses [27] for pseudo-Nambu–Goldstone bosons is done by following the work of Dashen. He calculated contributions to the masses of ordinary pions due to QED and weak interactions, for example. The derivation here is a combination of Dashen's work and the work in technicolor of Peskin and Preskill. Peskin and Preskill [28] begin by searching for the true vacuum of the theory. Ignoring the explicit breaking of chiral symmetry, the lowest energy state is highly degenerate. Denote by T^i and X^i the vector and axial vector generators respectively of the chiral symmetry. The vector generators commute with the chirally symmetric Hamiltonian while the axial ones don't, due to the spontaneous symmetry breaking. We will label a member of the degenerate vacuum states $|\Omega\rangle$. Since this will be invariant under

vector transformations,

$$T^i|\Omega\rangle = 0. \tag{3.34}$$

On the other hand, axial transformations will transform one vacuum state into another. We can define one of the degenerate vacua to be $|\Omega_0\rangle$ and define all the other vacua by the axial vector transformation that takes $|\Omega_0\rangle$ into them, which we can denote by the parameters α^i. When we introduce a new term in the Hamiltonian which explicitly breaks chiral symmetry, we find that the energies of the various vacua are shifted. This shift is given by

$$\Delta E = -\frac{1}{2}\sum_{\Lambda}\int d^4x D^{\mu\nu}(x)\langle\Omega(\alpha^i)|T(J^{\Lambda}_{\mu}(x)J^{\Lambda}_{\nu}(0))|\Omega(\alpha^i)\rangle \tag{3.35}$$

for a symmetry breaking of the form $\delta\mathcal{L} = J^{\Lambda}_{\mu}A^{\Lambda\mu}$. The vacuum $|\Omega(\alpha^i)\rangle$ is that vacuum obtained by starting with the vacuum $|\Omega_0\rangle$ and performing a transformation specified by the parameters α_i. $D^{\mu\nu}$ is the gluon propagator. The index Λ represents all the gauged generators. and the coupling constants are absorbed into J.

This energy shift will depend on which of the degenerate vacua we use. To find the true vacuum, we minimize ΔE,

$$\frac{\partial(\Delta E)}{\partial\alpha^i} = 0. \tag{3.36}$$

Using the true vacuum, $|0\rangle$, we can calculate the technipion mass matrix from current algebra. The result is

$$m^2_{ij} = \frac{1}{F_\pi}\langle 0|\left[Q^i,\left[Q^j,\delta H\right]\right]|0\rangle \tag{3.37}$$

where $Q^i = \int d^3x J^{i0}_A$ is the charge associated with the axial current, and δH is the Hamiltonian used to generate ΔE. It can also be shown, however, that

$$\frac{\partial^2}{\partial\alpha^i\partial\alpha^j}\Delta E\bigg|_{|0\rangle} = \langle 0|\left[Q^i,\left[Q^j,\delta H\right]\right]|0\rangle. \tag{3.38}$$

The left-hand side of (3.38) can be reduced to a function of group generators, which can be calculated, times a matrix element which depends only on technicolor, and so can be estimated from the corresponding quantity in QCD. The result is

$$m_{ij}^2 = \frac{1}{4\pi} M^2 \left\{ \sum_{\Lambda} \mathrm{Tr} \left([\Lambda_T, [\Lambda_T, X^i]] X^j - [\Lambda_X, [\Lambda_X, X^i]] X^j \right) \right\}. \tag{3.39}$$

The index T on Λ denotes a vector generator, while the index X denotes an axial vector generator. That is, each gauged generator Λ is a sum of a vector and an axial vector generator, denoted Λ_T and Λ_X. Also,

$$M^2 = \frac{4\pi}{F_\pi^2} \int d^4x D^{\mu\nu}(x) \langle 0 | T \left(J_\mu^T(x) J_\nu^T(0) - J_\mu^X(x) J_\nu^X(0) \right) | 0 \rangle, \tag{3.40}$$

where superscripts T and X denote vector and axial vector currents. M has been calculated in QCD, and its value is $.29 m_\rho$. Furthermore, in the large N limit, the ratio

$$\frac{\sqrt{N} M}{f_\pi} \tag{3.41}$$

is constant. From the QCD values, we get about 8. This gives us M for technicolor around 500 GeV. The other factors depend on the representation of the technipions in $SU(3)$. For the octets, we get $m(P_8) = (3\alpha_s)^{1/2} 500$ GeV ≈ 240 GeV. For the triplets we get $m(P_3) = \left(\frac{4}{3}\alpha_s\right)^{1/2} 500$ GeV ≈ 160 GeV.

The $P^\pm$ also obtain mass in a similar manner. This time, however, it is from the electroweak sector of the model, rather than QCD. As a result, the mass is much smaller, around 2 to 10 GeV. The P^0 and $P^{0'}$ are still massless at this point. Extended technicolor will give these particles masses, and will enhance the mass of the $P^\pm$. We will discuss extended technicolor consequences next.

3.4. Effects of Extended Technicolor

Extended technicolor was introduced as a way of coupling technifermions to ordinary fermions. In the process, ETC provides four-fermion couplings among ordinary fermions and among technifermions. The effects of this on the technipions is twofold. First, ETC gives couplings between the technipions and ordinary fermions, i.e., Yukawa couplings. Second, it contributes to the masses of the technipions.

The couplings of technipions to ordinary fermions due to ETC is not closely predicted unless we assume a particular ETC model. We won't do this, since, as already mentioned, there is no completely satisfactory ETC model. We can, however, make estimates with a few reasonable assumptions. These estimates are based on the fact that the technipions are the technicolor analogue of the Higgs, and such estimates are supported by ETC models.

The Higgs couplings to fermions are proportional to m_f/v, where m_f is the fermion mass, and v is again the vacuum expectation value (VEV) of the neutral Higgs field. This relationship holds because the coupling of the Higgs is linked to the "coupling" of the VEV. That is, the neutral Higgs field ϕ is related to the Higgs particle H by

$$\phi = H + v. \tag{3.42}$$

As a result, the coupling of any particle to the Higgs is the same as its coupling to the VEV, v. Since the coupling of a fermion to v is, by design, m/v, so is its coupling to the Higgs particle.

The same is true of technipions and the technifermion condensate. The VEV is $\langle 0|\bar{\Psi}\Psi|0\rangle$ while the technifermion content of a technipion is of the form $\bar{\Psi}\gamma_5\Psi$. When

we couple either of these to ordinary fermions, the γ_5 difference can be reconciled by a Fierz transformation, and so we expect the couplings of technipions to fermions to be $\sim m_f/F_\pi$. The exact constant of proportionality will be model dependent, but this gives us an estimate.

This estimate has been shown to hold in ETC models, such as the "monophagic" models [29] constructed by Ellis et al. In these models, all of the ordinary fermions of a particular charge get their masses from the same technifermion condensate. The advantage to such a model is that fermion couplings to neutral technipions are flavor independent. This suppresses flavor changing neutral currents due to technipion exchange. (The FCNCs due to ETC gauge boson exchange are still present.) In the models of Ellis et al., the proportionality constants are numbers close to 1, like $\sqrt{3}$ and $\sqrt{1/3}$.

Therefore, we define couplings of fermions to the neutral technipions we're interested in ($P^{0\prime}$ and $P_8^{0\prime}$) by

$$\mathcal{L}_{Pff} = iG\phi\bar{\psi}\gamma_5\psi + iG_8\phi_8^a\bar{\psi}T^a\gamma_5\psi \tag{3.43}$$

where G and G_8 are both proportional to m_f/F_π with proportionality constant of order 1. ϕ and ϕ_8^a stand for the technipions $P^{0\prime}$ and $P_8^{0\prime}$, and γ_5 is included for parity invariance.

Finally we calculate the ETC contribution to technipion masses. These masses arise from four-fermion terms of the form $\bar{\Psi}\Psi\bar{\Psi}\Psi$, where all four fermions are technifermions. The estimates for these masses vary greatly, because of the uncertainties of the exact form of the interaction, the magnitude of the technicolor condensate, and

the ETC scale. We can postulate an interaction of the form

$$\mathcal{L} = \frac{g_{etc}^2}{M_{etc}^2}[\bar{Q}Q\bar{L}L - \bar{Q}\gamma_5\sigma^\alpha Q\bar{L}\gamma_5\sigma L]. \tag{3.44}$$

Going back to (3.37) we see that we need to compute the vacuum expectation value of commutators involving charges and the Hamiltonian derived from (3.44). The charge for the $P^{0'}$ is given by

$$Q = \frac{1}{\sqrt{48}}(Q^\dagger\gamma_5 Q - 3L^\dagger\gamma_5 L) \tag{3.45}$$

(cf. Table 3.1). Computing the commutators gives

$$m_P^2 = \frac{1}{F_\pi}\frac{g_{etc}^2}{M_{etc}^2}\frac{40}{48}\langle 0|\bar{Q}Q\bar{L}L|0\rangle. \tag{3.46}$$

Putting in values for these constants, and assuming $\langle 0|\bar{Q}Q\bar{L}L|0\rangle \sim 3\langle 0|\bar{\Psi}\Psi|0\rangle^2$ we can compute the mass of $P^{0'}$. Most estimates of the light technipion masses are around 2 GeV $\leq m_P \leq$ 45 GeV for the two lightest neutral technipions, and about 5 GeV more for the two light charged ones. (The charged ones, recall, have mass from the electroweak sector of the standard model as well.) Since ETC mass is contributed to m^2 and not m, the contribution to the colored technipions, which are much heavier, will be smaller. Charged technipions have been experimentally ruled out (assuming the decay modes $P^+ \to \tau^+\nu, c\bar{s}$, and $c\bar{b}$ dominate) below 19 GeV, so we don't expect the neutral ones to be any lighter than about 15 GeV.

Finally, one should mention the effects of an enhanced technifermion condensate [19, 21] on the technipion masses. Recall that the possibility of and enhanced condensate was introduced by Appelquist et al. as a means of boosting the extended technicolor scale. This same condensate enhancement can lead to an increase in the technipion masses. In the most extreme case, the masses of the lightest technipions may be as high as a few hundred GeV.

Our survey of the masses and couplings of the technipions is complete. While we haven't actually computed the couplings of all the technipions, we have computed or estimated the couplings of the two particles that we'll be most interested in, the $P^{0\prime}$ and the $P_8^{0\prime}$. In order to be able to discover these particles, we need to know the production cross sections and the decay rates. The conventional wisdom [30] has been that the dominant decay modes of these particles are two-body decays such as gg and $\bar{f}f$. In Chapter 5, we'll see that this assumption was too hasty, and that the three-body decays cannot be ignored. Before we calculate the three-body decay widths, however, we will make a digression into the calculation of gluon polarization sums for processes with many gluons. This will be important when we calculate the decay $P^{0\prime} \to ggg$ for example.

4. GLUON POLARIZATION SUMS

4.1. The Trouble with Gluons

In a non-Abelian gauge theory such as QCD, calculating processes involving many gauge bosons can be a very tedious business. There are two main sources of complication. The first of these is the presence of Feynman vertices containing three or four gauge bosons. These are not present in an Abelian gauge theory such as QED. They often lead to many more diagrams, even in lowest order calculations. The second source of complication is the presence of the longitudinal polarization states of the gauge bosons. While these unphysical states are present in QED as well, they do not couple to any other part of the theory, and so they can be ignored. We can see this by looking at the couplings of ghost particles in QCD. These ghost particles are introduced to cancel longitudinal polarization states. Their only coupling (which is to one gluon) is proportional to the $SU(3)_c$ structure constants, f^{abc}. But these structure constants are characteristic only of non-Abelian gauge theories. In an Abelian gauge theory, this coupling does not exist. Therefore the longitudinal polarization states of the photon in QED do not couple to any other part of the theory, while the same states of the gluon couple to other gluons in QCD.

For internal gluons, these states are canceled by including, for every diagram containing a gluon loop, a corresponding diagram containing a ghost loop. For exter-

nal gluons, there are two standard ways for eliminating the unphysical states. The first is to eliminate the extra states when summing over polarization states. We can simply sum over only the physical states, and leave the unphysical states out of our summation. This is *not* simple, however, since the sum over all four polarization states takes on a much simpler form than the sum over two polarization states. In particular, the four-state sum is

$$\sum_{\lambda=1}^{4} \epsilon_\mu(\lambda,k)\epsilon_\nu(\lambda,k) = -g_{\mu\nu} \tag{4.1}$$

while the two-state sum is

$$\sum_{\lambda=1}^{2} \epsilon_\mu(\lambda,k)\epsilon_\nu(\lambda,k) = -g_{\mu\nu} + (k_\mu n_\nu + k_\nu n_\mu)/k\cdot n + n^2 k_\mu k_\nu/(k\cdot n)^2, \tag{4.2}$$

where k is the gluon momentum, λ is the polarization state, and n can be any four-vector orthogonal to the physical polarization states (i.e., $\epsilon\cdot n = 0$ for $\lambda = 1,2$). The use of (4.2) will eliminate the excess states, but it generates many more terms than (4.1).

Another way of eliminating the unphysical polarization states of external particles is by adding diagrams in which external gluon lines are replaced by ghost lines. One first computes the amplitude with the gluons, and squares it using (4.1). Then one calculates the square of the amplitude for processes in which different combinations of gluon lines are replaced by ghost lines. (Since the only ghost interaction contains two ghosts and one gluon, there will always be an even number of external ghost lines. Ghost lines, like fermion lines, never terminate at a vertex.) These are subtracted from the squared amplitude of the gluon process, and the result is the square of the amplitude for the gluon process, summed only over the physical polarization states.

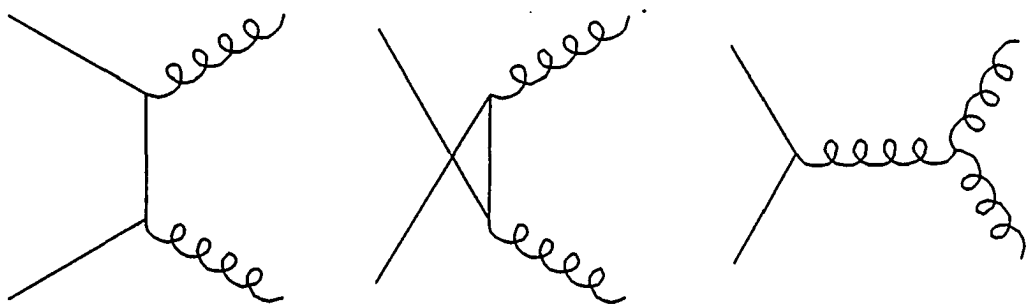

Figure 4.1. Diagrams for the process $gg \rightarrow \bar{q}q$

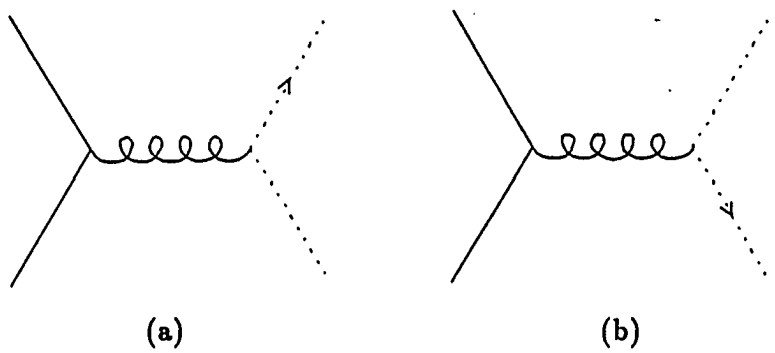

Figure 4.2. Ghost diagrams representing longitudinally polarized gluons in the initial state

As an easy example, consider the process $gg \to \bar{q}q$. The diagrams are given in Figure 4.1. If one chooses to use the polarization sum (4.1), then one needs to also consider the diagrams in Figure 4.2. These two diagrams represent different "processes" (the final state ghosts are not identical; one is a ghost, the other an anti-ghost) and so they are squared separately, not added and then squared. The squares of these two amplitudes are subtracted from the square of the gluon amplitude, and it is this result that is the correct form for the square of the amplitude, summed over the physical polarization states.

4.2. A Case in Which the Sum Can Be Simplified

Georgi et al. [31] noticed that there is a simpler method for dealing with the polarization sum when they calculated charm production at hadron colliders via $gg \to \bar{c}c$. This is exactly the process we just discussed, and we need to examine the same diagrams. We shall call the amplitude (stripped of its external polarization vectors) $T^{\mu\nu}$, and the individual diagrams $T_s^{\mu\nu}, T_t^{\mu\nu}$, and $T_u^{\mu\nu}$. We can compute these, and the result is

$$\begin{aligned} T_s^{\mu\nu} &= \frac{-g^2 f^{abc}}{(p_1+p_2)^2}\bar{u}(p_2)\gamma_\alpha T^c v(p_1)\left[(k_2-k_1)^\alpha g^{\mu\nu}+(2k_1+k_2)^\nu g^{\mu\alpha}\right. \\ &\qquad \left.+(-2k_2-k_1)^\mu g^{\nu\alpha}\right] \\ T_t^{\mu\nu} &= \frac{-ig^2}{(p_2-k_2)^2-m^2}\bar{u}(p_2)T^bT^a\gamma^\nu(\not{p}_2-\not{k}_2+m)\gamma^\mu v(p_1) \qquad (4.3) \\ T_u^{\mu\nu} &= \frac{-ig^2}{(p_2-k_1)^2-m^2}\bar{u}(p_2)T^aT^b\gamma^\mu(\not{p}_2-\not{k}_1+m)\gamma^\nu v(p_1). \end{aligned}$$

If the Ward–Takahashi identities,

$$k_{1\mu}T^{\mu\nu} = k_{2\nu}T^{\mu\nu} = 0, \qquad (4.4)$$

held, then we could use (4.1) for the polarization sum. This is because all the extra terms from (4.2) vanish. The identities do not hold, however, due to the presence of longitudinal gluon couplings in Figure 4.1c. Using conservation of energy, the mass-shell conditions, and the properties of the Dirac matrices and the u and v spinors, we can show that

$$k_{1\mu}T^{\mu\nu} = \frac{-g^2 f^{abc}}{(k_1+k_2)^2}\bar{u}(p_2)\ \not{k}_1 T^c v(p_1)k_2^\nu. \tag{4.5}$$

This is, in fact, just the term in $T_s^{\mu\nu}$ containing k_2^ν. For physical polarization states, this term vanishes, since $\epsilon_\nu(k_2,\lambda)k_2^\nu = 0$. Therefore, we can throw away the offending term in $T_s^{\mu\nu}$ (i.e., the k_2^ν term) without altering the result for the physical polarization states. If we look at $k_{2\nu}T^{\mu\nu}$, we find that we are left with only the k_1^μ term of $T_s^{\mu\nu}$, which can also be discarded for the same reason.

Therefore, if we discard all the terms in $T^{\mu\nu}$ which are proportional to k_1^μ or k_2^ν, we do not alter the amplitude for the physical polarization states, and we obtain an expression which satisfies the Ward–Takahashi identities. Using this expression as our new amplitude, we can sum over all four polarization states using (4.1) without calculating ghost diagrams. This trick can, in fact, be generalized [32]. We will now show this using the Slavnov–Taylor identities [33].

4.3. Simplifying Polarization Sums with the Slavnov–Taylor Identities

Consider a process with n gluons and m other particles (usually fermions). We can write the amplitude (again without the polarization vectors)

$$T_{\mu_1\ldots\mu_n}(k_1,\ldots,k_n;q_1,\ldots,q_m), \tag{4.6}$$

where k_i is the momentum of the ith gluon, μ_i is the Lorentz index associated with the ith gluon, and q_i is the momentum of the ith fermion. (We'll assume the other particles are fermions, although the arguments apply equally well if we have scalars.) Although we do not have the Ward–Takahashi identities, we do have the Slavnov–Taylor identities. The Slavnov–Taylor identities tell us

$$k_1^{\mu_1} T_{\mu_1 \ldots \mu_n} = k_{2\mu_2} S^{(12)}_{\mu_3 \ldots \mu_n} + k_{3\mu_3} S^{(13)}_{\mu_2 \mu_4 \ldots \mu_n} + \ldots + k_{n\mu_n} S^{(1n)}_{\mu_2 \ldots \mu_{n-1}}, \tag{4.7}$$

where $S^{(12)}_{\mu_3 \ldots \mu_n}$ is the amplitude in which the external gluons 1 and 2 have been replaced by ghosts of the same momentum and color, and the other S's are defined similarly. What will enable us to generalize the simplification of the previous section is the fact that every term on the right side of (4.7) is proportional to a gluon momentum with a Lorentz index that matches the index of the corresponding polarization vector. That is, each term is proportional to $k_i^{\mu_j}$, where $i = j$. For this reason, each term on the right vanishes when we contract it with the appropriate polarization vector ($\epsilon \cdot k = 0$).

Let us define a modified amplitude,

$$\tilde{T}_{\mu_1 \ldots \mu_n}(k_1, \ldots, q_m), \tag{4.8}$$

to be the original amplitude stripped of all terms proportional to $k_i^{\mu_i}$ for every i. This term will produce the same results as (4.6) for the physical polarization states. We must see whether

$$k_i^{\mu_i} \tilde{T}_{\mu_1 \ldots \mu_n} \tag{4.9}$$

is 0 for all i (up to n). We know that all terms in (4.9) must take on the form of those in the right side of (4.7). Since $\tilde{T}$ has no terms of that form, we must see if

the contraction with, for example, $k_1^{\mu_1}$ produces any terms of that form. If not, then we can assume (4.9) is 0. In order to produce such terms, $\tilde{T}$ must contain terms proportional to the metric $g_{\mu_1\mu_i}$ $(i \neq 1)$. This will give terms proportional to $k_1^{\mu_i}$. If we can take all the k's to be independent, then no terms proportional to $k_i^{\mu_i}$ are produced. Therefore, terms containing $g_{\mu_1\mu_i}$ cannot be contained in $\tilde{T}$. This is the case if there are fermions in the process. If the process consists solely of gluons, however, then conservation of energy provides a relationship between the momenta; they are not independent.

In the case where there are fermions, therefore, (4.9) is 0. We can use (4.1) for the polarization sum, provided we use $\tilde{T}$ as the amplitude. In the case where there are only gluons, however, this is not necessarily the case. Let's consider a possible term in $\tilde{T}_{\mu_1\ldots\mu_n}$ of the form

$$g_{\mu_1\mu_2} f_{\mu_3\ldots\mu_n}. \tag{4.10}$$

When we contract this with $k_1^{\mu_1}$ we get

$$k_{1\mu_2} f_{\mu_3\ldots\mu_n}. \tag{4.11}$$

It is quite possible for $\tilde{T}$ also to contain a term which, when contracted with $k_1^{\mu_1}$, looks like

$$(k_3 + \ldots + k_n)_{\mu_2} f_{\mu_3\ldots\mu_n}. \tag{4.12}$$

(For simplicity, all the momenta are incoming.) The sum of (4.11) and (4.12) is $-k_{2\mu_2} f_{\mu_3\ldots\mu_n}$, which is an allowed term according to the Slavnov–Taylor identity, (4.7). Therefore we cannot assume that our trick of dropping certain terms from the amplitude T to obtain $\tilde{T}$ will enable us to use the simpler polarization sum (4.1).

In fact, our trick doesn't work for the simplest physical process consisting solely of gluons, $gg \to gg$.

All is not lost, however. We can write one of the gluon momenta in T, say k_n, in terms of the others: $k_n = -(k_1 + ... + k_{n-1})$. Then the other $n-1$ momenta are independent. *After* we make this substitution, we create $\tilde{T}$ the same way as before, by lopping off terms proportional to $k_i^{\mu_i}$. Now the term (4.12) in $k_1^{\mu_1}\tilde{T}_{\mu_1...\mu_n}$ can't exist, because we've replaced $k_{n\mu_2}$ by $-(k_1 + ... + k_{n-1})_{\mu_2}$ and thrown out the $k_{2\mu_2}$ when we defined $\tilde{T}$. Hence $k_1^{\mu_1}\tilde{T}_{\mu_1...\mu_n} = 0$ and we can use the sum over all four polarization states for the first gluon. Similarly, we can use the simpler polarization sum for all of the gluons except the nth one. For the last gluon, we must use the more complicated sum (4.2).

To summarize, we have a prescription for simplifying polarization sums. In the case where there are particles involved which are not gluons, we simply discard all terms in the amplitude proportional to $k_i^{\mu_i}$. The new amplitude will satisfy the Ward–Takahashi identities, instead of the Slavnov–Taylor identities, and we are then able to use the sum over all four polarization states. In the case where we have only gluons, we express the momentum of one gluon in terms of all the others, and then discard terms just as before. We can use the sum over four polarization states for all the gluons except the one we singled out. For this one, we must still use the sum over only two states. In either case, the result is simpler. This will help us when we calculate decays of technipions into three gluons, as we shall see shortly.

We are not the only group to have found ways to simplify the problems of the gluon polarization sum. Another method [34] involves the use of helicity amplitudes instead of tensor amplitudes. This method works for theories with massless fermions

which interact in definite helicity states with the gauge bosons, and for which the axial-vector current is conserved. Still another method [35] embeds the gauge theory in a supersymmetric extension. The advantage of our method over these is in generality. Our method does not require that fermions be massless, and does not require a supersymmetric extension. We only require gauge invariance, a very general condition. Hence, this is the method we shall use in the next chapter when we are faced with the decay $P^{0\prime} \rightarrow ggg$.

5. TREE LEVEL DECAYS OF NEUTRAL TECHNIPIONS

5.1. The Two Body Decays

Based on coupling constant and phase space suppression, it has been believed that the dominant decay modes of technipions would be into two particles. Here, we will examine three body decay modes of the $P^{0\prime}$. Before we do this, however, we will look at the two body modes.

The two body decays will be dominated by $P^{0\prime} \to gg$ and $P^{0\prime} \to \bar{f}f$. Each process involves just one diagram (shown in Figure 5.1) and the amplitudes are given by

$$T_{gg} = 2i\Gamma\epsilon^{\mu\nu\alpha\beta}\delta^{ab}k_{1\alpha}k_{2\beta}\epsilon_{\mu}(1)\epsilon_{\nu}(2) \tag{5.1}$$

and

$$T_{\bar{f}f} = -G_f\bar{u}(p_1)\gamma^5 v(p_2). \tag{5.2}$$

In (5.1), the constant Γ is

$$\Gamma = \frac{-N_{TC}g^2}{16\sqrt{3}\pi^2 F_\pi}, \tag{5.3}$$

where N_{TC} is the number of technicolors (N for an $SU(N)$ gauge group), g is the QCD coupling constant, and $F_\pi = 125$ GeV is the technipion decay constant.

G_f (not to be confused with the Fermi constant G_F) in (5.2) is a constant which will in general depend on extended technicolor physics, which is mostly unknown to

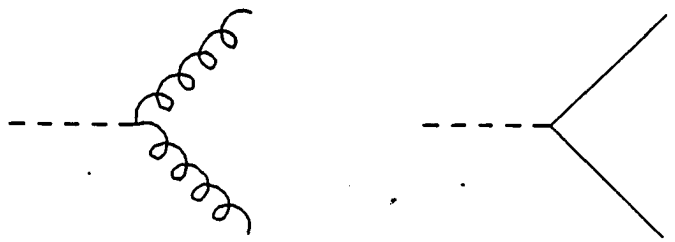

(a) (b)

Figure 5.1. Decays of $P^{0\prime}$ to two gluons (a) and two fermions (b)

us. We expect it, however, to be on the order of m_f/F_π, like the ordinary Higgs, although the coefficient may depend on which fermion we're talking about. For this reason, we believe that the $P^{0\prime}$ will decay mainly into the heaviest possible fermions, when it doesn't decay into gluons. In addition, we assume that the fermionic decays are mainly flavor conserving, since flavor violations here would lead to flavor changing neutral currents elsewhere in the theory.

We can easily calculate the widths of these decay modes, and when we do so we get

$$\Gamma(P^{0\prime} \to gg) = \frac{\Gamma^2 M^3}{2\pi} \tag{5.4}$$

and

$$\Gamma(P^{0\prime} \to \bar{f}f) = \frac{G_f^2}{8\pi}\left(M + 2\frac{m_f^2}{M}\right)\sqrt{1 - \frac{4m^2}{M^2}}, \tag{5.5}$$

where M is the mass of the $P^{0\prime}$, and m_f is the mass of the fermion, f. The fermion width is for a colorless fermion (e.g., the τ lepton). For quarks, we just multiply (5.5) by three. Figure 5.2 shows the relative branching ratios of the fermionic and gluonic decay modes, assuming a one family technicolor model with four technicolors ($N_{TC} =$

4). The coefficient of m/F_π in G_f is assumed to be 1 for each fermion. Changing G_f will affect the decay rate to the corresponding fermion, f, while assuming $N_{TC} \neq 4$ will affect the decay rate to gluons.

We can examine the $P^{0\prime}$ in the mass range from 15 GeV to a few hundred GeV. Since the $P^{\pm}$ have not been found up to 19 GeV, and these are expected to be only about 5 GeV heavier than the $P^{0\prime}$, we expect that the $P^{0\prime}$ cannot be much lighter than 15 GeV. In a theory with an enhanced technifermion condensate, the $P^{0\prime}$ could take on a mass as high as a few hundred GeV. There are few solid experimental constraints, just as there are few for the standard model Higgs. The $P^{0\prime}$ and the Higgs behave similarly.

5.2. The Three Body Decay Amplitudes

Early papers on technicolor phenomenology consider only these two body decays. We decided to consider the three body decays to see whether one could justify neglecting them. We ignore electromagnetic and weak decays such as $P^{0\prime} \to \bar{f}f\gamma$ just as we ignored, for example, $P^{0\prime} \to \gamma\gamma$ in the two body decays. The strong interaction decays will dominate these. There are two such decays to consider, $P^{0\prime} \to ggg$, and $P^{0\prime} \to \bar{q}qg$. The relevant diagrams are given in Figures 5.3 and 5.4. These diagrams are all simple extensions of the diagrams for two body decays except for the diagram consisting of the $P^{0\prime}ggg$ vertex. This vertex is necessary for gauge invariance, and in fact the expression for the vertex can be derived by imposing the Ward–Takahashi identity on the three gluon decay instead of resorting to more complicated methods such as extracting it directly from the Wess–Zumino–Witten Lagrangian.

One thing to notice is the fact that there are no important three body decays

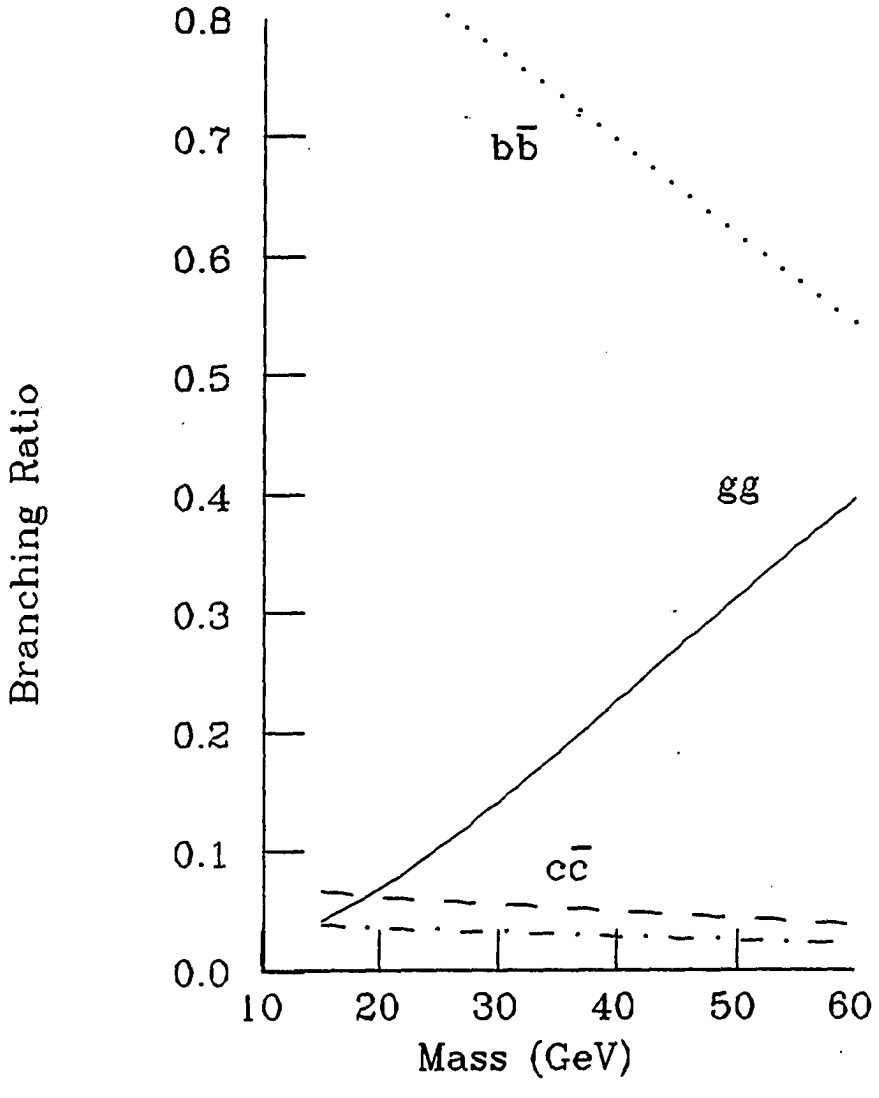

Figure 5.2. Branching ratios for the decays of $P^{0\prime}$, considering only the two body decays

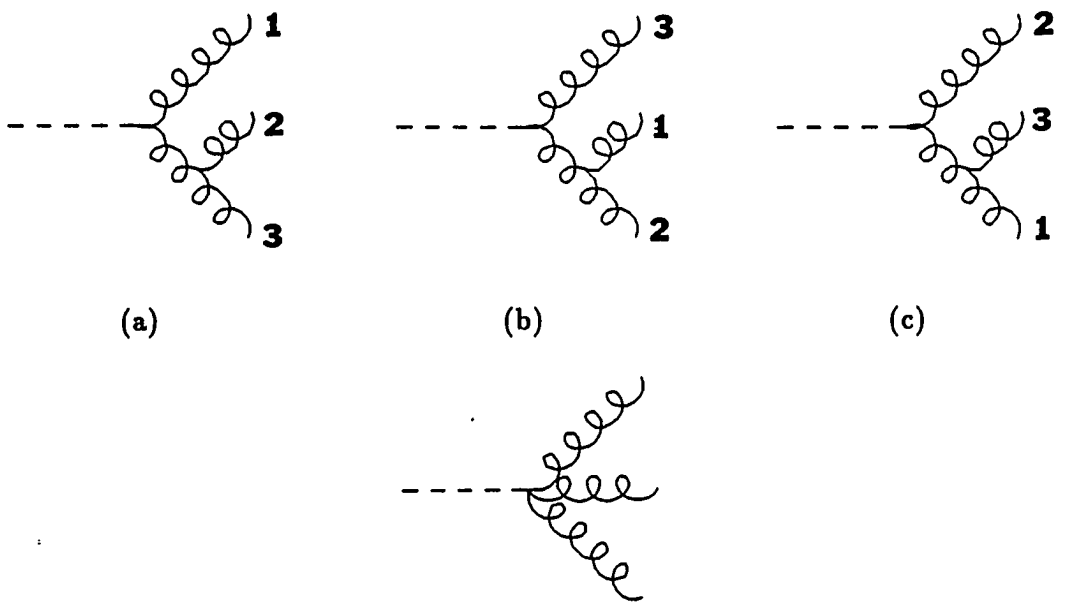

Figure 5.3. Diagrams for the decay $P^{0\prime} \rightarrow ggg$

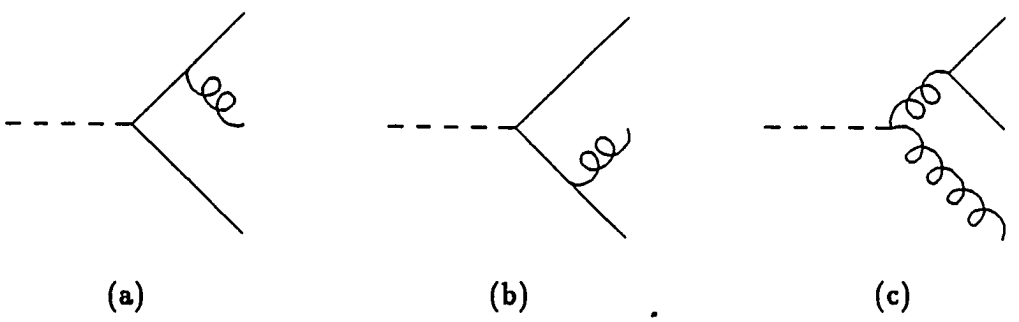

Figure 5.4. Diagrams for the decay $P^{0\prime} \rightarrow \bar{q}qg$

involving leptons. Considering the three body decays will reduce the branching ratio into taus.

We could in principle have many other vertices to consider in these processes. We will restrict ourselves somewhat, however. First, we only consider lowest order corrections in $\alpha_s = g^2/4\pi$. Second, we consider only lowest order in $1/F_\pi$. This means that we stick with operators of mass dimension totaling 5 or less in our Lagrangian. Higher order operators can be created by adding more fields or by adding more derivatives. As an example, we could consider a term such as

$$\phi\bar{\psi}\not{D}\gamma_5\psi \tag{5.6}$$

where D_μ is the usual covariant derivative, $\partial_\mu + igT^aG^a_\mu$, and ϕ and ψ are the $P^{0'}$ and quark fields, respectively. This term meets all the requirements that we need. It is gauge invariant and parity invariant. It also contributes to both two body and three body decays. It is a dimension 5 operator, and so it would be an operator that, within our restrictions, we would have to consider. The fact that fermions are involved, however, indicates that such a vertex would probably only arise in the presence of extended technicolor, and that the coefficient would be proportional to the fermion mass, just as it is for other fermion couplings which arise from ETC. Therefore, the coefficient must go as $1/F_\pi^2$. We will not consider such a term.

The restriction to lowest order in α_s is easily justified. At the energy we will be dealing with, $O(M)$, $\alpha_s \approx .2$ or less. Hence we suspect higher order corrections will be smaller. We should keep in mind, however, that this is exactly the assumption we are testing: whether or not higher order QCD corrections can be ignored. But if the order $O(\alpha_s)$ corrections are small compared to the tree level two body decays, then it is probably safe to assume that further corrections are even smaller.

The restriction to lowest order in $1/F_\pi$ is more complicated. Increasing powers of $1/F_\pi$ will in general be associated with more powers of gluon momenta. In other words, the expansion is really in terms of k/F_π, where k is a typical gluon momentum. For a $P^{0\prime}$ that is not too heavy, $k \ll F_\pi$ and the expansion is justified. For example, for a 30 GeV $P^{0\prime}$, no gluon momentum will be larger than 15 GeV, regardless of the number of gluons. Meanwhile, $F_\pi = 125$ GeV. On the other hand, if we have a greatly enhanced technifermion condensate, the momentum of a typical gluon could be more than 125 GeV. In this case our restriction to lowest order in k/F_π is suspect. We will keep our restriction, however, since abandoning it would make the problem unmanageable. Not only would we open the door to an infinite number of terms, but the coefficients of these terms are *a priori* undetermined. Furthermore, we are encouraged by the fact that the lowest order term in $1/f_\pi$ gives an adequate description of pion decays in QCD, in spite of the fact that $m_\pi > f_\pi$. Hence we will consider only the diagrams of Figures 5.3 and 5.4.

First we consider the decay $P^{0\prime} \to ggg$. Writing out the expressions for the four diagrams gives us (in Feynman gauge, $\xi = 1$)

$$\begin{aligned} T_{3g}^{\mu\nu\lambda} &= \frac{-2g\Gamma f^{abc}}{(k_2+k_3)^2}\epsilon^{\mu\rho\alpha\beta}k_{1\alpha}(k_2+k_3)_\beta\left[(-k_2+k_3)_\rho g^{\nu\lambda}+(-2k_3-\mathrm{k}_2)^\nu g_\rho^\lambda\right. \\ &\qquad \left.+(2k_2+\mathrm{k}_3)^\lambda g_\rho^\nu\right] \\ &\quad +(\text{cyclic permutations}) \\ &\quad +2g\Gamma f^{abc}\epsilon^{\alpha\mu\nu\lambda}(k_1+k_2+k_3)_\alpha, \end{aligned} \tag{5.7}$$

where we've stripped off the polarization vectors for the external gluons. The permutations in (5.7) are two terms like the first one, with cyclic permutations of the momenta and the Lorentz and color indices of the external gluons. The first three

terms correspond to the first three diagrams, while the last term corresponds to the diagram with the $P^{0\prime}ggg$ vertex.

In order to use the simpler form of the gluon polarization sum, we drop terms proportional to k_1^μ, k_2^ν, and k_3^λ, as discussed in the previous chapter. There are two such terms contained in each of the first three terms of $T_{3g}^{\mu\nu\lambda}$, and they are shown in bold print in (5.7).

The next step in calculating the decay rate into three gluons is to square the amplitude and sum over the polarization states and colors of the gluons. The color sum is easily performed using the identity

$$\sum_{a,b,c} f^{abc} f^{abc} = C_2(G)(N^2-1) \tag{5.8}$$

for $SU(N)$. In our case $C_2(G) = N = 3$ (this N is for QCD, not technicolor) but we'll leave it in this form.

Squaring the amplitude and doing the appropriate summations gives us

$$\begin{aligned}
|T_{ggg}|^2 \;=\; & 32g^2\Gamma^2 C_2(G)(N^2-1)\Bigg\{3(k_1\cdot k_2 + k_2\cdot k_3 + k_3\cdot k_1) \\
& +2\left[\frac{(k_1\cdot k_2)^3}{(k_2+k_3)^2(k_3+k_1)^2} + \frac{(k_2\cdot k_3)^3}{(k_3+k_1)^2(k_1+k_2)^2} \right. \\
& \qquad \left. + \frac{(k_3\cdot k_1)^3}{(k_1+k_2)^2(k_2+k_3)^2}\right] \\
& +2\left[\frac{(k_3\cdot k_1)^2 + (k_1\cdot k_2)^2}{(k_2+k_3)^2} + \frac{(k_1\cdot k_2)^2 + (k_2\cdot k_3)^2}{(k_3+k_1)^2} \right. \\
& \qquad \left. + \frac{(k_2\cdot k_3)^2 + (k_3\cdot k_1)^2}{(k_1+k_2)^2}\right] \\
& +3\left[\frac{(k_3\cdot k_1)(k_1\cdot k_2)}{(k_2+k_3)^2} + \frac{(k_1\cdot k_2)(k_2\cdot k_3)}{(k_3+k_1)^2} + \frac{(k_2\cdot k_3)(k_3\cdot k_1)}{(k_1+k_2)^2}\right]\Bigg\}.
\end{aligned} \tag{5.9}$$

We are also considering the process $P^{0\prime} \to \bar{q}qg$. The amplitude for this process

has two parts. One part comes from the Wess–Zumino–Witten Lagrangian and consists of a two gluon decay in which one gluon is off shell and produces a $\bar{q}q$ pair (Dalitz pair production). The other part comes from the two fermion extended technicolor decay in which one of the fermions emits a gluon. These are shown in Figure 5.4. It is apparent that in either case the fermion must couple directly to a gluon. Therefore, none of these decays will involve leptons.

The amplitude is given by

$$\begin{aligned} T^{\mu}_{\bar{q}qg} &= \frac{-2ig\Gamma}{(k_2+k_3)^2-m^2}\epsilon^{\mu\alpha\rho\sigma}k_{1\rho}(k_2+k_3)_\sigma \bar{u}(k_2)\gamma_\alpha T^a v(k_3) \qquad (5.10) \\ &\quad -gG_f\bar{u}(k_2)\left[\frac{\gamma^\mu(\not{k}_1+\not{k}_2+m)}{(k_1+k_2)^2-m^2}-\frac{(\not{k}_1+\not{k}_2+m)\gamma^\mu}{(k_1+k_3)^2-m^2}\right]\gamma_5 T^a v(k_3). \end{aligned}$$

Since the constant G_f is proportional to the fermion mass, we ignore the second term above for light quarks, including it in the rest of the calculation only in the case of the b quark. Each of the two terms satisfies the Ward–Takahashi identities individually, and so we have no worries with the polarization sum. The square of the amplitude is rather lengthy and not very enlightening, and we won't present it here.

Finally, in order to obtain the decay width we must integrate over Lorentz invariant three body phase space.

5.3. Phase Space Integration and the Infrared Divergence

Three body Lorentz invariant phase space takes on the form

$$(2\pi)^4\frac{d^4k_1}{(2\pi)^3}\frac{d^4k_2}{(2\pi)^3}\frac{d^4k_3}{(2\pi)^3}\delta(k_1^2-m_1^2)\delta(k_2^2-m_2^2)\delta(k_3^2-m_3^2)\delta^4(p-k_1-k_2-k_3), \quad (5.11)$$

where m_i is the mass of the ith particle and p is the total four-momentum of the initial state. Using this as our integration measure, we integrate $|T|^2$ over the entire

range of each momentum from $-\infty$ to ∞ (except for the 0th component which is always positive). The first three δ functions put the particles on mass shell, while the last one imposes conservation of energy.

In the three gluon case the three particles are massless, which simplifies the calculation. It also leaves us, however, with the problem of an infrared divergence. A typical term in $|T|^2$ contains, for example, $1/(k_1 + k_2)^2$. If the denominator is zero the integral can diverge. There are two ways that the integral can be zero. The first is if all components of either k_1 or k_2 are zero. This is kinematically allowed only because the gluons are massless. If, say, k_1 is zero, then the denominator is k_2^2, which is also zero. This type of divergence is called a soft gluon divergence. The second way that the denominator can be zero is if the two gluons travel parallel to each other. To see this, we note that if the gluons travel parallel, then the three vector $\mathbf{k}_1$ (the three-momentum) is proportional to $\mathbf{k}_2$. That is, $\mathbf{k}_1 = \alpha \mathbf{k}_2$. Then the zero components of the four momenta must be related similarly: $k_1^0 = \alpha k_2^0$. So

$$(k_1 + k_2)^2 = (1 + \alpha)^2 k_2^2 = 0. \tag{5.12}$$

This divergence is called a collinear divergence, and it is present only because both particles are massless.

While these divergences may seem to lead us to a divergent decay width, they are, in fact, not a fundamental problem with the theory. Rather, they are a reflection of the difference between theoretical wishes and experimental facts. We would like to always know the number of particles produced in any scattering process. It is a kinematic fact, however, that in some cases this is impossible, no matter how good our detectors are. The soft gluon divergence reflects the fact that a gluon with very low energy is undetectable. The collinear divergence reflects the fact that two gluons

traveling parallel are indistinguishable from a single gluon. In both of these cases, a three body process mimics a two body process, and so the distinction between three body processes and two body processes is blurred.

This problem is not peculiar to the process we're looking at, but is a very common occurrence in gauge theory. In general, any process involving a gluon (or photon) and two or more other particles in the final state will suffer from a soft gluon divergence, and any process ending with three or more particles including a gluon or photon and some other massless particle (such as another gluon or a massless quark) may contain a collinear divergence.

The solution to this problem comes about by looking at more than one process simultaneously. In the case at hand, we must look at the combined decay rates for $P^{0\prime} \rightarrow gg$ and $P^{0\prime} \rightarrow ggg$. If we calculate both processes out to the same order in α_s, we find not only the infrared divergence in the three body decay, but also an infrared divergence in the one loop corrections to the two body decay. These will in fact cancel, as we shall see later when we discuss the two body decays to one loop. Hence while both processes are infrared divergent, the sum of the two processes is infrared finite. While it is not possible to specify the decay rate to two gluons or to three gluons, it is possible (to this order in perturbation theory) to specify the combined decay rate to two or three gluons. If we go to the next order, we should run into problems with four gluon decay rates, but the resolution of that problem should be similar.

Of course, if we produce the $P^{0\prime}$ in the laboratory we will see it decay sometimes to two jets and sometimes to three jets, and it is useful to discuss the two decays separately. We can do this by regularizing the infrared divergence in some manner

that reflects our ability to distinguish a three body decay from a two body decay. A straightforward way of doing this is to integrate over less than the full range of three body phase space. In particular, we can impose limits on the invariant mass of any pair of gluons. We base our choice for these limits on the ability of experiments to resolve jets. That is, we need to know how much energy a soft gluon must have before it will produce an identifiable jet, and how large the invariant mass of a two gluon system must be before their fragmentation products are far enough apart to be resolved as separate jets.

5.4. Results of Three Body Decays

Most of the actual details of the phase space integration have been relegated to Appendix B. A few important ones must be mentioned here though. First of all, we used $\alpha_s = .2$ throughout the calculation of Ref. [36]. We took the number of technicolors, N_{TC}, to be 4. (The coupling Γ is directly proportional to both α_s and N_{TC}.) While the number of technicolors is unimportant to the actual symmetry breaking for which we introduced technicolor, there is a certain prejudice for $N_{TC} > 3$. This prejudice arises from the desire for grand unification. If we intend to unify technicolor with QCD at some higher scale, then we want the coupling constants of the two gauge groups to match at that scale. Both theories are assumed to be asymptotically free, and so the couplings decrease as we go to higher energy. Since at low energies the technicolor coupling is stronger, we would like the technicolor coupling constant to run more quickly than that of QCD. This will usually be true if there are more technicolors than colors ($N_{TC} > 3$). We took the coupling G_f to be just m_f/F_π. The other variable involved in the process is the infrared regularization.

We used an invariant mass cutoff of 4 GeV in all gg channels of the three gluon decay and, for massless quarks, in the $\bar{q}q$ channel of the $\bar{q}qg$ decay. For the $\bar{b}bg$ decay, we used an invariant mass cutoff of 7 GeV in the bg and $\bar{b}g$ systems, which corresponds to a gluon "mass" of about 1.7 GeV.

Our results are given in Figure 5.5. We see that for a relatively light $P^{0\prime}$ the $\bar{b}b$ decay mode dominates, but as the $P^{0\prime}$ gets heavier, the three gluon decay dominates. Among the other decay modes, the two gluon mode will typically be the largest. Meanwhile, the $\bar{\tau}\tau$ mode will be quite small. There are several caveats to remember, however, before interpreting this graph too strictly. First, these curves depend on the infrared cutoff chosen during the phase space integration. Second, the choice of a value for α_s is a somewhat tricky business. We in fact varied the cutoff in all these processes and used a running coupling constant for the decay modes involving quarks. (Using a running coupling constant for the three gluon decay mode is not possible because of the requirement of maintaining gauge invariance.) The effects of these modifications can change the branching ratios by at most 50% from what is shown in the graph. Finally, there is the uncertainty in the couplings, G_f, and the uncertainty in N_{TC}, which is contained in the coupling, Γ. Hence Figure 5.5 should not be taken as an exact prediction, but rather, as a guideline to the behavior of the $P^{0\prime}$ that is much different from what was previously believed.

The graph does not go beyond 60 GeV for the $P^{0\prime}$ mass. Since we completed this work, there have been indications [19] that the $P^{0\prime}$ mass may be larger than this. This possibility is treated in the work of Kuo, McKay, and Young [37].

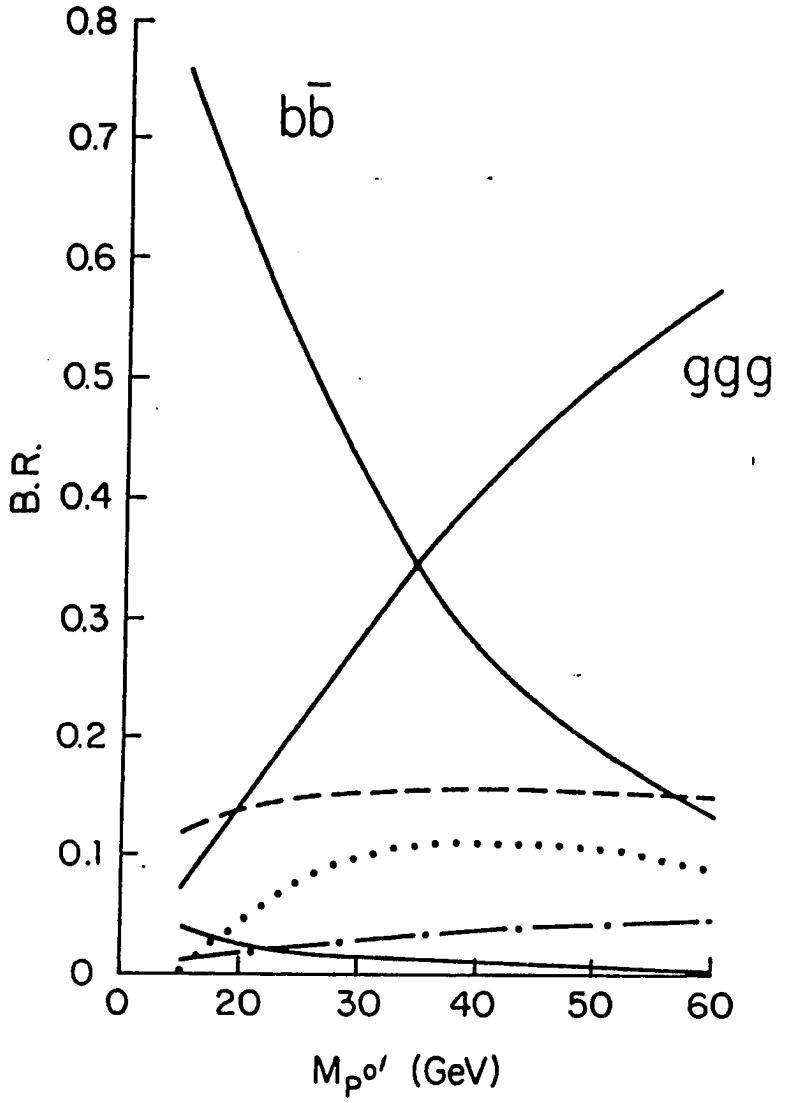

Figure 5.5. Branching ratios of the $P^{0\prime}$ as a function of mass, considering now the three body decays along with the two body decays. The dashed curve is $P^{0\prime} \to gg$, the dotted curve $P^{0\prime} \to \bar{b}bg$, the dot-dashed curve $P^{0\prime} \to \bar{q}qg$ for quarks lighter than the b, and the bottom solid curve is $P^{0\prime} \to \bar{\tau}\tau$

5.5. Production of $P^{0\prime}$ in Hadron Colliders

Encouraged by the high rate of three body decays, we decided to look for new modes of producing $P^{0\prime}$ in hadron collisions. The only mode previously considered was the gluon fusion diagram of Figure 5.6. We decided to examine the processes in Figure 5.7 as well. One should notice that the relation of the new processes to the first one is completely analogous to the relation of the three body decays to the two body ones. In fact, the production processes are all simply decay processes with some of the legs of the Feynman diagrams shifted from initial to final state or vice versa.

In perturbation theory, separate processes in calculations involving hadron collisions are defined by the final products and by the partons of the initial state. For example, $gg \to P^{0\prime}g$ is distinct from $\bar{q}q \to P^{0\prime}g$, even though the initial state involves the same hadrons. It is important to make this distinction, because we add all diagrams that describe the same process before we square the amplitude. Then to get the total cross section for $P^{0\prime}$ production we add the squared amplitudes for all processes. Finally, we integrate over phase space and convolute the initial state with the appropriate parton distribution functions.

The subprocess cross sections for producing the $P^{0\prime}$ are

$$\hat{\sigma}(\bar{q}q \to P^{0\prime}g) = \hat{s}\frac{d\sigma}{d\hat{t}}(\bar{q}q \to P^{0\prime}g) = \frac{\alpha_s^3(Q^2)}{27\pi^2 F_\pi^2}\frac{\hat{t}^2+\hat{u}^2}{\hat{s}^2}, \tag{5.13}$$

$$\hat{\sigma}(gq \to P^{0\prime}q + g\bar{q} \to P^{0\prime}\bar{q}) = \frac{\alpha_s^3(Q^2)}{72\pi^2 F_\pi^2} \cdot \frac{2M^2\hat{s}\hat{u} + (\hat{s}+\hat{u})\left(\hat{s}^2+\hat{u}^2 - M^2(\hat{s}+\hat{u})\right)}{\hat{s}\hat{t}^2}, \tag{5.14}$$

and

$$\hat{\sigma}(gg \to P^{0\prime} g) = \frac{\alpha_s^3(Q^2)}{16\pi^2 F_\pi^2} \cdot \frac{1}{\hat{s}} \left\{ M^2 \left[1 + M^2 \left(\frac{1}{\hat{s}} + \frac{1}{\hat{t}} + \frac{1}{\hat{u}} \right) + \frac{\hat{s}^2}{\hat{t}\hat{u}} + \frac{\hat{t}^2}{\hat{u}\hat{s}} + \frac{\hat{u}^2}{\hat{s}\hat{t}} \right] + \frac{\hat{u}\hat{t}}{\hat{s}} + \frac{\hat{s}\hat{u}}{\hat{t}} + \frac{\hat{t}\hat{s}}{\hat{u}} \right\}. \quad (5.15)$$

In these expressions, $\hat{s}$, $\hat{t}$, and $\hat{u}$ are the usual Mandelstam variables of the partons. In particular, in (5.14) $\hat{t}$ is the $g - P^{0\prime}$ invariant momentum transfer. M is the mass of the $P^{0\prime}$. Also,

$$\alpha_s(Q^2) = \frac{g_s(Q^2)^2}{4\pi} = \frac{4\pi}{7 \log\left(q^2/\Lambda^2\right)} \quad (5.16)$$

is the expression for the strong coupling constant assuming six flavors of quarks.

Because of the extra particle in the final state, the kinematics of this process are much different from the kinematics of the single particle final state of Figure 5.6. In particular, the $P^{0\prime}$ from the lowest order process is produced at rest in the parton frame, while in our processes, the $P^{0\prime}$ is produced with some momentum. Hence one can produce the $P^{0\prime}$ with high transverse energy, and this is the possibility we will investigate.

We will look at the production of $P^{0\prime}$ as a function of transverse momentum ($p_\perp$) at zero rapidity. Rapidity is defined as

$$y = \frac{1}{2} \log \left(\frac{E + p_L}{E - p_L} \right), \quad (5.17)$$

where E is the beam energy, and p_L , the longitudinal momentum, is the component of the particle's momentum along the beam. Zero rapidity means that the particle in question travels perpendicular to the beam.

The total cross section for a hadron process is obtained from taking the cross section for the parton process and integrating over all initial parton states, using

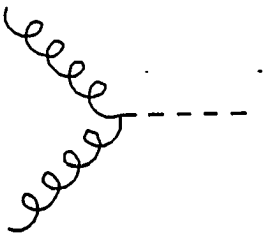

Figure 5.6. Lowest order process for producing $P^{0\prime}$ in hadron collisions

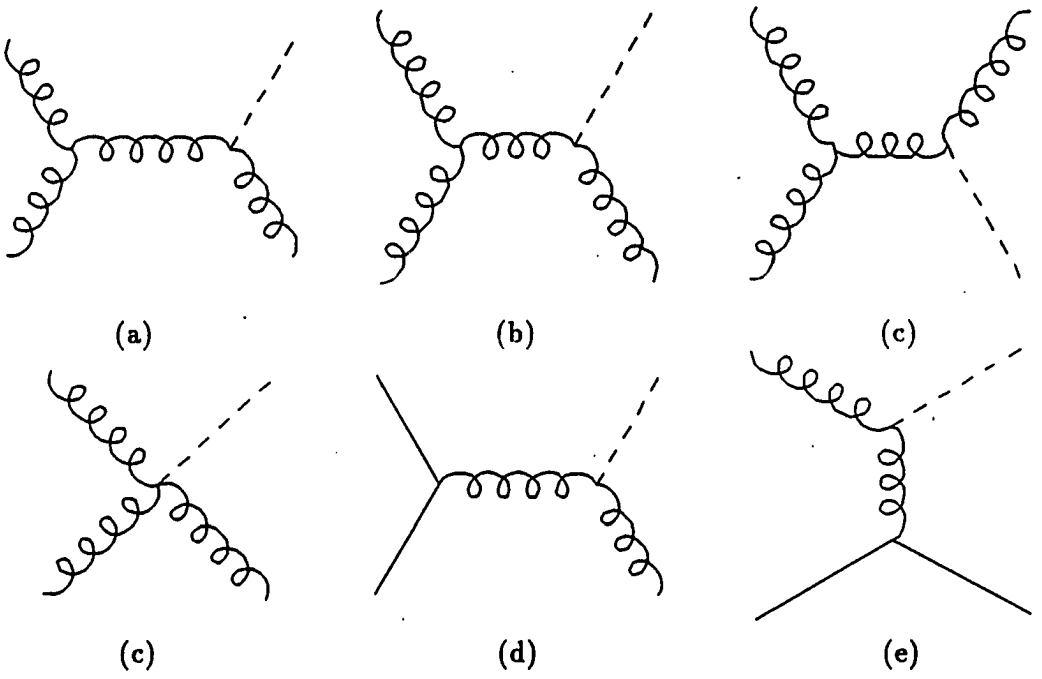

Figure 5.7. Higher order processes for producing $P^{0\prime}$ in hadron collisions

parton distribution functions. In terms of $\hat{\sigma}$,

$$\sigma(pp \to X) = \int_0^1 dx_a\, f_1(x_a) \int_0^1 dx_b\, f_2(x_b) \int d\hat{t}\, \frac{\hat{\sigma}(\hat{s},\hat{t},\hat{u})}{\hat{s}}, \tag{5.18}$$

where f_1 and f_2 are the parton distributions for the subprocess parton(1)+parton(2) $\to$ X.

Instead of x_a, x_b, and $\hat{t}$, we want x_a, y, and $p_\perp$. (Any variable will do for the first one, but x_a is convenient since we already have it in (5.18).) We make the variable change and set $y = 0$. This gives us

$$\left.\frac{d\sigma}{dp_\perp dy}\right|_{y=0} = 2p_\perp \int_{x_{\min}}^1 dx_a \frac{f_1(x_a,Q^2) f_2(x_b,Q^2) \hat{\sigma}(\hat{s},\hat{t},\hat{u})}{x_a s + u - M^2}, \tag{5.19}$$

where

$$x_{\min} = \frac{-u}{s + t - M^2}. \tag{5.20}$$

Also, we've explicitly included the dependence of the structure functions on Q^2, the energy at which we are probing the hadrons. We take this to be $Q^2 \approx {p_\perp}^2$.

In (5.19) we must express all quantities in terms of x_a, y, and $p_\perp$. We can do this via

$$\begin{aligned}
t &= -\sqrt{s} M_\perp e^{-y} + M^2, \\
u &= -\sqrt{s} M_\perp e^{y} + M^2, \\
\hat{s} &= x_a x_b s, \\
\hat{t} &= -\sqrt{s} x_a M_\perp e^{-y} + M^2, \\
\hat{u} &= -\sqrt{s} x_b M_\perp e^{y} + M^2, \\
M_\perp^2 &= {p_\perp}^2 + M^2,
\end{aligned} \tag{5.21}$$

and

$$x_b = \frac{-x_a t - (1 - x_a) M^2}{x_a s + u - M^2}.$$

The only thing left to remember is that in the cases where the initial partons are different, such as in $gq \to P^{0\prime}q$, the initial quark could come from either hadron 1 or hadron 2, and we must take the two cases separately and add them. (This is just a factor of two when the initial hadrons are identical.)

The final result is displayed in Figure 5.8. In this graph, we have plotted the cross section for producing $P^{0\prime}$ at zero rapidity in hadron collisions as a function of $p_\perp$. We have done this for $\sqrt{s} = 2$ and 40 TeV in $\bar{p}p$ and pp collisions, respectively. For comparison, we have included the same cross sections for $W^\pm$ production. For $P^{0\prime}$ mass in the range of 10s of GeV, the curves are insensitive to the mass. The curves are also reasonably insensitive to the choice of parton distribution functions. This particular plot is for $M = 40$ GeV, and the distribution functions are Duke and Owens's set 1 [38].

We can see that at Tevatron energy, $\sqrt{s} = 2$ TeV, the rate of production at high $p_\perp$ is low. At SSC, ($\sqrt{s} = 40$ TeV) on the other hand, the cross section is much higher. Also, the decline as one goes to higher $p_\perp$ is less than that for the $W^\pm$, so that above $p_\perp \approx .6$ TeV, the $P^{0\prime}$ will be produced in greater abundance than $W^\pm$. These two characteristics of $P^{0\prime}$ production compared to $W^\pm$ production is due to the momentum dependence of the $P^{0\prime}gg$ coupling. This momentum dependence, absent in the $W^\pm\bar{q}q$ coupling, causes the cross sections for $P^{0\prime}$ processes to decrease less rapidly as energy increases. With an integrated luminosity of 10^7nb^{-1} at the SSC, we expect to find $10^4 - 10^5$ $P^{0\prime}$ events with .4 TeV $< p_\perp <$ .8 TeV and $-1/2 < y < 1/2$. These would show up mainly as the decay products of the $P^{0\prime}$ opposite a single jet. A closer examination of the background for $P^{0\prime}$ events and the prospects of observing the $P^{0\prime}$ has been conducted by W.-C. Kuo [39].

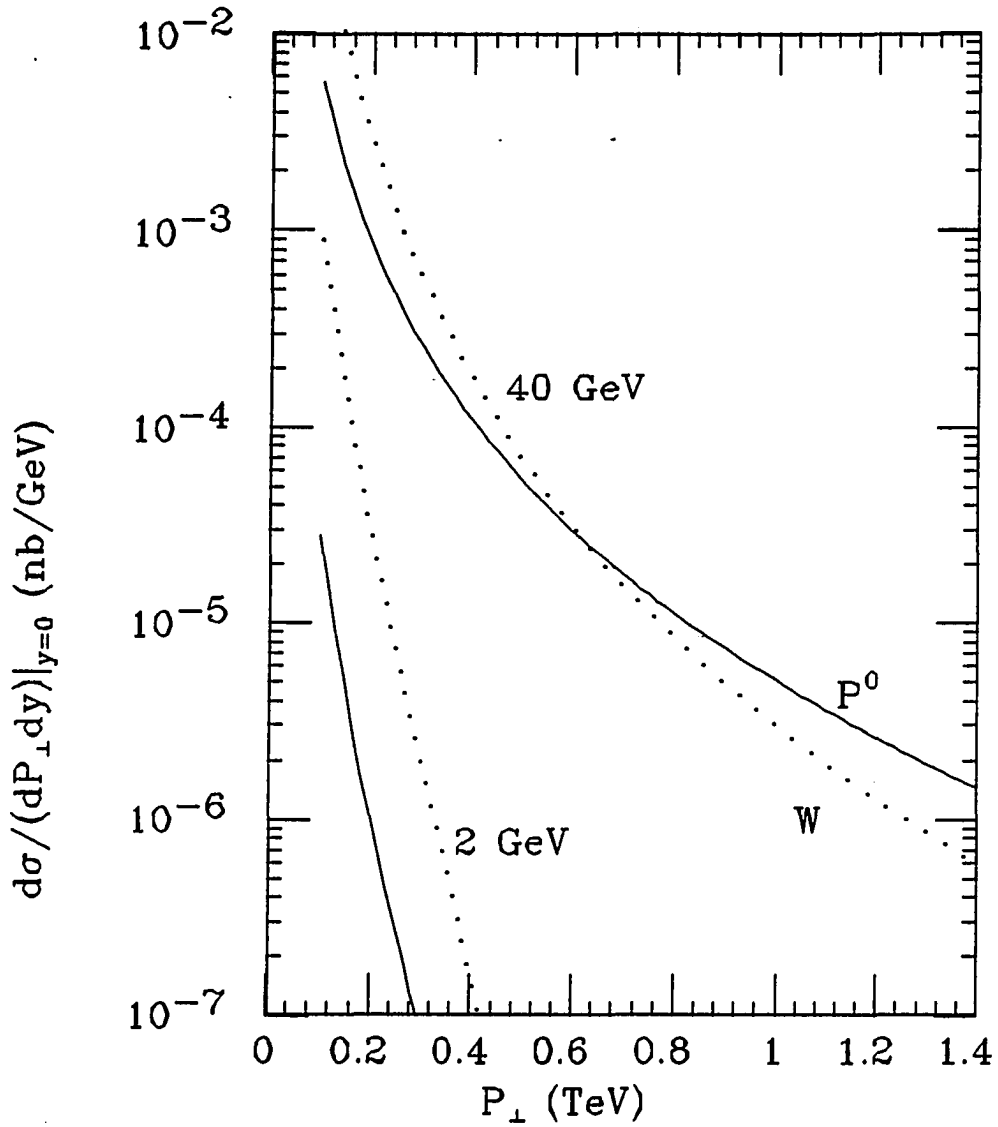

Figure 5.8. Cross section for producing $P^{0\prime}$ as a function of transverse momentum. The solid curves are for the $P^{0\prime}$, while the dotted curves are for $W^{\pm}$. The upper curves are for $\sqrt{s}$ = 40 TeV, while the lower curves are for $\sqrt{s}$ = 2 TeV

We can therefore conclude two things from this work. First, previous assumptions that the dominant decay modes of the $P^{0'}$ are two body decays are unjustified. Our calculation of three body decays indicates that these decays are just as important, if not dominant. Second, one can produce more of these particles than was previously believed, and in fact, one can produce large numbers of these particles at high transverse momentum in a machine such as the SSC.

Finally, there is one last caveat. The three body decay modes which we have calculated are $\mathcal{O}(\alpha_s)$ times the two body decays. There are, in fact, corrections to the two body decay modes *which are of this same order.* If we want a truly fair comparison between the two and three body decay modes, we must calculate these corrections. These corrections are fraught with difficulties, as we shall see when we calculate them in Chapter 7. But first, we must discuss the topic of renormalization.

6. RENORMALIZATION

It is never hard to find trouble in field theory. —Bjorken and Drell

6.1. Why We Need to Renormalize

In order to calculate corrections to the two body decay modes of the $P^{0\prime}$ and the $P_8^{0\prime}$, we must go beyond "tree level" calculations and investigate one loop Feynman diagrams. When we do, we run into a new problem. To illustrate the problem, let us examine a sample piece of a Feynman diagram which will enter into our calculation. The piece we'll examine, and a full diagram containing it, are shown in Figure 6.1.

We can write down the amplitude for this piece. For diagrams with loops we find that not all the momenta are fixed by momentum conservation at the vertices. In the diagram of Figure 6.1a, we must integrate over the internal momentum l. Then the amplitude is

$$-T(F)g^2\delta^{ab}\int\frac{d^4l}{(2\pi)^4}\mathrm{Tr}\left[\gamma_\nu\frac{1}{\not l-m}\gamma_\mu\frac{1}{\not l-\not k-m}\right], \tag{6.1}$$

where $T(F)$ is defined by $\mathrm{Tr}(T^aT^b)=T(F)\delta^{ab}$.

The trouble is in the integration at large l. As $l\to\infty$ the numerator goes as l^4 while the denominator goes as l^2. As a result, the integral is quadratically divergent. (Actually, one can show that due to gauge invariance the quadratic divergence cancels, and the integral is only logarithmically divergent.) Hence the expression for this

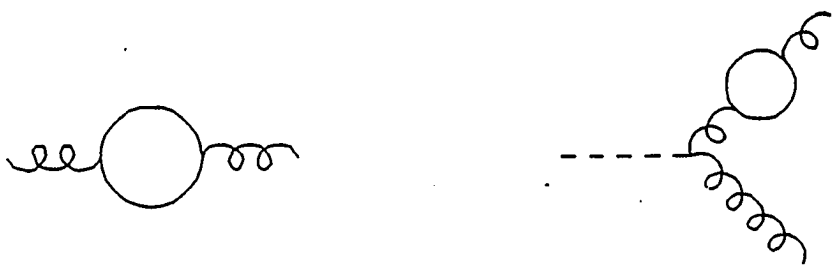

(a) (b)

Figure 6.1. A one loop correction (a) and a process containing it (b)

diagram is not defined. In fact, most of the diagrams beyond tree level in the processes $P^{0\prime} \to gg$, $P^{0\prime} \to \bar{f}f$, $P_8^{0\prime} \to gg$, and $P_8^{0\prime} \to \bar{f}f$ have this same problem, as do most processes involving loops. Our perturbation expansion seems to fail as soon as we go past lowest order in almost any process. If we are to continue to use perturbation theory, we must find some way around this ultraviolet divergence problem.

The program for dealing with these divergences and making perturbation theory work is called renormalization [40]. Since we are unable to expand Green functions of our fields in terms of the coupling constant and quark masses of the original Lagrangian (without divergences), we'll expand Green functions of different fields in terms of different coupling constants and different masses. We choose the new fields, coupling constants, and masses to be functions of the old ones in such a way that the perturbation expansion in terms of the new parameters is convergent. The values of these new parameters will be determined from experiments. In principle, we must be able to make the expansion finite to all orders. In practice, we need only renormalize to the order in which we wish to calculate.

The first step in the process is regularization. We must replace the divergent amplitude with a finite amplitude that is equivalent to the divergent one in some limit. The next step is to write a new Lagrangian which has almost the same form as the original one. The Lagrangian that we start with we call the bare Lagrangian. The quantities in the bare Lagrangian, such as the fields, couplings, and masses, we call bare quantities. The new, renormalized Lagrangian has the same form as the bare Lagrangian except for the addition of counterterms. The new Lagrangian, however, is expressed in terms of renormalized quantities instead of bare quantities. The quantities that are replaced are the couplings, the masses, and the fields themselves. The counterterms take on the same form as the ordinary terms of the Lagrangian, except that the coefficients are divergent, but well defined within any renormalization scheme. These terms are chosen to cancel the (regularized) divergences in the Feynman diagrams, which are now expressed in terms of the renormalized parameters. There is quite a bit of freedom in choosing them. The exact choice of counterterms, along with the constraint that the two Lagrangians must be equal, determines the relationship between the renormalized quantities and the bare quantities. When we're finished, we have a Lagrangian which we can expand in a perturbation series and obtain finite results to all orders when we take the limit in our regularization.

6.2. Regularization

There are several ways in which we can regularize ultraviolet divergences. For example, we can simply cut off the momentum integrals at some value. This will give us the correct expression for the amplitude in the limit that the cutoff approaches infinity. This is straightforward, but has the drawback that in a gauge theory this

method is not gauge invariant. Since QCD is a gauge theory, we desire a gauge invariant regularization. Such a method exists [41], and it is called dimensional regularization.

The premise of dimensional regularization is that the momentum integrals in loop diagrams are divergent because the integrals take place in a fixed number (four) of space-time dimensions. If we were allowed to adjust the number of dimensions of the integration, according to the form of the integral, we could obtain finite results. Then we can take the limit as the number of dimensions approaches four.

In order to do this, we need to first of all be able to express all the familiar formulas for tensors and gamma matrices in an arbitrary number of dimensions. This is tricky in the case of the gamma matrices (especially γ_5) and the Levi-Civita tensor, $\epsilon^{\mu\nu\alpha\beta}$. A good collection of the formulas can be found scattered in reference [42]. The other thing we need to be able to do is to calculate integrals such as

$$\int \frac{d^d l}{(2\pi)^d} \frac{1}{(l^2 + 2l \cdot Q - P^2)^n}, \tag{6.2}$$

for (integer) values of d for which the integral is convergent. Once we have performed the integral, we can analytically continue the result to arbitrary (including non-integral) d. Some useful formulas in dimensional regularization [42] are

$$g_{\mu\nu} g^{\mu\nu} = d \tag{6.3}$$

$$\{\gamma^\mu, \gamma^\nu\} = 2g^{\mu\nu} \tag{6.4}$$

$$\mathrm{Tr}\, I = 2^{d/2} \tag{6.5}$$

$$\gamma^\mu \gamma_\mu = d \tag{6.6}$$

$$\gamma^\mu \gamma_\nu \gamma_\mu = (2 - d)\gamma_\nu, \tag{6.7}$$

$$\mathrm{Tr}\,(\gamma^\mu\gamma^\nu) = 2^{d/2}g^{\mu\nu}, \tag{6.8}$$

$$\mathrm{Tr}\left(\gamma^\mu\gamma^\nu\gamma^\alpha\gamma^\beta\right) = 2^{d/2}\left(g^{\mu\nu}g^{\alpha\beta} - g^{\mu\alpha}g^{\nu\beta} + g^{\mu\beta}g^{\nu\alpha}\right), \tag{6.9}$$

where d is the number of dimensions, and I is the identity matrix in Dirac spinor space. The presence of I is understood in some of the above expressions such as the right side of (6.4). Equation (6.5) is often replaced by $\mathrm{Tr}I = 4$ [42]. This will also affect (6.8) and (6.9) similarly. The only overall effect will be a factor of 2 in the quantity μ^2, which will be defined soon. This corresponds to a renormalization group transformation.

Also,

$$\int \frac{d^dl}{(2\pi)^d}\frac{1}{(l^2-P^2)^n} = i(-1)^n\frac{\Gamma(n-d/2)}{\Gamma(n)}\frac{(P^2)^{d/2-n}}{(4\pi)^{d/2}} \tag{6.10}$$

$$\int \frac{d^dl}{(2\pi)^d}\frac{l^2}{(l^2-P^2)^n} = i(-1)^{n-1}\frac{d}{2}\frac{\Gamma(n-d/2-1)}{\Gamma(n)}\frac{(P^2)^{d/2-n+1}}{(4\pi)^{d/2}}. \tag{6.11}$$

When we integrate an expression (over all l) in which the denominator is symmetric in l, we can make the replacement

$$l_\mu l_\nu \to \frac{1}{d}l^2 g_{\mu\nu}. \tag{6.12}$$

These formulas will get us through most of the regularization we will need to do.

We can now go back to the diagram of Figure 6.1 and the expression (6.1). In an arbitrary number of dimensions it is

$$-T(F)g^2\delta^{ab}(\mu^2)^{2-d/2}\int\frac{d^dl}{(2\pi)^d}\mathrm{Tr}\left[\gamma_\nu\frac{\not l+m}{l^2-m^2}\gamma_\mu\frac{\not l-\not k+m}{(l-k)^2-m^2}\right]. \tag{6.13}$$

The parameter μ^2 is an arbitrary constant of dimension (mass)^2, included so that the coupling constant is dimensionless while the integral (6.13) stays at dimension 2. To

perform the integral, we use the relation

$$\frac{1}{ab} = \int_0^1 dx \frac{1}{[a(1-x)+bx]^2} \tag{6.14}$$

to combine the factors in the denominator. Then we can shift the integration variable so that the denominator resembles those in (6.10) and (6.11). We can also take the trace of gamma matrices. Then we perform the momentum integral to get

$$2ig^2 T(F)\delta^{ab}(k_\mu k_\nu - k^2 g_{\mu\nu}) 2^{d/2}(\mu^2)^{2-d/2}\frac{\Gamma(2-d/2)}{(4\pi)^{d/2}} \tag{6.15}$$
$$\cdot \int_0^1 dx\, x(1-x)[-k^2 x(1-x)+m^2]^{d/2-2}.$$

We next define $\epsilon = 2 - d/2$ and expand (6.15) in ϵ. Using the fact that $\Gamma(\epsilon) \approx \frac{1}{\epsilon} - \gamma_E$ for small ϵ, where $\gamma_E \approx .577$ is Euler's constant, we can extract the divergent part to get

$$\frac{ig^2\delta^{ab}}{(4\pi)^2}\frac{4}{3}T(F)(k_\mu k_\nu - k^2 g_{\mu\nu})\frac{1}{\epsilon}. \tag{6.16}$$

The rest of the terms are convergent in the limit $\epsilon \to 0$, which corresponds to four dimensions. We can regularize divergences in the other diagrams similarly.

So far, the continuation to an arbitrary number of dimensions has been relatively straightforward. All of the Lorentz structures we've encountered, the metric tensor, γ_μ, etc. are written as easily in d dimensions as in 4. Our work, however, will also require us to deal with the Levi-Civita tensor ($\epsilon^{\mu\nu\alpha\beta}$) and γ_5. These objects require special consideration.

6.3. $\epsilon^{\mu\nu\alpha\beta}$ and γ_5 in Dimensional Regularization

In an arbitrary number of space-time dimensions, d, the Levi-Civita tensor is a completely anti-symmetric tensor with d indices. We are stuck, however, with a

theory that is rooted in four-dimensional Minkowski space. In continuing our four-dimensional scattering or decay amplitudes to d dimensions, we are not free to change the number of indices on our tensors, and so even as we continue to arbitrary dimensions the Levi-Civita tensor must be represented as an object with four indices. There is no obviously correct way to do this.

The problem with γ_5 is similar, and in fact related. In four dimensions, one can define γ_5 in terms of $\epsilon^{\mu\nu\alpha\beta}$ by

$$\gamma_5 \propto \epsilon^{\mu\nu\alpha\beta}\gamma_\mu\gamma_\nu\gamma_\alpha\gamma_\beta. \tag{6.17}$$

Because of the presence of γ_5 in weak interactions of the standard model, many people have worked on and written about the d-dimensional extension of γ_5. Less work has been done on $\epsilon^{\mu\nu\alpha\beta}$.

There are two obvious prescriptions which come to mind for generalizing γ_5. The first of these is to make γ_5 a covariant object. That is, we define

$$\gamma_5 = i\gamma^0\gamma^1\ldots\gamma^{d-1}, \tag{6.18}$$

which implies (for d even)

$$\{\gamma_5, \gamma_\mu\} = 0 \qquad \text{for all } \mu. \tag{6.19}$$

The other possibility is to keep γ_5 a strictly four-dimensional object,

$$\gamma_5 = i\gamma^0\gamma^1\gamma^2\gamma^3, \tag{6.20}$$

which will lead to the mixed commutation relations

$$\begin{aligned} \{\gamma_5, \gamma_\mu\} &= 0 \qquad && \mu = 0, 1, 2, \text{ or } 3 \\ [\gamma_5, \gamma_\mu] &= 0 && \mu > 3. \end{aligned} \tag{6.21}$$

The latter definition (6.20) has the disadvantage of not being Lorentz covariant, and this can make calculations very messy when one is forced to use (6.21). In addition, the non-covariant definition often must be applied with caution. Körner, Nasrallah, and Schilcher [43] have examined the decay $b \to s + H$ (a process which is forbidden at tree level but can occur at one loop) using a four-dimensional γ_5. They found that in this scheme the charged current must be changed from $\frac{1}{2}\bar{s}\gamma_\mu(1-\gamma_5)b$ to $\frac{1}{4}\bar{s}(1+\gamma_5)\gamma_\mu(1-\gamma_5)b$ in order to obtain the correct result. In the case of a covariant γ_5, these two expressions are the same. In the case of a four-dimensional γ_5, however, only the latter expression leads to strictly left-handed couplings to $W^\pm$. It also leads to a charged current with only four components.

't Hooft and Veltman [41] used dimensional regularization to examine the triangle diagrams which lead to the ABJ anomaly (see Chapter 3). They found that the covariant definition of γ_5, (6.18), breaks the vector Ward–Takahashi identities and leaves the axial vector identity intact. On the other hand, we prefer to leave the vector identities intact. The four-dimensional definition (6.20) achieves this, violating only the axial vector Ward–Takahashi identity. From this, it appears that the strictly four-dimensional definition of γ_5 is more suitable than the covariant definition.

The four-dimensional definition has problems, however, in other situations. Chanowitz, Furman, and Hinchliffe [44] have shown that in processes involving fermion loops with an even number of γ_5's, spurious anomalies (apparent anomalies with no physical basis) are introduced. In this case it is necessary to use the covariant γ_5.

In fact, Chanowitz et al. use a prescription for γ_5 which is different from either of the two mentioned above. First, they assume a fully anti-commuting γ_5 as in (6.19).

Second, they assume

$$\mathrm{Tr}(\gamma_5\gamma^\mu\gamma^\nu\gamma^\alpha\gamma^\beta) = 4i\epsilon^{\mu\nu\alpha\beta}, \tag{6.22}$$

for μ, ν, α and β all in four dimensions. This is not a complete definition of γ_5. Moreover, it suffers from inconsistencies. If one considers the quantity

$$\mathrm{Tr}(\gamma_5\gamma^\mu\gamma^\nu\gamma^\alpha\gamma^\beta\gamma^\rho\gamma_\rho), \tag{6.23}$$

one finds that there is more than one way of computing it. One is to simply replace $\gamma^\rho\gamma_\rho$ with d and use (6.22). Another (albeit roundabout) way of calculating this is to shift the last gamma matrix (γ_ρ) to the front of the trace (this is still allowed in any number of dimensions) and then permute it to the right with the other gamma matrices until it is next to γ^ρ again. Then one can contract and take the trace as before. In fact, the two courses do not lead to the same result except in four dimensions. The results differ by $\mathcal{O}(d-4)$.

Chanowitz et al. do not consider this to be a weak point of their convention, but rather, claim that this ambiguity is a manifestation of the anomaly. Recall that when we discussed the anomaly in Chapter 3, we found an ambiguity in the final result due to different possible momentum assignments. We then chose the momentum assignment that preserved the Ward–Takahashi identities which we wanted to preserve the most. Here, we choose an expression for (6.23) which is consistent with the four dimensional result, and again preserves the Ward–Takahashi identities which we deem most precious (usually the vector identities.) The first method, simply replacing $\gamma^\rho\gamma_\rho$ with d in (6.23), reproduces 't Hooft and Veltman's result for the anomaly.

Many other people have worked on generalizing γ_5 to d dimensions, and yet the issue has not been fully resolved to this day. On the other hand, the work done

on $\epsilon^{\mu\nu\alpha\beta}$ in dimensional regularization is less extensive, due to its absence in the standard model.

Breitenlohner and Maison [45] advocated a strictly four-dimensional tensor in the late seventies. Their only use of $\epsilon^{\mu\nu\alpha\beta}$, however was to define γ_5 as in (6.17). The most relevant work on the d-dimensional Levi-Civita tensor has been done by Bos [46].

Bos in fact examines the Wess–Zumino–Witten model, just as we are doing here, although he examines it in only two dimensions. The advantage to working in two dimensions is that one can derive a few exact results. Then working perturbatively, one can calculate the same results and compare. Bos examines two conventions for $\epsilon^{\mu\nu}$. The first is to take a strictly two-dimensional definition. That is, we take

$$\epsilon^{\mu\nu} = 0 \qquad \text{whenever} \qquad \{\mu,\nu\} \neq \{0,1\}. \tag{6.24}$$

The other option Bos discusses is a covariant convention. The rules here are that we take the tensor to be anti-symmetric as usual, and

$$\epsilon^{\mu\nu}\epsilon^{\alpha\beta} = -F(d)(g^{\mu\alpha}g^{\nu\beta} - g^{\mu\beta}g^{\nu\alpha}), \tag{6.25}$$

where $F(d)$ is an analytic function and $F(2) = 1$. One should note that this is not a complete definition. For example, if $d > 2$, one can use (6.25) to derive an expression for ϵ^{01} and ϵ^{02}. Comparing these results with the expression for $\epsilon^{01}\epsilon^{02}$ derivable from (6.25), we are forced into the result $F(d) = 0$ for $d > 2$. This is not consistent with our constraints of continuity and $F(2) = 1$. This shouldn't bother us much, however, since we don't require the values of individual components of $\epsilon^{\mu\nu}$; we only require covariant combinations such as (6.25).

Bos supports the non-covariant convention, however, for two reasons. First, there are inconsistencies lurking in the covariant convention which are more serious than the one we just mentioned. For example, in evaluating the quantity

$$\epsilon^{\mu\nu}\epsilon^{\rho\sigma}\epsilon_{\nu\rho} \qquad (6.26)$$

one can use (6.25) on either the first two tensors or the last two tensors. If one demands the same result in each case, one must require $(d-2)F(d)=0$. This would imply that $F(d)=0$ whenever $d \neq 2$. Coupled with our requirement that $F(2)=1$, we see that one cannot smoothly take the limit $d \rightarrow 2$ as required in dimensional regularization.

This situation is very similar to the ambiguities in the γ_5 convention of Chanowitz et al., and therefore would not seem to be too great an objection. In fact, if one subscribes to the philosophy of Chanowitz et al., one might be inclined to search for occurrences of this ambiguity to see if they are associated with anomalies. Bos has a second objection to the covariant prescription for $\epsilon^{\mu\nu}$, however, which we shall see is more damning.

One can derive several exact results in the two-dimensional Wess–Zumino–Witten model. Among these are constraints on renormalization group constants. Bos rederives a couple of these perturbatively, and compares the perturbative result with the exact one. In the cases he studies, only with the two-dimensional Levi-Civita tensor (6.25) do the answers match. This strongly indicates that one should sacrifice Lorentz covariance and use the two-dimensional prescription.

Our problem is different from Bos's, in spite of the fact that both are applications of the Wess–Zumino–Witten Lagrangian. Bos examines mostly bubble diagrams with no external lines in his work. Furthermore, he does not gauge his Lagrangian, and

so he has no particles which must be kept massless. Therefore, he does not have to deal with the infrared divergences in our calculations. We, on the other hand, must include cancellation of infrared divergences at the top of our list of criteria. If the infrared divergences don't cancel, then we don't get a sensible result.

There are two prescriptions that we've tried that bear mentioning. First of all, the covariant $\epsilon^{\mu\nu\alpha\beta}$ leads to a cancellation of the infrared divergences. Bos's result in the two-dimensional theory, however, discourages one from using this prescription.

The other prescription to try is the four-dimensional $\epsilon^{\mu\nu\alpha\beta}$. In this case, one must decide whether the external momenta are four-dimensional objects or d-dimensional objects. This is because when we square the matrix element in the two gluon decay of the $P^{0'}$, for example, we get expressions like

$$\epsilon^{\mu\nu\alpha\beta}\epsilon_{\mu\nu\rho\sigma}k_{1\alpha}k_{2\beta}k_1^\rho k_2^\sigma, \tag{6.27}$$

where k_1 and k_2 are the gluon momenta. In the four-dimensional case,

$$\epsilon^{\mu\nu\alpha\beta}\epsilon_{\mu\nu\rho\sigma} = -2\left(\underline{g}^\alpha_\rho\underline{g}^\beta_\sigma - \underline{g}^\alpha_\sigma\underline{g}^\beta_\rho\right) \tag{6.28}$$

where underlined quantities hereafter will denote quantities that are truncated to four dimensions. Then for (6.27) we get

$$\epsilon^{\mu\nu\alpha\beta}\epsilon_{\mu\nu\rho\sigma}k_{1\alpha}k_{2\beta}k_1^\rho k_2^\sigma = -2\left[\underline{k}_1^2\underline{k}_2^2 - (\underline{k}_1\cdot\underline{k}_2)^2\right]. \tag{6.29}$$

If we take k_μ to be a four-dimensional object, then $\underline{k}_1\cdot\underline{k}_2 = k_1\cdot k_2$, and $\underline{k}^2 = k^2 = 0$. If k_μ is a d-dimensional object, then $\underline{k}_1\cdot\underline{k}_2 = k_1\cdot k_2 + \mathcal{O}(\varepsilon)$, etc. The leading term in the infrared divergence is $\mathcal{O}(1/\varepsilon^2)$, and so the difference between k in d dimensions and k in four dimensions can be infrared divergent.

It is common in dimensional regularization to take external momenta to be four-dimensional quantities while taking only loop momenta to be d-dimensional. This is a problem in our case, however, since in the three body decays it is necessary to perform the phase space in d dimensions, in order to regularize the infrared. Hence we are integrating external momenta over all possible values in d dimensions. It would, furthermore, be rather inconsistent to handle the external momenta differently in the three body and two body cases. Therefore, we will take all external momenta to be d-dimensional.

This prescription also leads to a cancellation of infrared divergences. From the point of view of infrared divergence cancellation, we are free to choose whichever prescription we prefer. The only other information we have is the work of Bos. Therefore, we will follow Bos and take the strictly four-dimensional definition of the Levi-Civita tensor. The lack of Lorentz covariance will make the calculation very tedious (see Appendix B), but the only indication we have is that this prescription is more correct. Now we can continue with our discussion of renormalization.

6.4. Renormalization

As we've already said, the process of renormalization consists of defining new quantities (coupling constants, masses, and fields) which are similar to the bare quantities, but will give finite results in perturbation theory. We shall demonstrate the process with QCD [47].

We start with the QCD Lagrangian:

$$\mathcal{L} = -\frac{1}{4}\hat{G}_0^{a\mu\nu}\hat{G}^a_{0\mu\nu} - \frac{1}{2\xi_0}(\partial^\mu G^a_{0\mu})^2 + (\partial_\mu c^a_0)^\dagger(\partial^\mu c^a_0) + \bar{\psi}_0(i\,\partial\!\!\!/ - m_0)\psi_0$$

$$
\begin{aligned}
&+g_0 f^{abc}(\partial_\mu G^a_{0\nu})G^{b\mu}_0 G^{c\nu}_0 - \frac{g_0^2}{4} f^{abc} f^{ade} G^{b\mu}_0 G^{c\nu}_0 G^d_{0\mu} G^e_{0\nu} \\
&+g_0 f^{abc}(\partial^\mu c^a_0)^\dagger c^b_0 G^c_{0\mu} - g_0 \bar{\psi}_0 \not{G}^a_0 T^a \psi_0,
\end{aligned}
\tag{6.30}
$$

where $\hat{G}^a_{\mu\nu} = \partial_\mu G^a_\nu - \partial_\nu G^a_\mu$. The hat on $\hat{G}$ is to distinguish it from the gauge covariant $G^a_{\mu\nu}$ which contains $\hat{G}^a_{\mu\nu}$ plus the terms in the second line of (6.30). The 0's denote the fact that the fields, the coupling and the quark mass here are bare quantities. We now define the renormalized quantities:

$$
\begin{aligned}
g_0 &= Z_g^{-1} g \\
\psi_0 &= Z_2^{1/2} \psi \\
G^a_{0\mu} &= Z_3^{1/2} G^a_\mu \\
c^a_0 &= Z_4^{1/2} c^a \\
\xi_0 &= Z_5 \xi \\
m_0 &= m + \delta m.
\end{aligned}
\tag{6.31}
$$

We will see later that $Z_3 = Z_5$.

We can rewrite the Lagrangian in terms of the renormalized quantities. This gives us

$$
\begin{aligned}
\mathcal{L} \;=\; & -\frac{1}{4} Z_3 \hat{G}^{a\mu\nu} \hat{G}^a_{\mu\nu} - \frac{1}{2\xi} Z_3 Z_5^{-1} (\partial^\mu G^a_\mu)^2 + Z_4 (\partial_\mu c^a)^\dagger (\partial^\mu c^a) \\
& + Z_2 \bar{\psi}(i \not{\partial} - m)\psi - Z_2 \delta m \bar{\psi}\psi \\
& + Z_g^{-1} Z_3^{3/2} g f^{abc} (\partial_\mu G^a_\nu) G^{b\mu} G^{c\nu} - Z_g^{-2} Z_3^2 \frac{g^2}{4} f^{abc} f^{ade} G^{b\mu} G^{c\nu} G^d_\mu G^e_\nu \\
& + Z_g^{-1} Z_4 Z_3^{1/2} g f^{abc} (\partial^\mu c^a)^\dagger c^b G^c_\mu - Z_g^{-1} Z_2 Z_3^{1/2} g \bar{\psi} \not{G}^a T^a \psi.
\end{aligned}
\tag{6.32}
$$

Finally we can write this in the form that will be most useful to us. This is

$$
\mathcal{L} \;=\; -\frac{1}{4} \hat{G}^{a\mu\nu} \hat{G}^a_{\mu\nu} - \frac{1}{2\xi} (\partial^\mu G^a_\mu)^2 + (\partial_\mu c^a)^\dagger (\partial^\mu c^a) + \bar{\psi}(i \not{\partial} - m)\psi
$$

$$
\begin{aligned}
&+gf^{abc}(\partial_\mu G^a_\nu)G^{b\mu}G^{c\nu} - \frac{g^2}{4}f^{abc}f^{ade}G^{b\mu}G^{c\nu}G^d_\mu G^e_\nu \\
&+gf^{abc}(\partial^\mu c^a)^\dagger c^b G^c_\mu - g\bar{\psi}\,\not{G}^a T^a \psi \\
&-\frac{1}{4}(Z_3-1)\hat{G}^{a\mu\nu}\hat{G}^a_{\mu\nu} - \frac{1}{2\xi}(Z_3Z_5^{-1}-1)(\partial^\mu G^a_\mu)^2 + (Z_4-1)(\partial_\mu c^a)^\dagger(\partial^\mu c^a) \\
&+(Z_2-1)\bar{\psi}(i\not{\partial}-m)\psi - Z_2\delta m\bar{\psi}\psi \qquad (6.33) \\
&+(Z_g^{-1}Z_3^{3/2}-1)gf^{abc}(\partial_\mu G^a_\nu)G^{b\mu}G^{c\nu} \\
&-(Z_g^{-2}Z_3^2-1)\frac{g^2}{4}f^{abc}f^{ade}G^{b\mu}G^{c\nu}G^d_\mu G^e_\nu \\
&+(Z_g^{-1}Z_4Z_3^{1/2}-1)gf^{abc}(\partial^\mu c^a)^\dagger c^b G^c_\mu - (Z_g^{-1}Z_2Z_3^{1/2}-1)g\bar{\psi}\,\not{G}^a T^a\psi.
\end{aligned}
$$

The first three lines of (6.33) are identical in form to the bare Lagrangian (6.30), except that the bare quantities are replaced by the renormalized quantities. The rest of (6.33) is referred to as the counterterm Lagrangian. We choose the various renormalization constants (Z_i and δm) such that calculations of physical quantities are finite. To lowest order (tree diagrams) all quantities are already finite, so $Z_i = 1$ and $\delta m = 0$. In higher orders, the renormalization constants take on the form $Z_i = 1 + \mathcal{O}(\alpha_s)$ and $\delta m = \mathcal{O}(\alpha_s)$. Hence we treat the counterterms as perturbations.

Now we move on to the business of actually calculating some of these renormalization constants. We'll start with corrections to the fermion propagator. The only one loop diagram is shown in Figure 6.2a. The renormalization will be easier if we put the correction in the form

$$-i\Sigma(\not{p}) = -i\{A + (\not{p}-m)[B + C(\not{p})]\}, \qquad (6.34)$$

where $C(\not{p})$ is ultraviolet convergent, and $C(m) = 0$. This is not quite as straightforward as it looks, due to the presence of an infrared divergence.

From (6.34) we see that $B = \partial\Sigma/\partial\not{p}|_{\not{p}=m}$, and $A = \Sigma(m)$. When we calculate

(a)

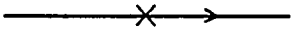

$$\frac{3ig^2C_2(F)}{(4\pi)^2}m\left(\frac{1}{\epsilon}-\gamma_E+\log 4\pi\right)$$

(b)

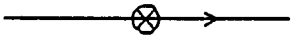

$$-i(\not{p}-m)\frac{g^2C_2(F)}{(4\pi^2)}\left(\frac{1}{\epsilon}-\gamma_E+\log 4\pi\right)$$

(c)

Figure 6.2. Quark propagator correction and counterterms

this one loop diagram, using dimensional regularization, we get

$$\begin{aligned}\Sigma(\not{p}) &= \frac{g^2 C_2(F)}{(4\pi)^2}(4\pi\mu^2)^{\epsilon}\Gamma(\epsilon)\int_0^1 dx[-(2-2\epsilon)\not{p}(1-x)+(4-2\epsilon)m] \\ &\quad \cdot[m^2 x - p^2 x(1-x)]^{-\epsilon}. \end{aligned} \tag{6.35}$$

Setting $\not{p} = m$ and expanding in ϵ gives us

$$A = \frac{3g^2 C_2(F)}{(4\pi)^2} m\left(\frac{1}{\epsilon} - \gamma_E + \log\frac{4\pi\mu^2}{m^2} + \frac{4}{3}\right). \tag{6.36}$$

Next, we take the derivative of Σ with respect to $\not{p}$ in order to obtain B:

$$\begin{aligned}\frac{\partial\Sigma}{\partial\not{p}} &= \frac{g^2 C_2(F)}{(4\pi)^2}(4\pi\mu^2)^{\epsilon}\Gamma(\epsilon)\int_0^1 dx\left\{-2(1-\epsilon)(1-x)[m^2 x - p^2 x(1-x)]^{-\epsilon}\right. \\ &\quad +2\epsilon\not{p}x^{-\epsilon}(1-x)[-2(1-\epsilon)\not{p}(1-x)+(4-2\epsilon)m] \\ &\quad \left.\cdot[m^2 - p^2(1-x)]^{-1-\epsilon}\right\}. \end{aligned} \tag{6.37}$$

At this point, we can see two different kinds of divergences in (6.37). The first is represented by the $\Gamma(\epsilon)$ to the left of the integral sign. This is the ultraviolet divergence. The second term of the integrand has a coefficient $\sim \epsilon$, and so this term is ultraviolet convergent. A new divergence becomes apparent, however, when we let $\not{p} \to m$ in (6.37). As we go on mass shell (which we must do, remember, to obtain the constant B), the last expression in brackets in (6.37) becomes

$$[m^2 x]^{-1-\epsilon}, \tag{6.38}$$

which causes the x integral to diverge at the lower limit for $\epsilon \geq 0$. This divergence is an infrared divergence, since it only appears as we go on mass shell.

Note that the term containing the infrared divergence is, in fact, ultraviolet finite. In order to regularize ultraviolet divergences, we normally assume $\epsilon > 0$,

corresponding to $d < 4$. Since there is no ultraviolet divergence in this term, however, we are free to analytically continue to $\varepsilon < 0$. Taking $\varepsilon < 0$ in (6.37) will allow us to go on shell and still be able to evaluate the x integral. Hence, we use a parameter ε which is greater than 0 to regularize ultraviolet divergences, while we use a parameter $\varepsilon < 0$ to regularize infrared divergences. We will distinguish between these two cases by attaching subscripts, ε_u and ε_i, to denote ultraviolet and infrared divergences.

We complete our calculation of B by taking $\not{p} = m$ and expanding in ε. This gives us

$$B = \frac{g^2 C_2(F)}{(4\pi)^2}\left[-\left(\frac{1}{\varepsilon_u} - \gamma_E + \log\frac{4\pi\mu^2}{m^2}\right) - 2\left(\frac{1}{\varepsilon_i} - \gamma_E + \log\frac{4\pi\mu^2}{m^2}\right) - 4\right]. \quad (6.39)$$

Now that we know A and B, we can calculate C. This is rather tedious, and we won't be needing C for our work, so we won't bother.

Now we must discuss the choice of counterterms. The counterterms which are relevant to quark propagator renormalization are

$$(Z_2 - 1)\bar{\psi}(i\not{\partial} - m)\psi - Z_2\delta m\bar{\psi}\psi. \quad (6.40)$$

In principle, the renormalization constants Z_2 and δm determine the Feynman rules for the counterterm diagrams of Figures 6.2b and c. Diagrams containing these counterterms are then added into the amplitude along with loop diagrams. In practice, however, we work backwards. First we calculate the loop diagrams, with their ultraviolet divergences. Then we decide what we want to subtract from the loop diagrams, and choose the Feynman rules for Figures 6.2b and c accordingly. Once we have chosen the Feynman rules for the counterterms, this choice will determine the renormalization constants Z_2 and δm, since the Lagrangian (6.40) must reproduce these Feynman rules.

There is a great deal of freedom in how we choose our counterterms. The only non-negotiable constraint is that we must choose them in such a way as to cancel the ultraviolet divergences. We also would like to make our subtractions in some systematic way, rather than doing so haphazardly. Usually the counterterms are chosen to meet some boundary condition on certain Green functions (for example, on shell renormalization), or they are chosen to take on some particular form (for example, $\overline{\text{MS}}$). In Figures 6.2b and c, we have included the Feynman rules that will result from the choice of subtraction that we will make below.

One of the most common conventions for choosing the counterterms is called "on shell" renormalization. In on shell renormalization, we choose the counterterms in such a way that for a particle on mass shell ($\not{p} = m$) the sum of the propagator corrections (loop diagrams + counterterms) is 0. This is convenient for many theories. Unfortunately, QCD is not one of them. If we were to do all our renormalization on shell, the infrared divergences would not cancel. Instead, we shall resort to a method called modified minimal subtraction ($\overline{\text{MS}}$) [48].

In minimal subtraction (MS) [49], we subtract only the pole, $1/\varepsilon$, from $\Sigma(p)$. By doing this, we will not encounter infrared divergences in our renormalization constants. Minimal subtraction also has the advantage that it is very easy to do. Modified minimal subtraction is based on the observation that with no more effort than in minimal subtraction we can make the final corrected propagator a bit simpler. It turns out that in dimensional regularization, wherever we find a $1/\varepsilon$ we will also find $-\gamma_E + \log 4\pi$. In modified minimal subtraction, we subtract these terms also.

This choice of subtraction procedure is reflected in the expressions for the Feynman rules of Figures 6.2b and c. Since these Feynman rules must be obtained from

(a) (b) (c)

$$\frac{-ig^2}{(4\pi)^2}\delta^{ab}(k^2 g_{\mu\nu} - k_\mu k_\nu)\left[\tfrac{5}{3}C_2(G) - \tfrac{4}{3}T(F)\right] \cdot \left(\tfrac{1}{\varepsilon} - \gamma_E + \log 4\pi\right)$$

(d)

Figure 6.3. Gluon propagator corrections and counterterm

the counterterms of (6.40), we have determined the renormalization constants δm and Z_2. These are

$$\delta m = -\frac{3g^2 C_2(F)}{(4\pi)^2} m \left(\frac{1}{\varepsilon_u} - \gamma_E + \log 4\pi\right), \tag{6.41}$$

and

$$Z_2 = 1 - \frac{g^2 C^2(F)}{(4\pi)^2}\left(\frac{1}{\varepsilon_u} - \gamma_E + \log 4\pi\right). \tag{6.42}$$

In our calculations, we will be interested in quark propagator corrections only for external lines. Corrections to external lines carry additional complications which we will discuss later. In the meantime, we have calculated two of our six renormalization constants. We can now move on to corrections to the gluon propagator, and to the renormalization constants Z_3 and Z_5.

The gluon propagator corrections are shown in Figure 6.3. Just as before, we need to calculate these diagrams, and choose the renormalization constants such that the counterterms cancel the divergences. Adding up the diagrams of Figures 6.3a, b, and c gives us

$$i\delta^{ab}(k^2 g_{\mu\nu} - k_\mu k_\nu)\Pi(k^2) \tag{6.43}$$

where

$$\begin{aligned}\Pi(k^2) \;=\; & \frac{g^2}{(4\pi)^2}\left\{\frac{5}{3}C_2(G)\left(\frac{1}{\varepsilon} - \gamma_E + \log 4\pi + \frac{31}{15}\right)\left(\frac{-k^2}{\mu^2}\right)^{-\varepsilon}\right. \\ & -\frac{4}{3}T(F)\left[\frac{1}{\varepsilon} - \gamma_E + \log\frac{4\pi\mu^2}{2m^2} + \frac{5}{3} + \frac{4m^2}{k^2}\right. \\ & \left.\left. -2(1+\frac{2m^2}{k^2})\sqrt{\frac{1}{4}-\frac{m^2}{k^2}}\log\left(\frac{\sqrt{\frac{1}{4}-\frac{m^2}{k^2}}+\frac{1}{2}}{\sqrt{\frac{1}{4}-\frac{m^2}{k^2}}-\frac{1}{2}}\right)\right]\right\}.\end{aligned} \tag{6.44}$$

$C_2(G)$ is the second order Casimir invariant for the adjoint representation of the gauge group, defined by $f^{acd}f^{bcd} = C_2(G)\delta_{ab}$. For $SU(N)$, $C_2(G)$ is just N. $T(F)$ is defined by $\mathrm{Tr}(T^aT^b) = T(F)\delta^{ab}$. For the fundamental representation of $SU(N)$ this is usually taken to be $1/2$. The first line of (6.44) is the contribution from the gluon and ghost diagrams, while the rest is from fermion loops, and must be summed over all quarks.

Separating the ultraviolet from the infrared divergences in the gluonic contribution to (6.44) is tricky, due to the factor $(-k^2/\mu^2)^{-\varepsilon}$. As we go on shell ($k^2 \to 0$), this factor is either 0 or divergent, depending on the sign of ε. We can handle this situation in our $\overline{\mathrm{MS}}$ scheme as follows. First, we leave $\Pi(k^2)$ off shell, and extract the ultraviolet divergence. In regularizing the ultraviolet divergence, we take $\varepsilon > 0$.

This corresponds to working in fewer than four dimensions, which is appropriate for regularizing the ultraviolet. Then we perform modified minimal subtraction, as usual. With the ultraviolet divergences removed, we are now free to take $\epsilon < 0$. This is the appropriate condition for regularizing infrared divergences. (Ultraviolet divergences arise from integrating in too many dimensions, infrared divergences from too few.) Now that $\epsilon < 0$, we can go on mass shell with impunity, since $(k^2)^{-\epsilon} \to 0$ as $k^2 \to 0$.

We'll ignore the fermion contribution for now, since the subtraction for that ultraviolet divergence is straightforward, and there is no infrared divergence. Since we're leaving the gluon off shell for now, we can expand in ϵ to obtain the ultraviolet divergence. This gives us

$$\Pi^g(k^2) = \frac{g^2}{(4\pi)^2}\frac{5}{3}C_2(G)\left[\frac{1}{\epsilon_u} - \gamma_E + \log 4\pi + \log\left(\frac{\mu^2}{-k^2}\right) + \frac{31}{15}\right], \tag{6.45}$$

where the superscript g indicates that we are including only the gluon and ghost loop contributions, and ignoring the fermion contribution. We can now read off the ultraviolet divergence, and in the spirit of $\overline{\text{MS}}$, we subtract

$$\Pi_0^g = \frac{g^2}{(4\pi)^2}\frac{5}{3}C_2(G)\left(\frac{1}{\epsilon_u} - \gamma_E + \log 4\pi\right). \tag{6.46}$$

Then for our renormalized propagator correction, we get

$$\begin{aligned}\Pi_R^g(k^2) &= \Pi^g(k^2) - \Pi_0^g \\ &= \frac{g^2}{(4\pi)^2}\frac{5}{3}C_2(G)\left[\left(\frac{1}{\epsilon_i} - \gamma_E + \log 4\pi\right)\left\{\left(\frac{-k^2}{\mu^2}\right)^{-\epsilon_i} - 1\right\}\right. \\ &\qquad \left. + \frac{31}{15}\left(\frac{-k^2}{\mu^2}\right)^{-\epsilon_i}\right].\end{aligned} \tag{6.47}$$

For $k^2 \neq 0$, the expression (6.47) is convergent in the limit $\epsilon \to 0$. Therefore, we have removed the ultraviolet divergence. Any remaining divergence must be infrared,

and so we are justified in using the subscript i on the ε's of (6.47). Since we no longer need to regularize the ultraviolet, we can now take $\varepsilon_i < 0$. This is the appropriate condition for regularizing infrared divergences. Once we do this, then we can go on shell. As $k^2 \to 0$, $(-k^2/\mu^2)^{-\epsilon_i} \to 0$, so that

$$\Pi_R^g(0) = -\frac{g^2}{(4\pi)^2}\frac{5}{3}C_2(G)\left(\frac{1}{\varepsilon_i} - \gamma_E + \log 4\pi\right). \tag{6.48}$$

Remember that we've left off the quark loop corrections. If we take the quarks to be massive, then there is no infrared problem associated with quark loops. If we have massless quarks, then there is an infrared problem, and we handle it just as we did for the case of gluon and ghost loops. We will take our quarks to be massive here. Including the quark loop contributions, we find that we must subtract

$$\Pi_0 = \frac{g^2}{(4\pi)^2}\left[\frac{5}{3}C_2(G) - \frac{4}{3}T(F)\right]\left(\frac{1}{\varepsilon_u} - \gamma_E + \log 4\pi\right), \tag{6.49}$$

and

$$\Pi_R(0) = \frac{g^2}{(4\pi)^2}\left[-\frac{5}{3}C_2(G)\left(\frac{1}{\varepsilon_i} - \gamma_E + \log 4\pi\right) - \frac{4}{3}T(F)\log\frac{\mu^2}{2m^2}\right]. \tag{6.50}$$

The contribution of the counterterms to the gluon self energy is denoted by the diagram of Figure 6.3d. Fixing Z_3 so that we obtain the correct counterterm, we find

$$\begin{aligned} Z_3 &= 1 + \Pi_0 \\ &= 1 + \frac{g^2}{(4\pi)^2}\left(\frac{5}{3}C_2(G) - \frac{4}{3}T(F)\right)\left(\frac{1}{\varepsilon_u} - \gamma_E + \log 4\pi\right). \end{aligned} \tag{6.51}$$

In principle, the counterterm $-\frac{1}{2\xi}(Z_3 Z_5^{-1} - 1)(\partial^\mu G_\mu^a)^2$ will also contribute to the gluon self energy. We have achieved our cancellation without it, however, and any divergence from this term would only spoil what we've worked so hard to achieve. Therefore, we set $Z_5 = Z_3$, and we've eliminated this term. One should also notice

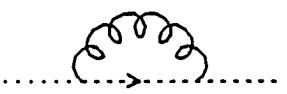

Figure 6.4. Ghost propagator correction

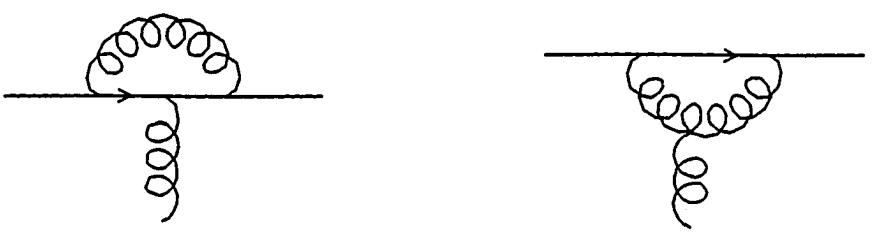

(a) (b)

Figure 6.5. The fermion vertex corrections

at this point that we've done all calculations in Feynman gauge ($\xi = 1$). In other gauges we would have different expressions for the renormalization constants. The results of physical calculations should, of course, be the same in any gauge.

We have now calculated four of our six renormalization constants. We can calculate Z_4 from the diagram in Figure 6.4, and Z_g from the diagrams in Figure 6.5. Here we give only the results. The calculation of Z_4 is very similar to the calculation of Z_3. The result is

$$Z_4 = 1 + \frac{g^2 C_2(G)}{(4\pi)^2} \frac{1}{2} \left(\frac{1}{\epsilon_u} - \gamma_E + \log 4\pi \right). \tag{6.52}$$

The constant Z_g is chosen to cancel the divergence from the vertex correction.

Actually, we could use the corrections to any vertex to obtain this constant. It may be rather worrisome that at this point we have corrections to four different vertices, all of which contain divergences, to renormalize, while we only have one renormalization constant left to choose. In fact this is not a problem. We can choose any vertex (three gluon, four gluon, ghost–gluon, or fermion–gluon) to calculate Z_g, and the result will be that all divergences will be canceled in all corrections. This result has been shown to hold to all orders, and is a consequence of the Slavnov–Taylor identities discussed earlier. Another way of stating this result is that after renormalization, the coupling constants for all vertices are still equal. Renormalization preserves gauge invariance! [50]

With this in mind, we choose to work with the fermion–gluon vertex. When we do this, we find

$$Z_g = 1 + \frac{g^2}{(4\pi)^2}\left[\frac{11}{6}C_2(G) - \frac{2}{3}T(F)\right]\left(\frac{1}{\varepsilon_u} - \gamma_E + \log 4\pi\right). \qquad (6.53)$$

Finally, the last counterterms are given in Figure 6.6. We have finished renormalizing QCD. We have created a new Lagrangian which is equivalent to the old one, but which gives finite results in a perturbation expansion. With our results of this section, we can calculate any process to one loop order and obtain a finite result. Before we see whether we can apply the techniques and results of this section to the effective Lagrangian that we've created for technipions, we have two more issues to deal with concerning renormalization in general. The first is the relationship between the delicate cancellation of infrared divergences and our choice of renormalization scheme.

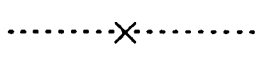

$$\frac{ig^2 C_2(G)}{2(4\pi)^2}\delta^{ab}k^2\left(\frac{1}{\epsilon}-\gamma_E+\log 4\pi\right)$$

(a)

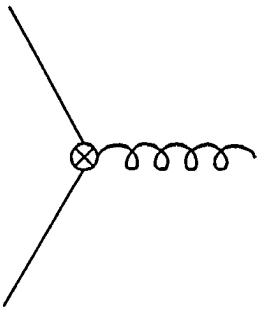

$$\frac{ig^3}{(4\pi)^2}T^a\gamma_\mu[C_2(G)+C_2(F)]\left(\frac{1}{\epsilon}-\gamma_E+\log 4\pi\right)$$

(b)

Figure 6.6. The ghost counterterm (a), and the vertex counterterm (b)

6.5. Renormalization and the Infrared Divergences

In Chapter 5 we stated without proof that the infrared divergences between the two gluon decay and the three gluon decay will cancel, and the resultant sum of the two decay widths will be finite. However, we have also discussed the freedom we have in choosing our renormalization constants. In the current chapter, we chose a renormalization scheme in which the renormalization constants have no infrared divergences in them. This is not a necessity. The renormalization of QED, for example, is usually performed on mass shell. This results in an infrared divergence in the renormalization constant Z_2. If we had renormalized QCD on shell, we would have introduced infrared divergences in many of the renormalization constants. Hence the infrared divergence of the decay $P^{0\prime} \rightarrow gg$ depends on our renormalization scheme, while that of the three gluon decay does not. Our hopes for canceling these divergences ride on our choice of renormalization scheme! This leads us to the question: what scheme is correct?

Our first instinct might be to try on shell renormalization, since this works for QED. Unfortunately, it does not work for QCD. Yao [51] and Sugamoto [52] for example, have examined the infrared problem in simple QCD processes such as $qq \rightarrow qq$ (along with the corresponding process $qq \rightarrow qqg$) and $qg \rightarrow qg$ or qgg. They performed the renormalization on shell, and their conclusion was that the infrared divergences cancel when expanding with the *bare* coupling constant. However, we know that in order to cancel the ultraviolet divergences we must renormalize the coupling constant. We could employ some haphazard scheme in which we renormalize the propagators on shell, and then choose a counterterm for the vertices in such a way that the coupling renormalization constant remains infrared finite. We prefer,

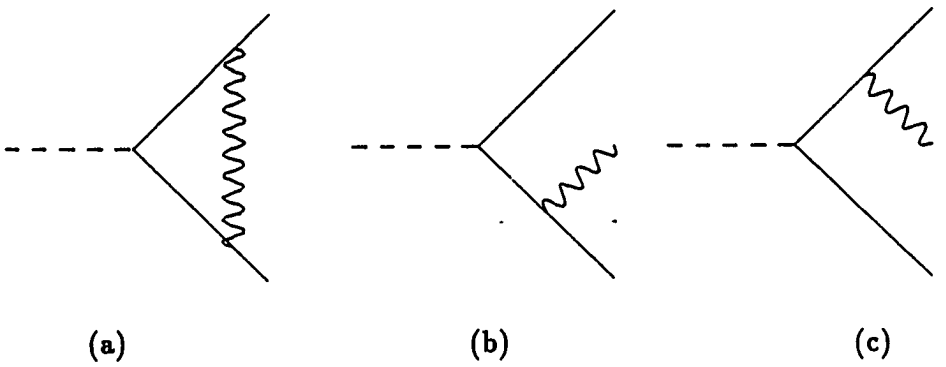

Figure 6.7. Scalar decaying to $\bar{f}f$ (a) and *bremsstrahlung* corrections (b) and (c)

however, to avoid the haphazard whenever possible.

Our $\overline{\text{MS}}$ scheme seems to be a likely candidate. Producing a complete set of renormalization constants with no infrared divergences in any of them is at first glance appealing, especially considering the fact that in the on shell scheme the problem seems to lie in the infrared divergence of the coupling renormalization constant. We've examined various processes in varying depth. In addition to the processes in this work, we've also examined in detail a process of a scalar particle decaying into a massless charged fermion–anti-fermion pair via a Yukawa coupling. The fermions can emit a *bremsstrahlung* photon, and this process is infrared divergent. We have also looked in less detail at the infrared divergences in the process $qg \rightarrow qg(g)$, and an electron scattering off a static Coulomb potential with possible *bremsstrahlung*. In the examples we've examined in the quest to find the right scheme, $\overline{\text{MS}}$ renormalization works.

In fact, there is a pattern to the cancellation. Figure 6.7a shows one of the diagrams for the one loop QED corrections to a scalar decaying to a massless charged

$\bar{f}f$ pair. The infrared divergence in this diagram arises from the possibility that the photon may be soft or collinear with one of the fermions. One can unhook the photon from the lower leg in Figure 6.7a and obtain the *bremsstrahlung* diagram of Figure 6.7b. One can also unhook the photon from the upper leg and obtain the diagram of Figure 6.7c. The infrared divergence in the product of these two *bremsstrahlung* diagrams will cancel the infrared divergence from the product of Figure 6.7a and the diagram obtained by removing the photon entirely. This pattern of cancellation holds for other diagrams for this process, as well as other processes.

Another way of illustrating this is through the "bubble" diagrams of Figure 6.8. Figure 6.9 shows two different ways of cutting the diagram of Figure 6.8a. When we cut this bubble diagram along one of the dotted lines, and put the cut lines on mass shell, we obtain a pair of diagrams for either the process $\phi \to \bar{f}f$ or $\phi \to \bar{f}f\gamma$. In Figure 6.9a, we get the tree level diagram for $\phi \to \bar{f}f$ and the one loop diagram of Figure 6.7a. This corresponds to a cross term between these two diagrams in the square of the amplitude of this process. Cutting the bubble as in Figure 6.9b gives us the diagrams of Figure 6.7b and c for the process $\phi \to \bar{f}f\gamma$. This corresponds to a cross term between these diagrams in the square of the amplitude of $\phi \to \bar{f}f\gamma$. When we add up the terms corresponding to all possible cuts of the bubble of Figure 6.8a (or any other bubble) the infrared divergences will all cancel. This pattern holds for other processes, as for example the technipion decays we are interested in.

6.6. External Lines in Off Shell Renormalization

We close this chapter with a discussion of external line corrections [53] in an off shell renormalization scheme, such as $\overline{\text{MS}}$. There are two intricacies that we shall

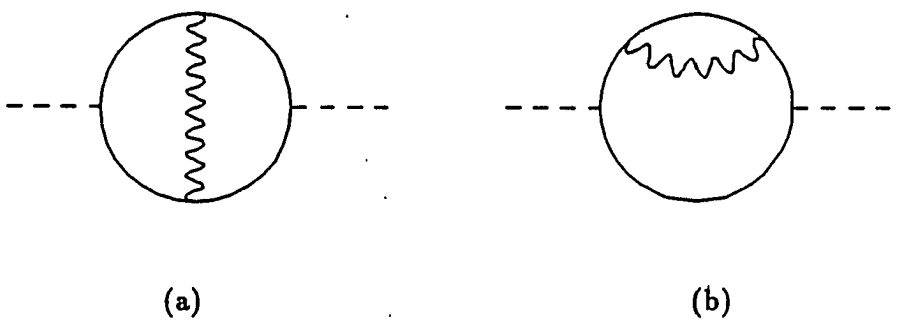

Figure 6.8. Bubble diagrams for $\phi \rightarrow \bar{f}f(\gamma)$

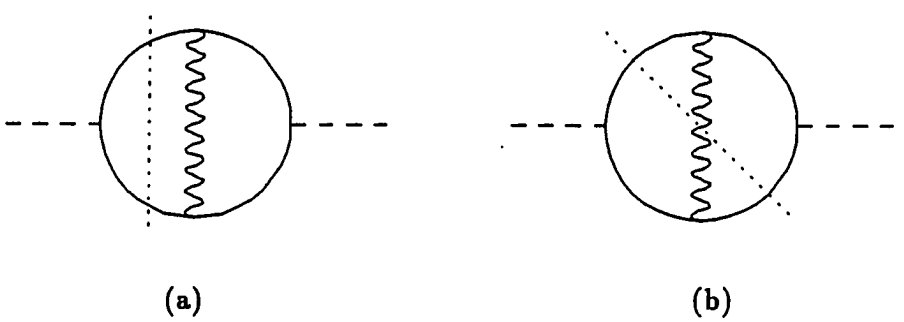

Figure 6.9. Bubble diagram with cuts to show pattern of infrared divergence cancellation

discuss. The first one concerns the pole in the propagator for massive particles in off shell renormalization, and applies to internal lines as well as external ones. The second one addresses the fact that there are renormalization constants in the reduction formula, and in the relation between bare and renormalized Green functions.

In a general renormalization scheme, the renormalized corrections to the quark propagator can be written in the form

$$-i\Sigma_R(\not p) = -i\{A_f + (\not p - m)[B_f + C(\not p)]\}, \tag{6.54}$$

where, recall, $C(\not p)$ is ultraviolet convergent and $C(m) = 0$. The subscripts f denote the fact that we've included the counterterms in $\Sigma_R(\not p)$ and so A_f and B_f are finite quantities. They are what remain of the A and B of equation (6.34) after we make the subtraction. If we had renormalized on shell, then A_f and B_f would be zero.

To one loop, the renormalized two point Green function in momentum space is

$$\tilde{G}_R^{(2)}(\not p) = \frac{i}{\not p - m} + \frac{i}{\not p - m}\left[-i\{A_f + (\not p - m)[B_f + C(\not p)]\}\right]\frac{i}{\not p - m}. \tag{6.55}$$

We expect the two point Green function to have a simple pole, which we then associate with the mass of the particle. This is not the case here, however, due to the presence of A_f.

In order to recover a simple pole in our propagator, we express $\tilde{G}_R^{(2)}(\not p)$ as a sum over bubbles, as illustrated in Figure 6.10. We can add up all these bubbles, to obtain

$$\begin{aligned}
\tilde{G}_R^{(2)}(\not p) &= \frac{i}{\not p - m} + \frac{i}{\not p - m}[-i\Sigma_R(\not p)]\frac{i}{\not p - m} + \cdots \\
&= \frac{i}{\not p - m}\left(\frac{1}{1 - \frac{\Sigma_R(\not p)}{\not p - m}}\right) \\
&= \frac{i}{\not p - m - \Sigma_R(\not p)}.
\end{aligned} \tag{6.56}$$

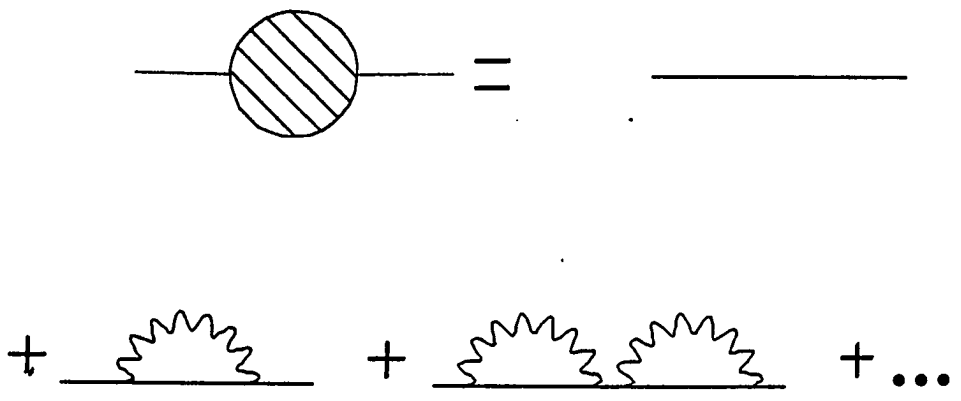

Figure 6.10. Sum of bubble diagrams, used to evaluate the two point Green function

Note that this is not exact. While we have summed over all bubbles, each bubble is only calculated out to a certain order in α_s; in our case, first order.

In accordance with our notion of a particle's mass, we define the physical mass, m_P, to be the pole in (6.56):

$$m_P - m - \Sigma_R(m_P) = 0. \tag{6.57}$$

That is,

$$m_p - m - A_f - (m_P - m)[B_f + C(m_p)] = 0. \tag{6.58}$$

We are only interested in lowest order. Since $m_P - m$ is $\mathcal{O}(\alpha_s)$, the last term in (6.58) is higher order, and we ignore it. Then

$$m_p = m + A_f. \tag{6.59}$$

Now we can express the two point Green function in terms of the physical quark mass, m_P:

$$\begin{aligned} \tilde{G}_R^{(2)}(\not{p}) &= \frac{i}{\not{p} - m - \{A_f + (\not{p} - m)[B_f + C(\not{p})]\}} \\ &= \frac{i}{\not{p} - m_P - (\not{p} - m_p)[B_f + C(\not{p})]}. \end{aligned} \tag{6.60}$$

We are free to use m_P instead of m in the last term in the denominator, since the difference between the two is higher order. Factoring out $\not{p} - m_P$ gives us

$$\tilde{G}_R^{(2)}(\not{p}) = \frac{i}{\not{p} - m_p}\{1 - [B_f + C(\not{p})]\}^{-1}. \tag{6.61}$$

If the propagator we're correcting is an external line, then we have a factor $-i(\not{p} - m_P)$ along with (6.61). As we go on mass shell, $C(m_P) \approx C(m) = 0$ (to one loop). Then for each external quark line, the one loop correction consists of a factor

$$(1 - B_f)^{-1}. \tag{6.62}$$

It is interesting to note that we could avoid this whole business of summing over bubbles if we chose to ignore the presence of A_f. Then we would still have a simple pole in our propagator, and we could evaluate the corrections just by considering the Feynman rules for the diagrams containing external line corrections (along with the appropriate counterterms, of course). It is not difficult to see that to lowest order this leads to the exact same result, a factor of $1 + B_f$ ($\approx (1 - B_f)^{-1}$) for each external line. In other words, our choice of A_f, or equivalently our choice of mass counterterm δm, has no bearing on the final result. We can actually take $A_f = 0$ in our calculation and make life easier on ourselves.

Finally, we discuss the effect of off shell renormalization arising from the presence of renormalization constants in the reduction formula and the relationship between

bare and renormalized Green functions. We will continue to look at fermion fields, but the result will be general. The S-matrix for a process involving fermions (to keep the notation manageable, we'll assume only particles, no anti-particles) is

$$\langle k_1,\ldots,k_n|S|k_1',\ldots,k_m'\rangle = \frac{1}{(n!m!)^{1/2}}\bar{Z}^{-(n+m)/2} \tag{6.63}$$
$$\cdot \lim_{\not{k}_i\to m_P}\prod_i[-i\bar{u}(k_i)(\not{k}_i - m_P)]\,\tilde{G}_0^{(n+m)}(k_1,\ldots,k_m')\prod_i\left[-i(\not{k}_i' - m_P)u(k_i')\right],$$

where $\tilde{G}_0^{(n+m)}$ is the Fourier transform of the bare Green function

$$G_0^{(n+m)}(x_1,\ldots,y_m) = \langle 0|T[\psi_0(x_1),\ldots,\bar{\psi}_0(y_m)]|0\rangle. \tag{6.64}$$

The factor $\bar{Z}$ is a proportionality constant [54] relating the bare fields to the asymptotic "in" and "out" fields.

When we calculate Feynman diagrams after renormalization, we are calculating Green functions of renormalized fields. Since the bare and renormalized fields are related by $\phi_0 = Z_2^{1/2}\phi$, we see from (6.64) that the renormalized Green functions are related to the bare Green functions by

$$G_0^{(n+m)}(x_1,\ldots,y_m) = Z_2^{(n+m)/2}G_R^{(n+m)}(x_1,\ldots,y_m), \tag{6.65}$$

and now we can write the S-matrix

$$\langle k_1,\ldots,k_n|S|k_1',\ldots,k_m'\rangle = \frac{1}{(n!m!)^{1/2}}\left(\frac{\bar{Z}}{Z_2}\right)^{-(n+m)/2} \tag{6.66}$$
$$\cdot \lim_{\not{k}_i\to m_P}\prod_i[-i\bar{u}(k_i)(\not{k}_i - m_P)]\,\tilde{G}_R^{(n+m)}(k_1,\ldots,k_m')\prod_i\left[-i(\not{k}_i' - m_P)u(k_i')\right],$$

The constant $\bar{Z}$ is independent of our renormalization scheme. If we renormalize on shell, then our field operator renormalization constant, Z_2, is equal to $\bar{Z}$ [55]. That is,

$$\bar{Z} = Z_{2P}, \tag{6.67}$$

where from here on the subscript P will denote quantities in an on shell, or "physical" renormalization scheme. The subscript R will be attached to quantities denoting some other renormalization scheme (for example, $\overline{\text{MS}}$). Then if we renormalize on shell, the Z's in (6.66) cancel. Since we have been forced away from on shell renormalization by the constraint of infrared divergence cancellation, we must investigate the consequences [53] of $Z_{2R} \neq \tilde{Z}$. Mainly, we have to evaluate the quantity

$$\mathcal{Z} \equiv \frac{Z_{2P}}{Z_{2R}}, \tag{6.68}$$

which occurs in (6.66).

To calculate $\mathcal{Z}$, we return to the two point Green function, $\tilde{G}_R^{(2)}(\not{p})$. For any renormalization scheme, we know that

$$\tilde{G}_R^{(2)}(\not{p}) = Z_2^{-1}\tilde{G}_0^{(2)}(\not{p}). \tag{6.69}$$

Then taking a ratio of Green functions in the two renormalization schemes, we find

$$\mathcal{Z} = \frac{Z_{2P}}{Z_{2R}} = \frac{\tilde{G}_R^{(2)}(\not{p})}{\tilde{G}_P^{(2)}(\not{p})}. \tag{6.70}$$

But we saw earlier that in any renormalization scheme,

$$\lim_{\not{p}\to m_P} \tilde{G}_R^{(2)}(\not{p}) = \frac{i}{(\not{p} - m_P)(1 - B_f)}. \tag{6.71}$$

In on shell renormalization, $B_f = 0$ by design, and so from (6.70) and (6.71) we see that

$$\mathcal{Z} = \frac{1}{1 - B_f}. \tag{6.72}$$

From the reduction formula (6.66) and the definition of $\mathcal{Z}$, we see that associated with each line we have a factor

$$(1 - B_f)^{1/2}. \tag{6.73}$$

Combining this with the factor $(1 - B_f)^{-1}$ that we found earlier, we see that the result of this last detail is that the external lines are corrected by a factor of only

$$(1 - B_f)^{-1/2}. \tag{6.74}$$

In lowest order, we can expand this, and see that we get $1 + \frac{1}{2}B_f$ instead of the factor $1 + B_f$ that we would expect from considering the Feynman rules alone. This means that after calculating all the external line corrections from the Feynman diagrams, *we must divide all the external line corrections by two!* This result holds just as true for scalars and gauge bosons.

This is the last step in our renormalization procedure. We have renormalized the fields and parameters of QCD in such a way that the ultraviolet divergences cancel. We have also introduced a regularization scheme for infrared divergences which can be used in both virtual corrections and, as we shall see, real corrections to physical processes. Our next step is to see whether the machinery we have unfolded here can be used to settle the divergences (both ultraviolet and infrared) in the technipion decays governed by our effective Lagrangian. We shall see in Chapter 7 that, in fact, almost all of the ultraviolet and all of the infrared divergences will cancel when we follow the recipe we've just laid out.

7. TWO BODY DECAYS TO ONE LOOP

7.1. Preliminaries

Now we are ready to attack the one loop corrections to two body decays of neutral technipions. In calculating these processes, we will encounter both ultraviolet and infrared divergences. We will have to regularize these, and remove them if we intend to arrive at a final result for the decay widths of these particles. Once this is done, we can finally give a more complete description of the decays of neutral technipions to one loop in QCD corrections.

The four processes that we will examine (in varying degrees of depth) are $P^{0\prime} \to gg$, $P^{0\prime} \to \bar{q}q$, $P_8^{0\prime} \to gg$, and $P_8^{0\prime} \to \bar{q}q$. The diagrams are shown in Figures 7.1, 7.2, 7.3, and 7.4. First we will address the question of the ultraviolet divergences, and whether they can be eliminated as they are in ordinary QCD.

7.2. The Ultraviolet Divergences

QCD has been proven to be a renormalizable theory. Hence we expect to be able to make the divergences cancel in QCD, as we did in the last chapter. The theory we consider here, QCD plus the effective technipion Lagrangian, may not be so well behaved. In fact, this theory is not renormalizable. One necessary condition for renormalizability is that the Lagrangian contain no terms with operators of mass

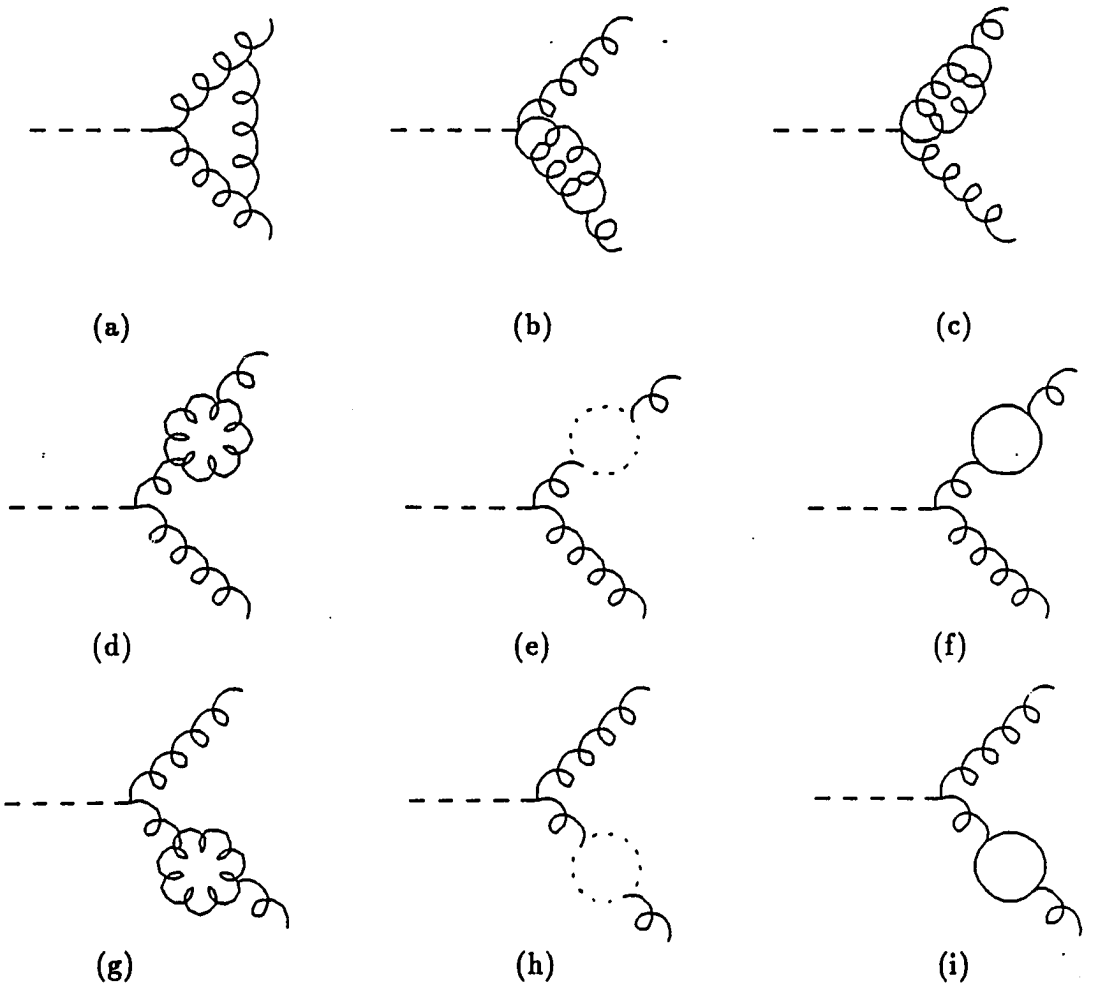

Figure 7.1. Diagrams for the decay $P^{0\prime} \rightarrow gg$

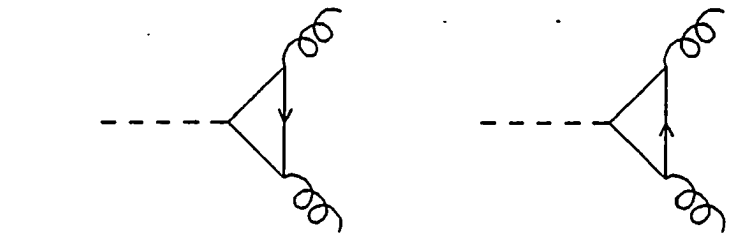

(j)

(k)

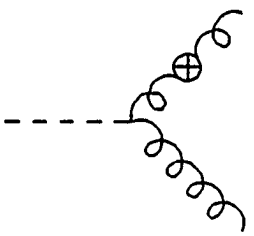

(l)

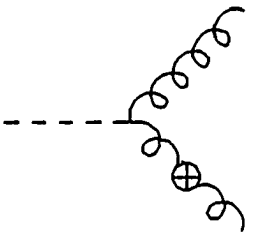

(m)

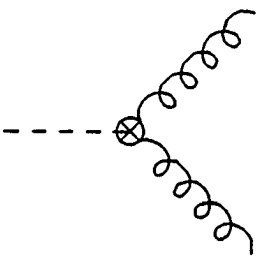

(n)

$$-\frac{4ig^2\Gamma C_2(G)}{(4\pi)^{\frac{d}{2}}}\epsilon^{\mu\nu\alpha\beta}\delta^{ab}k_{1\alpha}k_{2\beta}\left(\frac{1}{\varepsilon}-\gamma_E+\log 4\pi\right)$$

Figure 7.1. (continued)

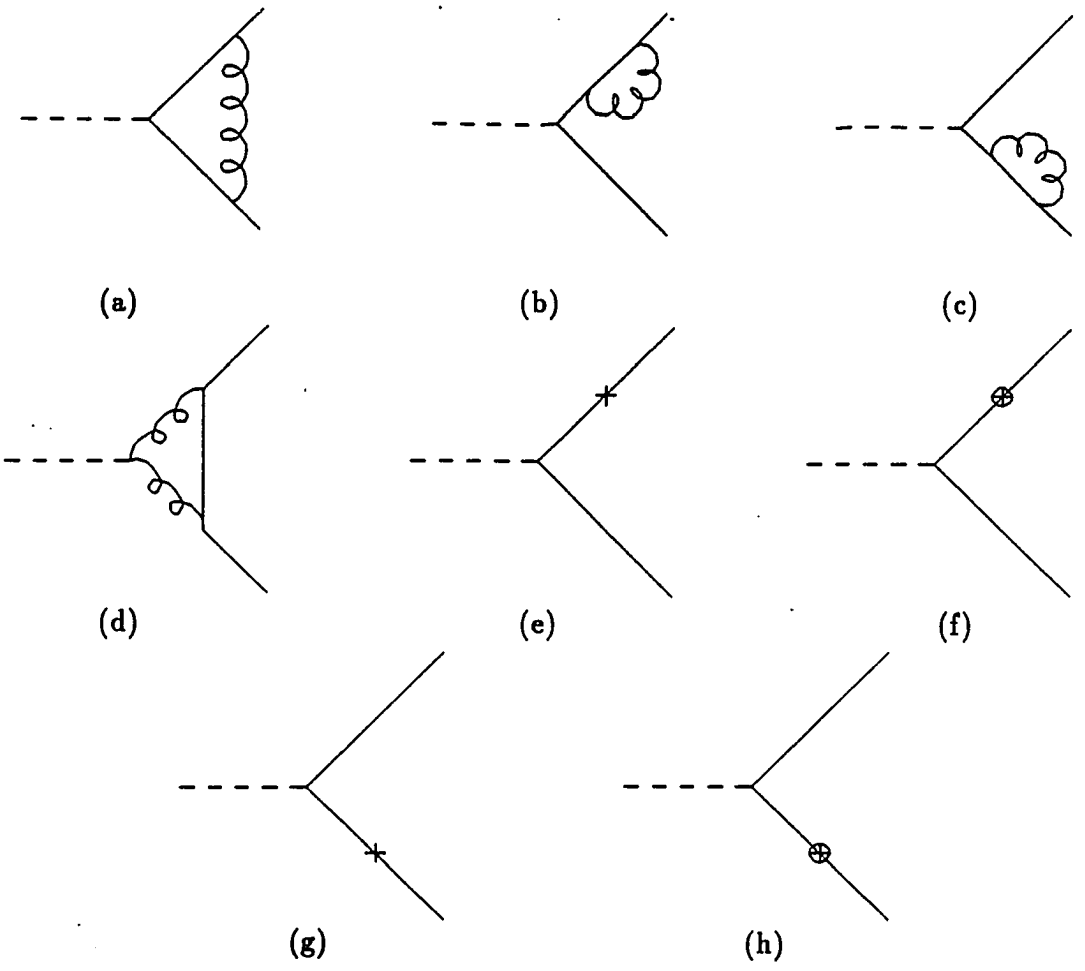

Figure 7.2. Diagrams for the decay $P^{0\prime} \rightarrow \bar{f}f$

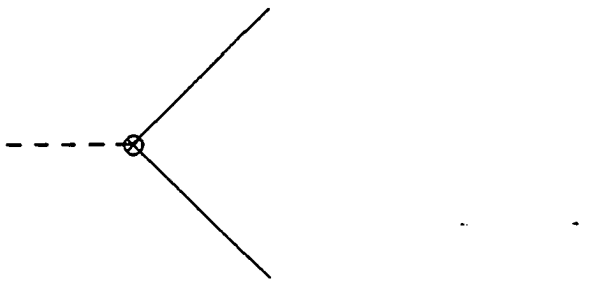

(i)

Figure 7.2. (continued)

dimension greater than four. The mass dimension of an operator here means the sum of the dimensions of the field operators and derivatives which it contains. A sample term in our Lagrangian is $\frac{1}{4}\Gamma\phi_0 G^{a\mu\nu}\tilde{G}^a_{\mu\nu}$ (recall, $\tilde{G}^a_{\mu\nu} = \epsilon_{\mu\nu\alpha\beta}G^{a\alpha\beta}$). The field ϕ_0 has dimension one. Each of the operators $G^a_{\mu\nu}$ and $\tilde{G}^a_{\mu\nu}$ has dimension two. This gives us a total of five. Hence a theory containing this term cannot be renormalizable. We therefore have good reason to suspect that even for the relatively simple one loop processes we are contemplating, we may not be able to make the ultraviolet divergences cancel. It turns out that the situation is not hopeless, as we shall see.

Before we examine the diagrams for the first process, $P^{0'} \rightarrow gg$, we have a very important decision to make concerning the Wess–Zumino–Witten Lagrangian. This Lagrangian contains fields for the technipions, as well as gluon fields and the parameters g and F_π. It is crucial to state whether these quantities are bare quantities or renormalized quantities. The perturbative expansion to one loop is done with renormalized quantities to avoid ultraviolet divergences in QCD. If the quantities in the Wess–Zumino–Witten Lagrangian are renormalized quantities, then we can use them with no further modification. If, however, they are bare quantities, then we must

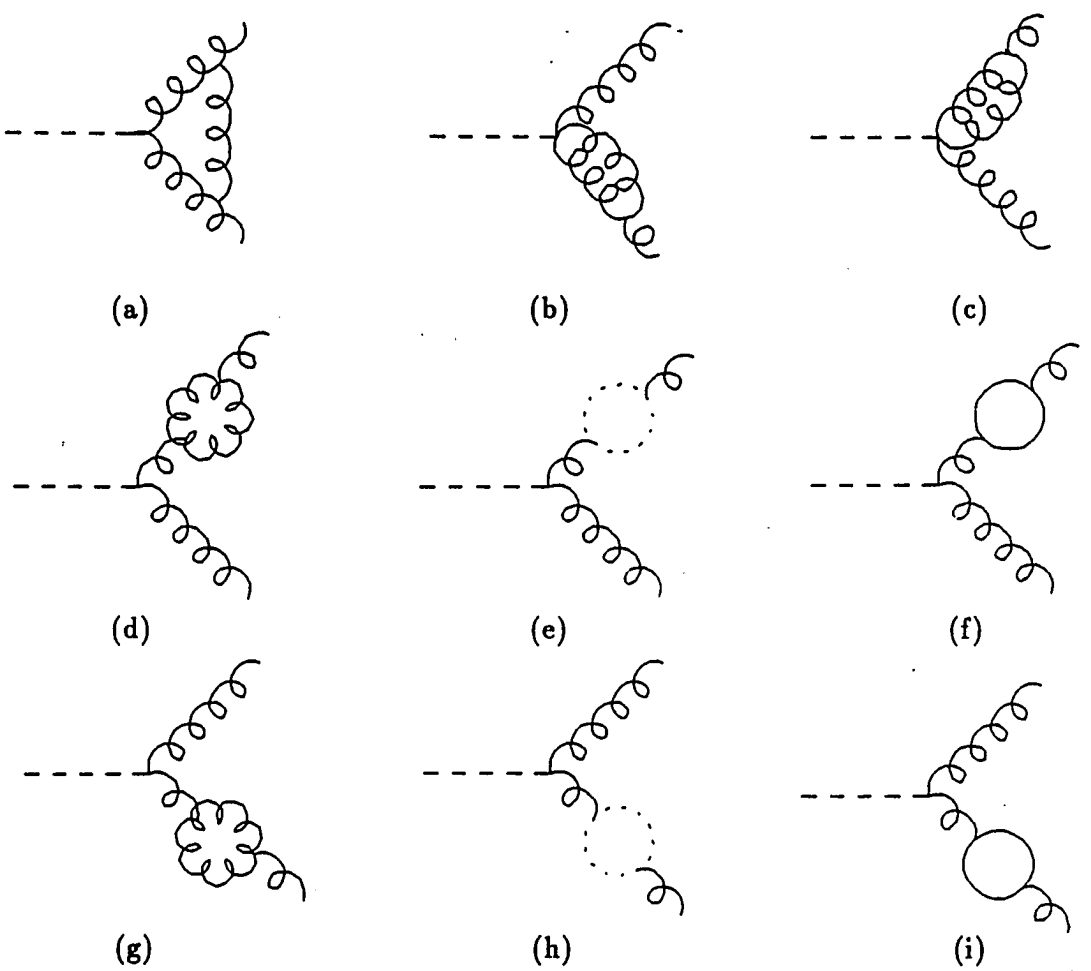

Figure 7.3. Diagrams for the decay $P_8^{0\prime} \to gg$

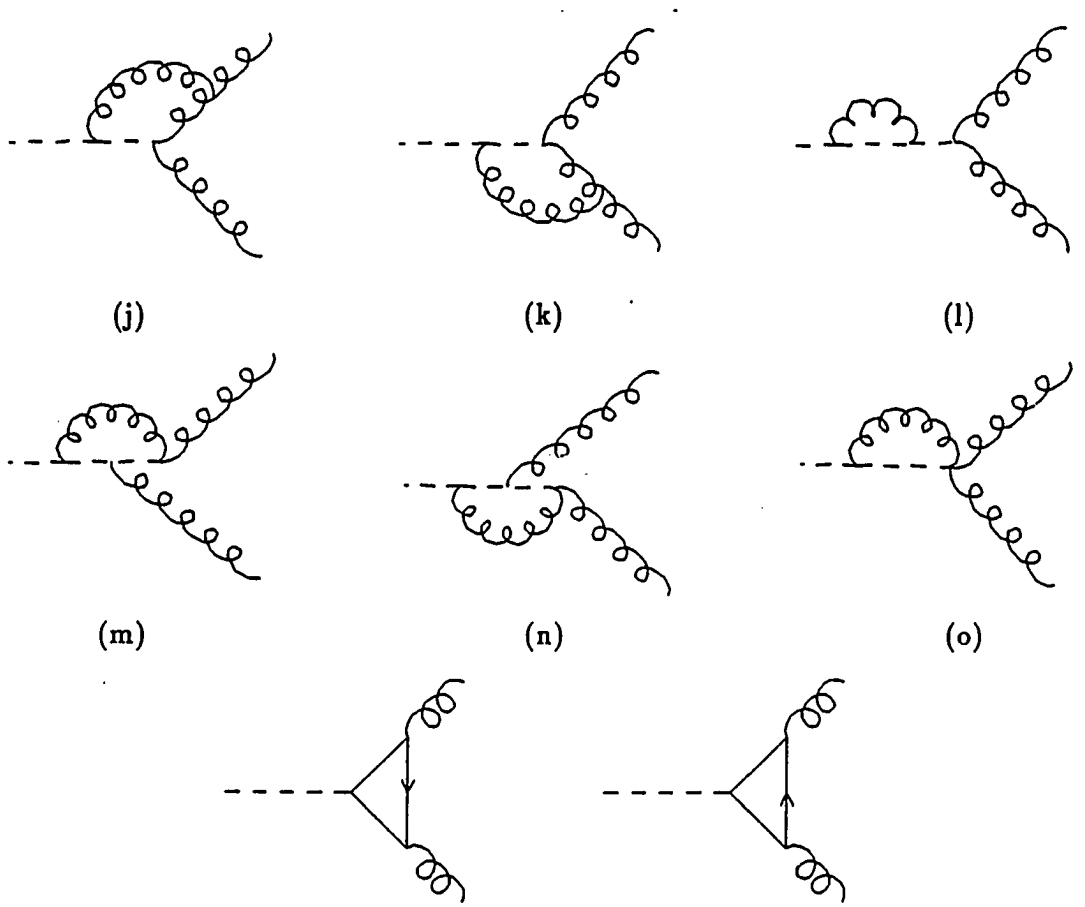

Figure 7.3. (continued)

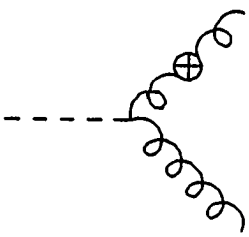

(r)

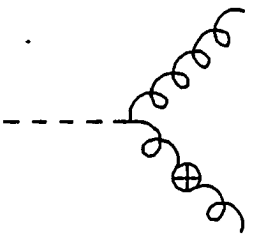

(s)

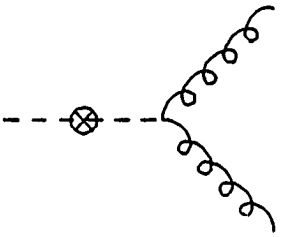

(t)

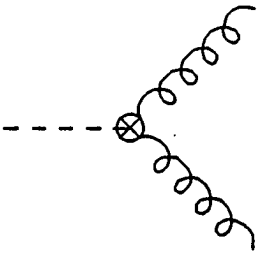

$$\frac{-2ig^2\Gamma' C_2(G)}{(4\pi)^2}\epsilon^{\mu\nu\alpha\beta}d^{abc}k_{1\alpha}k_{2\beta}\left(\frac{1}{\epsilon}-\gamma_E+\log 4\pi\right)$$

(u)

Figure 7.3. (continued)

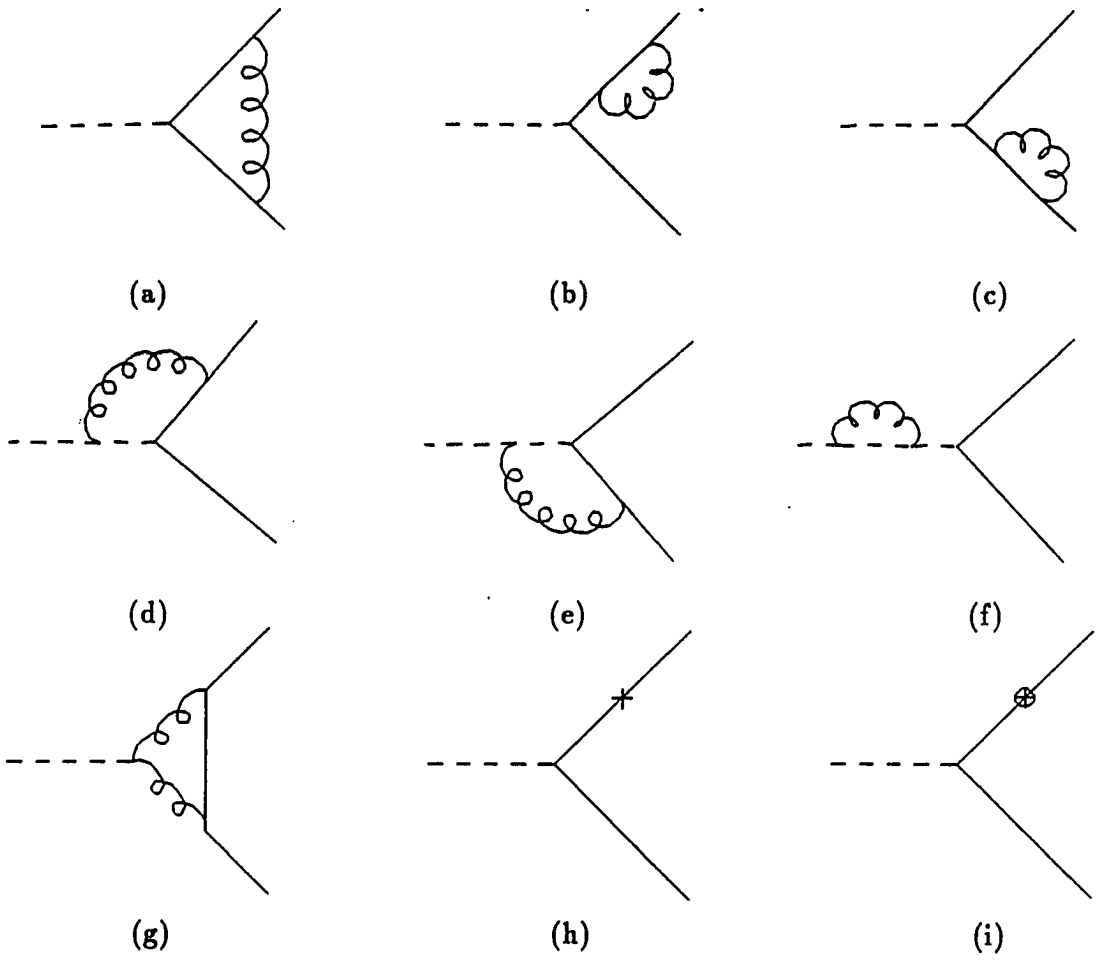

Figure 7.4. Diagrams for the process $P_8^{0\prime} \to \bar{f}f$

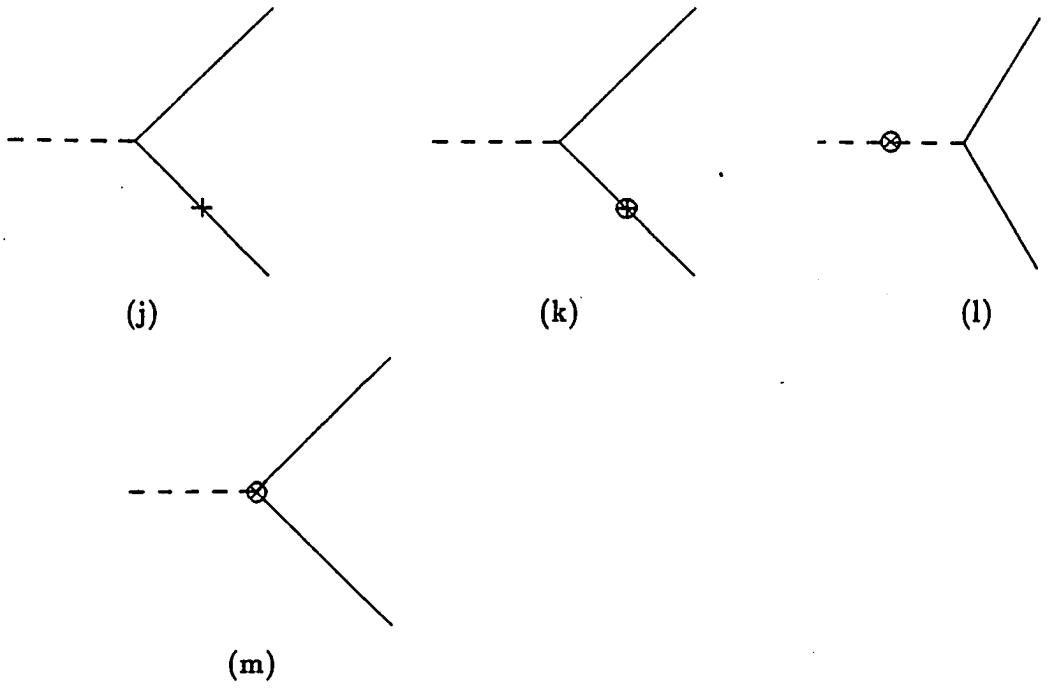

Figure 7.4. (continued)

express these in terms of the renormalized quantities. This will give us new terms like the original ones, except that they will be multiplied by various renormalization constants, Z_i. These constants, when expanded, will lead to counterterms, just as they did in QCD. These counterterms will play a role in the cancellation (or lack of cancellation) of ultraviolet divergences.

The key to resolving this question is in Witten's derivation of the anomalous Lagrangian. While we will not exhibit Witten's derivation here, upon examining it one can see that at no time does Witten resort to any kind of perturbation expansion or renormalization. The ungauged Lagrangian is derived solely from symmetry and topology considerations. The gauged Lagrangian is the minimal Lagrangian containing the ungauged Lagrangian and possessing gauge invariance. Hence we can take these quantities to be bare quantities. Similarly, we assume that the quantities in the extended technicolor terms in our effective technipion Lagrangian are bare quantities as well, although this is admittedly less certain since we are assuming no particular extended technicolor model, and know very little about the ETC sector of the theory.

The relation between the bare and renormalized couplings, g_0 and g are dictated by QCD renormalization, as is the relation between $G^a_{0\mu}$ and G^a_μ, and between m_{f0} and m_f. The only quantities that we may need or want to renormalize in our technipion Lagrangian are ϕ, ϕ^a, and F_π. (Since we will be using 0's to denote bare quantities, we no longer use a 0 in our symbol for the $P^{0'}$. From here on, ϕ will denote the renormalized $P^{0'}$ and ϕ^a will denote the renormalized $P^{0'}_8$. We will attach 0's to these to denote bare fields.) With these considerations in mind, we can examine the ultraviolet divergences in technipion decays.

The first process we will examine in our attempt to renormalize the non-renor-

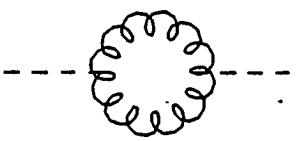

Figure 7.5. Propagator correction to $P^{0'}$

malizable (to one loop) is $P^{0'} \to gg$. The diagrams for this are shown in Figure 7.1. The first thing to notice is that to lowest order there is no correction to the $P^{0'}$ propagator. We could include the $P^{0'}$ propagator correction of Figure 7.5, but since the $P^{0'}gg$ vertex is $\mathcal{O}(g^2)$, this correction is $\mathcal{O}(g^4)$, which is higher than the order to which we're working. Hence we ignore this.

Next we calculate the counterterm, Figure 7.1n. The term in our Lagrangian that generates this counterterm is

$$\mathcal{L}_{P^{0'}gg} = -\frac{N_{TC}g_0^2}{16\sqrt{3}\pi^2 F_\pi}\epsilon^{\mu\nu\alpha\beta}\phi_0(\partial_\mu G^a_{0\nu})(\partial_\alpha G^a_{0\beta}). \tag{7.1}$$

We obtain the counterterm by substituting renormalized quantities for the bare quantities in (7.1), These substitutions are given by

$$\begin{aligned} \phi_0 &= \phi \\ g_0 &= Z_g^{-1} g \\ G^a_{0\mu} &= Z_3^{1/2} G^a_\mu. \end{aligned} \tag{7.2}$$

We derived Z_g and Z_3 in the last chapter. The technipion is not renormalized here because there is no propagator correction for the $P^{0'}$. (This will not be the case for

the $P_8^{0\prime}$.) Making the substitution, we get

$$\mathcal{L}_{P^{0\prime}gg} = \Gamma\epsilon^{\mu\nu\alpha\beta}\phi(\partial_\mu G^a_\nu)(\partial_\alpha G^a_\beta) \cdot\left\{1 - \frac{2g^2C_2(G)}{16\pi^2}\left(\frac{1}{\epsilon} - \gamma_E + \log 4\pi\right)\right\}, \tag{7.3}$$

where Γ is $-\frac{N_TCg^2}{16\sqrt{3}\pi^2F_\pi}$. The second term in braces is the counterterm we're looking for. This leads to the Feynman rule of Figure 7.1n. Note that we are not introducing any renormalization here beyond QCD. Our counterterm arises simply by expressing the bare QCD coupling constant in terms of the renormalized coupling constant, and the relationship between these is completely determined by QCD alone.

The ultraviolet divergences in the diagrams of Figures 7.1d, e, f, g, h, and i are, by design, exactly canceled by the counterterms of Figures 7.1l and m. Hence we will not concern ourselves for now with their ultraviolet divergences. This leaves us with only the diagrams of Figures 7.1a, b, c, j, and k. The ultraviolet divergence of 7.1a is

$$\frac{ig^2\Gamma C_2(G)}{16\pi^2}\delta^{ab}\epsilon^{\mu\nu\alpha\beta}\epsilon(1)_\mu\epsilon(2)_\nu k_{1\alpha}k_{2\beta}\frac{10}{\epsilon}. \tag{7.4}$$

The two diagrams 7.1b and c are equal. Their sum contains the ultraviolet divergence

$$\frac{ig^2\Gamma C_2(G)}{16\pi^2}\delta^{ab}\epsilon^{\mu\nu\alpha\beta}\epsilon(1)_\mu\epsilon(2)_\nu k_{1\alpha}k_{2\beta}\frac{-6}{\epsilon}. \tag{7.5}$$

Finally, the diagrams of Figures 7.1j and k are convergent. Adding up the divergences of (7.4), (7.5), and the counterterm of Figure 7.1n, we arrive at the result that the sum of all contributions to $P^{0\prime} \to gg$ at one loop is ultraviolet convergent.

The ultraviolet cancellation for the decay $P_8^{0\prime} \to gg$ is identical except for one minor difference. The $P_8^{0\prime}$ propagator correction leads to a renormalization of the field, ϕ^a. The renormalization constant Z_8 associated with this contributes to the

counterterm, which takes on the form:

$$2i\Gamma' \epsilon^{\mu\nu\alpha\beta} d^{abc} k_{1\alpha} k_{2\beta} (Z_8^{1/2} Z_3 Z_g^{-2} - 1), \tag{7.6}$$

where

$$\Gamma' = \frac{-N_{TC} g^2}{8\sqrt{2}\pi^2 F_\pi}. \tag{7.7}$$

The decays of technipions to quarks are not so well behaved. The diagrams for these processes are shown in Figures 7.2 and 7.4. First we'll address the counterterm of Figure 7.2i. The coefficient of the $P^{0'}\bar{q}q$ coupling is proportional to m_0/F_π, where m_0 is the appropriate bare quark mass. When we rewrite this in terms of the renormalized quark mass, which is defined by the relationship $m_0 = m + \delta m$ which we introduced when we renormalized QCD, we get a $P^{0'}\bar{q}q$ vertex proportional to m and a counterterm proportional to the renormalization constant δm. This counterterm leads to the Feynman rules of Figure 7.2i. The ultraviolet divergence from this counterterm cancels the divergence from diagrams 7.2a. A counterterm for the $P_8^{0'}\bar{q}q$ coupling arises similarly, and this is shown in Figure 7.4m. The divergence here cancels the ultraviolet divergences in the diagrams of Figures 7.4a, d, and e. This still leaves the diagrams of Figures 7.2d and 7.4g which come from the Wess–Zumino–Witten action, rather than extended technicolor interactions. There is no counterterm to cancel these divergences, and so we will handle them by introducing an ultraviolet cutoff in the loop integration.

7.3. Results of $P^{0'} \to gg(g)$

Because of the entanglement of the infrared divergences, we cannot calculate the rate of $P^{0'} \to gg$ in isolation. Hence we calculate the sum of the rates of the two

processes $P^{0'} \to gg$ and $P^{0'} \to ggg$. As we discussed in Chapter 6, there are two ways to treat the Levi-Civita tensor in dimensional regularization, and they lead to different results. Here, we will present the results of both methods, although the non-covariant prescription for $\epsilon^{\mu\nu\alpha\beta}$ is preferred. The details of the phase space calculation in an arbitrary number of dimensions are contained in Appendix B. The result is

$$\begin{aligned}\Gamma(P^{0'} \to gg) + \Gamma(P^{0'} \to ggg) = \frac{\alpha_s \Gamma^2 M^3}{32\pi^2} C_2(G)(N^2-1) \\ \cdot \left[27 - \frac{65}{6}c + \frac{11}{3}\log\frac{\mu^2}{M^2} - \frac{4}{3}\sum_f \frac{T(F)}{C_2(G)}\log\frac{\mu^2}{2m_f^2}\right] \\ + \sum_f \frac{\alpha_s \Gamma G_f M m_f T(F)(N_2-1)}{16\pi^2} h(f).\end{aligned} \tag{7.8}$$

In (7.8), $\Gamma = -\frac{N_{TC}\alpha_s}{4\pi\sqrt{3}F_\pi}$, α_s is the strong fine structure constant, $g^2/4\pi$, and N is 3 (the number of colors in QCD). Also, M is the mass of $P^{0'}$, μ^2 is an arbitrary mass scale introduced by the renormalization, and m_f is the mass of the quark f. The sums in (7.8) are over all quarks. G_f is a constant, assumed to be $\sim \frac{m_f}{F_\pi}$, but unknown without the details of extended technicolor interactions (or whatever mechanism one uses to give mass to fermions), and $C_2(G)$ and $T(F)$ are group theory factors which in our case are 3 and 1/2 respectively. Finally, $h(f)$ is a function which depends on the quark mass. For quarks less than half the $P^{0'}$ mass ($m_f < M/2$), we get

$$h(f) = -\pi^2 + \log^2\left(\frac{\frac{4m_f^2}{M^2}}{\left(1+\sqrt{1-\frac{4m_f^2}{M^2}}\right)^2}\right), \tag{7.9}$$

while for $m_f > M/2$ we get

$$h(f) = -\pi^2 - 4\arctan^2\sqrt{\frac{4m^2}{M^2}-1} + 4\pi\arctan\sqrt{\frac{4m^2}{M^2}-1}. \tag{7.10}$$

One should note the absence of the parameter ε in (7.8). This quantity has no infrared divergence, and so we freely take the limit $\varepsilon \to 0$.

The parameter c in (7.8) reflects our uncertainty in the regularization of $\epsilon^{\mu\nu\alpha\beta}$. If we take the Lorentz non-covariant prescription, then $c = 0$. If we take the covariant prescription, then $c = 1$. We see that the two scenarios give results which are very similar in form, differing only in one term. However, we also see that the difference is appreciable. The dependence of the final result on the regularization of $\epsilon^{\mu\nu\alpha\beta}$ is not negligible. Henceforth, we will stick with non-covariant prescriptions for $\epsilon^{\mu\nu\alpha\beta}$ and γ_5.

Figure 7.6 shows the result of our calculations for the decays $P^{0\prime} \to gg(g)$. We took the number of technicolors to be four, and the $P^{0\prime}\bar{f}f$ coupling to be am_f/F_π, choosing $a = 1$. We took α_s to be the running coupling constant with five flavors of quarks, and evaluated it at the $P^{0\prime}$ mass. We also set $\mu = M$. Finally, we chose $m_t = 125$ GeV. Putting these values into (7.8) gives us the solid curve of Figure 7.6.

The other two curves are the result of an attempt to separate the gluon decays into two body and three body decays. We did this by calculating the three gluon decay as in Chapter 5, with an infrared cutoff of 5 GeV in the invariant mass of any gluon system. A jet from a single gluon should have invariant mass 0. A two gluon system with an invariant mass of 5 GeV or more should be distinguishable from a single gluon. The dotted line in Figure 7.6 represents the three gluon decays derived in this manner. The dashed curve represents the two gluon decays (and three gluon decays in which one of the gluons is soft or two of them are nearly collinear), and is obtained by subtracting the dotted line from the solid line.

The graph shows that this result is absurd above about 75 GeV. The decay rate

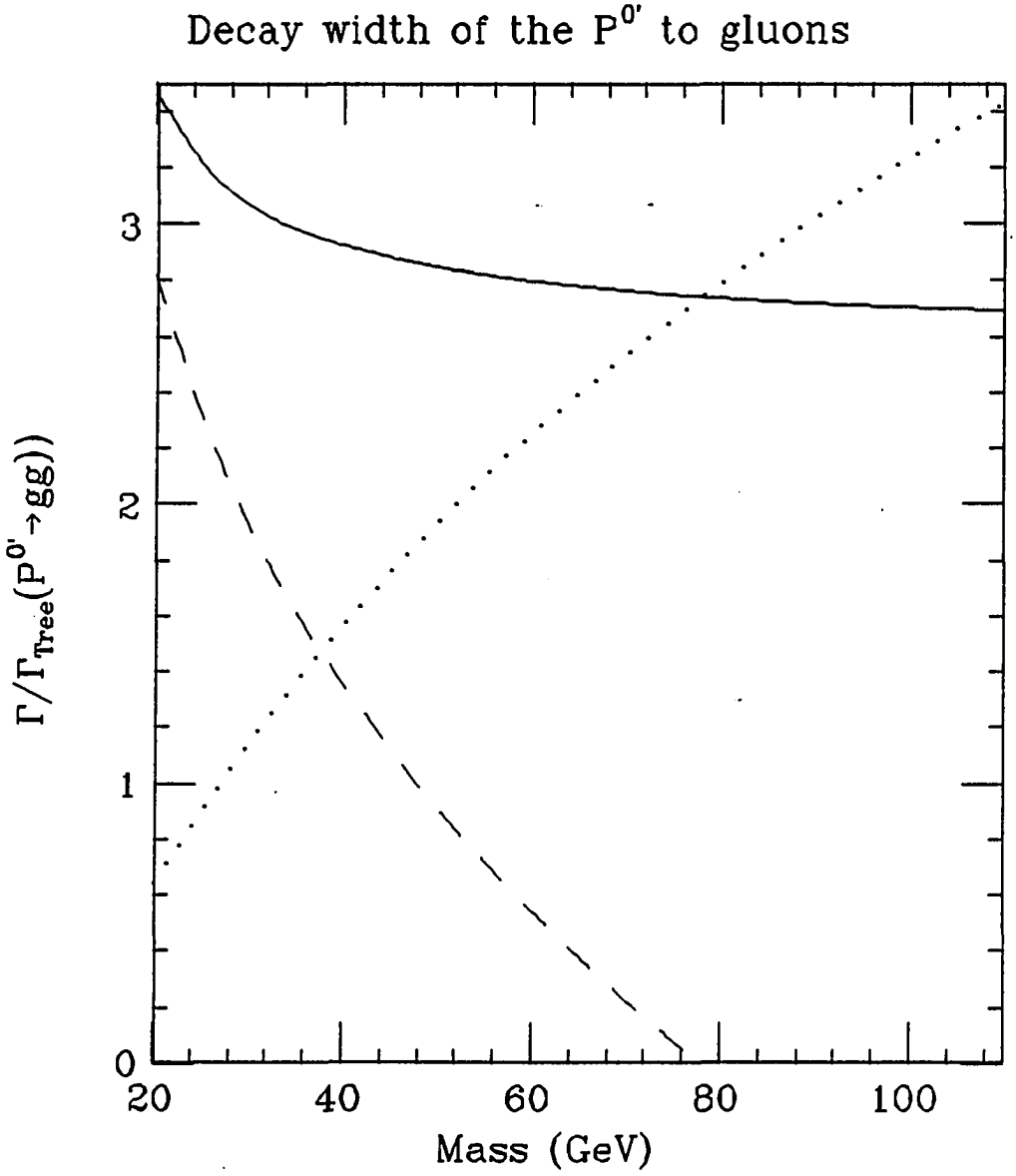

Figure 7.6. Decay width of $P^{0'}$ to gluons, relative to the tree level decay. The solid line is the total, while the dashed line and dotted line are the decays to 2 and 3 gluons respectively

to two gluons drops below zero at this point. As the mass of $P^{0\prime}$ increases, the 5 GeV cutoff goes deeper and deeper into the infrared divergence of the three gluon decay. This causes the three body decay width to rise rapidly, and the two body decay width drops. We could, of course, choose a higher cutoff than 5 GeV, but this would only push the problem to a higher mass $P^{0\prime}$. Of course, if we push the cutoff too high, then the entire physical meaning of the cutoff is lost, as we start to exclude events from the three body decays which could be experimentally resolved into a three body decay. Hence we are unable to sensibly separate the gluon decays of the $P^{0\prime}$ into three body and two body decays. The infrared divergences are too severe. The fact that we get an absurd result does not mean that we have done the calculation wrong in some way. It means simply that the infrared divergences in higher order terms is severe enough to be comparable to the corrections we've done, and so the higher orders cannot be ignored if we wish to separate the decays into two gluon and three gluon decays.

Figure 7.7 shows the $\mathcal{O}(\alpha_s)$ corrections to the decay width of $P^{0\prime} \rightarrow gg(g)$, broken up into three separate contributions. The first contribution (the solid line) is from diagrams containing only gluons and ghosts (besides the $P^{0\prime}$ itself, of course). These include all the three body decay diagrams and interference terms between the tree level two gluon decay and the two body diagrams of Figures 7.1a, b, c, d, e, g, h (with the appropriate counterterms). The second contribution (dashed line) comes from the quark triangle diagrams of Figures 7.1j and k. The final contribution (dotted line) comes from quark loop corrections to the gluon propagator (Figures 7.1f, i, and appropriate counterterms). The sum of the three curves of Figure 7.7 is one unit less than the solid curve of Figure 7.6. The difference is that the tree level contribution,

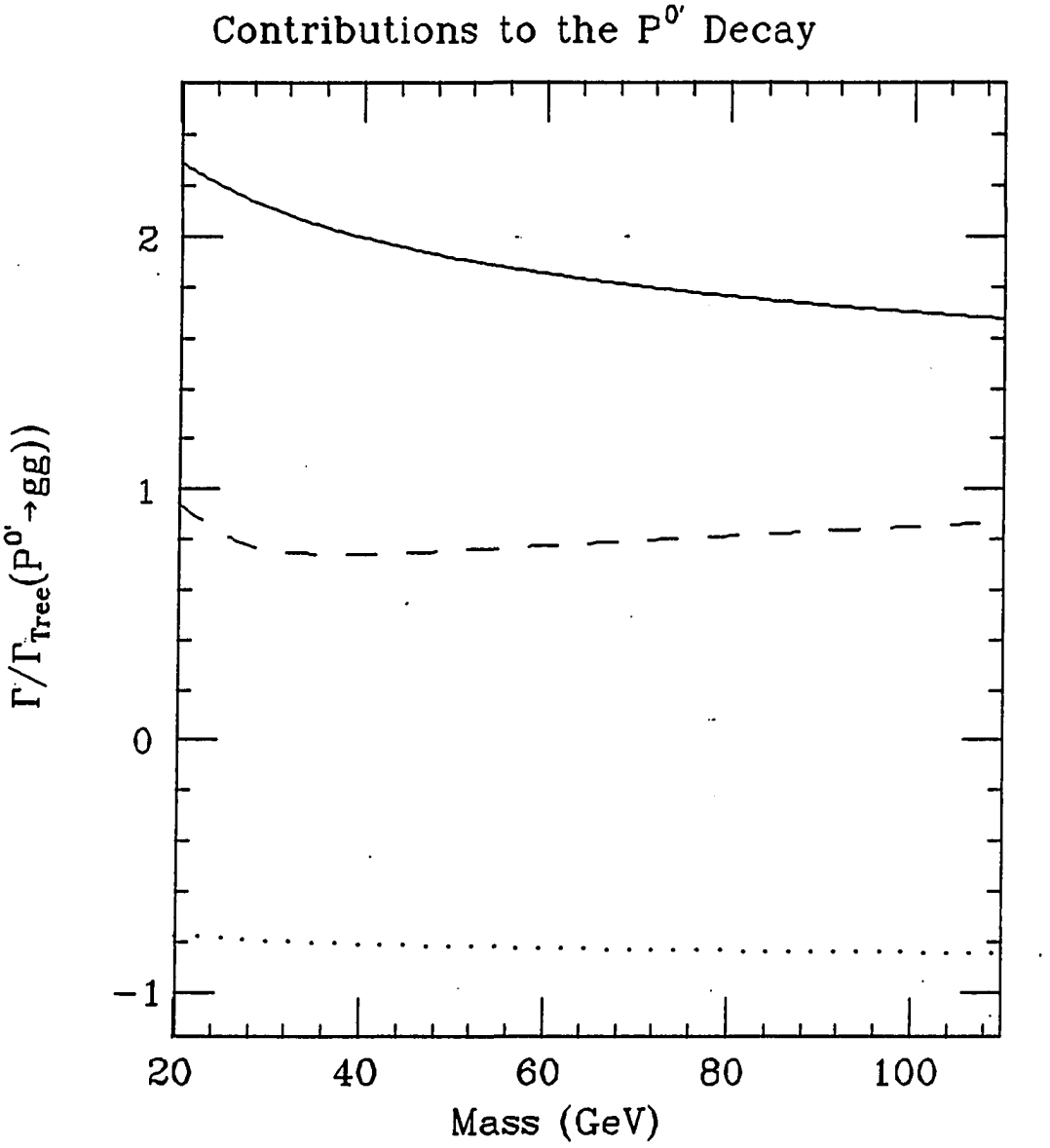

Figure 7.7. Decay width of $P^{0'} \rightarrow gg(g)$, separated by the various virtual processes effecting the decays. The solid line is the contribution from diagrams containing only gluons. The dashed line is from the quark triangle diagrams The dotted line is from quark loop corrections to the gluon propagator

which is 1 in our units, is included in the curves of Figure 7.6.

The quark triangle contribution comes mainly from the t quark. This is especially true for higher mass $P^{0\prime}$. One might expect this contribution to drop dramatically as the $P^{0\prime}$ mass increases. The reason for this is that the width for decays involving the $P^{0\prime}gg$ and $P^{0\prime}ggg$ vertices have a coefficient that goes as M^3, while the overall coefficient in decays involving the $P^{0\prime}\bar{f}f$ vertices goes as Mm_f^2. Hence the quark triangle contribution should decrease swiftly relative to the tree level two gluon decay, and relative to all the other curves of Figure 7.7. However, as the $P^{0\prime}$ mass increases, the virtual t quarks in the loop are closer and closer to mass shell, which provides an enhancement resulting in a slight overall increase in this contribution to the overall width, relative to the tree level gluonic decay width.

In Figure 7.7, the quark triangle contribution is taken to be the same sign as the tree level contribution and the all gluon corrections. There is no reason to assume that this is the case. The parameter a in $G_f = am_f/F_\pi$ could just as easily be negative as positive. Since G_f comes from extended technicolor and the constant Γ comes from the Wess–Zumino–Witten Lagrangian, we have no information *a priori* about the relative signs of these constants. For positive a, we have constructive interference between the quark loop diagrams and the tree level diagram, but we should in general also consider the case of destructive interference as well.

The contribution from quark loop corrections to the gluon propagator, on the other hand, is unambiguously negative. There is, in fact, a very good reason for this. In the limit of massless quarks, there is an infrared divergence in the quark loop diagrams. This infrared divergence is canceled by an infrared divergence in the square of the diagram of Figure 7.8 for the decay $P^{0\prime} \to \bar{q}qg$. Since the square of this diagram

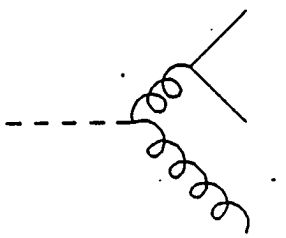

Figure 7.8. A diagram in the decay $P^{0\prime} \to \bar{q}qg$

must be positive and the infrared divergences must cancel, the contribution from the quark loop diagrams must be negative. Also, because of the infrared divergence in the massless quark limit, the largest part of this contribution comes from the lightest quarks.

Because of the infrared divergence, the quark loop contribution in Figure 7.7 is probably unrealistically large. Excluding all of the decay $\bar{q}qg$ of Figure 7.8 from the two gluon decays assumes that we can distinguish, for example, the decay $P^{0\prime} \to \bar{u}ug$ in which the two quarks are collinear from the decay $P^{0\prime} \to gg$. The u quark is simply not massive enough to allow this distinction experimentally, and so we must also consider decays to quarks while we consider decays to gluons.

7.4. Results of $P^{0\prime} \to \bar{q}qg$

Considering decays to quarks as well as gluons brings on a new problem. Namely, we must now perform loop integrals and phase space integrals in an arbitrary number of dimensions with massive particles. (Although we now have massive particles, we still have gluons, and so we still have infrared divergences to regularize.) The combined difficulties of massive particles, arbitrary number of dimensions, and lack of

Lorentz covariance (we still have $\epsilon^{\mu\nu\alpha\beta}$ and γ_5 in the calculation) render the problem intractable. So now we consider the quarks to be massless, at least for the purpose of phase space and loop integrals, except for the t quark, and we assume that the t quark is too heavy for the $P^{0\prime}$ to decay into. The first assumption will not hurt us much, since the $P^{0\prime}$ is almost certainly at least four times as heavy as the b quark. The second assumption is also a safe one, since the lower limit on the t quark mass is around 85 GeV, and the $P^{0\prime}$ mass can only be heavier than 170 GeV through an extreme case of condensate enhancement [19, 20, 21]. Therefore, while it is not impossible that the $P^{0\prime}$ could decay into $\bar{t}t(g)$, it is unlikely.

One should beware that we cannot completely assume the quarks to be massless. In the first place, the coupling $P^{0\prime}\bar{q}q$ is proportional to the quark mass, and so taking quarks to be massless here would eliminate many diagrams that we expect to be significant. Second, some terms which do not actually contain this coupling turn out to be proportional to the mass of a quark. We do not wish to throw these terms out. Instead, we will keep quarks massive in the coupling constant G_f; and for other terms that are proportional to the quark mass, we will keep the lowest order dependence on the quark mass. Effectively, this amounts to taking quarks to be massless in propagators and in the phase space integral, while keeping them massive in the numerators of expressions.

Once we decide to consider massless quarks, we of course introduce new infrared divergences, such as the divergence we just encountered which was formerly regularized by the quark mass. With the entanglement of the infrared divergences between the competing decay mechanisms, it would be a tedious business to separate each of the four decay modes, $P^{0\prime} \to gg$, $P^{0\prime} \to ggg$, $P^{0\prime} \to \bar{q}q$, and $P^{0\prime} \to \bar{q}qg$. Further-

more, we've already seen that this is futile. Hence we just present the total width, first in units of the tree level width, and then the absolute total width.

Finally, it is at this time that we must confront our remaining ultraviolet divergence, from the diagram in Figure 7.2d. Recall that this diagram has an ultraviolet divergence that was not canceled by any counterterms. We cannot use dimensional regularization for this divergence, since that would leave us with the parameter ϵ at the end of our calculation. This parameter, the difference between the number of space-time dimensions and four, has absolutely no physical significance. Instead, we opt for an ultraviolet cutoff, Λ. At the end of the calculation, we can choose the mass scale Λ to be at the scale at which our model is no longer valid. As an example, in employing a cutoff in radiative corrections to Fermi weak interaction theory, one can obtain good results by taking the cutoff to be around the $W^{\pm}$ mass [56]. This is the scale at which four Fermi weak interactions are superseded by the Glashow–Salam–Weinberg model. In the case of our technipion effective Lagrangian, we choose our scale to be about the scale where technipions become observable, which should be around a few TeV. The dependence on Λ will be logarithmic, and so a factor of two or so will make only a small difference.

We start with the amplitude for the diagram of Figure 7.2d:

$$\mathcal{M} = \qquad (7.11)$$
$$2g^2\Gamma C_2(F)\epsilon^{\mu\nu\alpha\beta}\int\frac{d^dl}{(2\pi)^d}\frac{\bar{u}(k_1)\gamma_\alpha(\not{l}+m)\gamma_\beta v(k_2)(l-k_1)_\mu(l+k_2)_\nu}{l^2(l-k_1)^2(l+k_2)^2}.$$

Next, we use Feynman parameter integrals to combine the factors in the denominator, and shift the integration variable to make the denominator symmetric. This gives us

$$\mathcal{M} = 2g^2\Gamma C_2(F)\epsilon^{\mu\nu\alpha\beta}\int_0^1 dxdy2y\int\frac{d^dl}{(2\pi)^d} \qquad (7.12)$$

$$\left\{\frac{\bar{u}(k_1)\gamma_\alpha \not{l}\gamma_\beta v(k_2)[l_\mu(k_1+k_2)_\nu]}{(l^2-Q^2)^3}\right.$$
$$\left.-\frac{m(1-y)^2\bar{u}(k_1)\gamma_\alpha\gamma_\beta v(k_2)k_{1\mu}k_{2\nu}}{(l^2-Q^2)^3}\right\}, \tag{7.13}$$

where $Q^2 = -y^2x(1-x)$. We have now separated the ultraviolet from the infrared divergences. The first term is infrared finite, while the second term is ultraviolet finite. We now insert a factor

$$\frac{-\Lambda^2}{l^2-\Lambda^2} \tag{7.14}$$

in the first term. In the limit $\Lambda \to \infty$, this factor is just 1. For finite Λ, however, this will serve to regularize the loop integral. We can then take $d = 4$ in the first term as well. After that, we continue integrating in a straightforward manner.

It may seem a bit artificial inserting the factor of equation (7.14) in the middle of the calculation. If we attempt to insert the factor earlier in the calculation, however, then we have problems separating the ultraviolet from the infrared divergences. Hence it is necessary that we wait until this point in the calculation to insert the ultraviolet regularization. The rest of the calculation involves nothing new, except for the phase space integrations, summarized in Appendix B.

Finally, we arrive at an expression for the total decay width of the $P^{0\prime}$ where Γ_0 is the lowest order decay width given in Chapter 5:

$$\Gamma(P^{0\prime}) = \Gamma_0(P^{0\prime}) \tag{7.15}$$
$$+\frac{\alpha_s}{32\pi^2}\left\{\Gamma^2(N^2-1)C_2(G)M^3\left[27+\frac{11}{3}\log\frac{\mu^2}{M^2}\right]\right.$$
$$+\Gamma^2(N^2-1)T(F)M^3\left[\frac{4}{3}n_f\left(-\log\frac{\mu^2}{M^2}+\log 2-\frac{53}{15}\right)-\frac{4}{3}\log\frac{\mu^2}{2m_t^2}\right]$$
$$\left.+2\Gamma G_t M m_t T(F)(N^2-1)\left[-\pi^2-4\arctan^2\sqrt{\frac{4m_t^2}{M^2}-1}+4\pi\arctan\sqrt{\frac{4m_t^2}{M^2}-1}\right]\right.$$

$$+\sum_f G_f^2 C_2(F) NM \left[6\log\frac{m_f^2}{M^2}+25\right]$$
$$-12\sum_f \Gamma G_f m_f M C_2(F) N\left(\log\frac{\Lambda^2}{M^2}+2\right)\Bigg\}.$$

The variables here are the same as in equation (7.8) with the additions that the subscript t denotes specifically the t quark, and Λ is our ultraviolet cutoff.

Figure 7.9 shows the $\mathcal{O}(\alpha_s)$ corrections to the decays of the $P^{0\prime}$ in units of the tree level decay. The corrections are less than or about equal to the tree level width. In obtaining the curve of Figure 7.9, we used the following choices for our parameters:

- $N_{TC} = 4$
- $G_f = \frac{m_f}{F_\pi}$
- $\alpha_s(P^2) = \alpha_s(M^2)$ for five quark flavors, so that $\alpha_s \approx .15$ at 50 GeV
- $\mu = M$
- $m_t = 125$ GeV
- $F_\pi = 125$ GeV
- $\Lambda = 3$ TeV.

There are two interesting characteristics to this curve. The first is that the corrections, taken as a whole, are not as overwhelming compared to the total tree level decay as the corrections to the gluon decays were compared to the tree level gluon decay. The reason for this is that the tree level decays are dominated by $P^{0\prime} \to \bar{b}b$. Since we are dividing the corrections by the lowest order decays, including

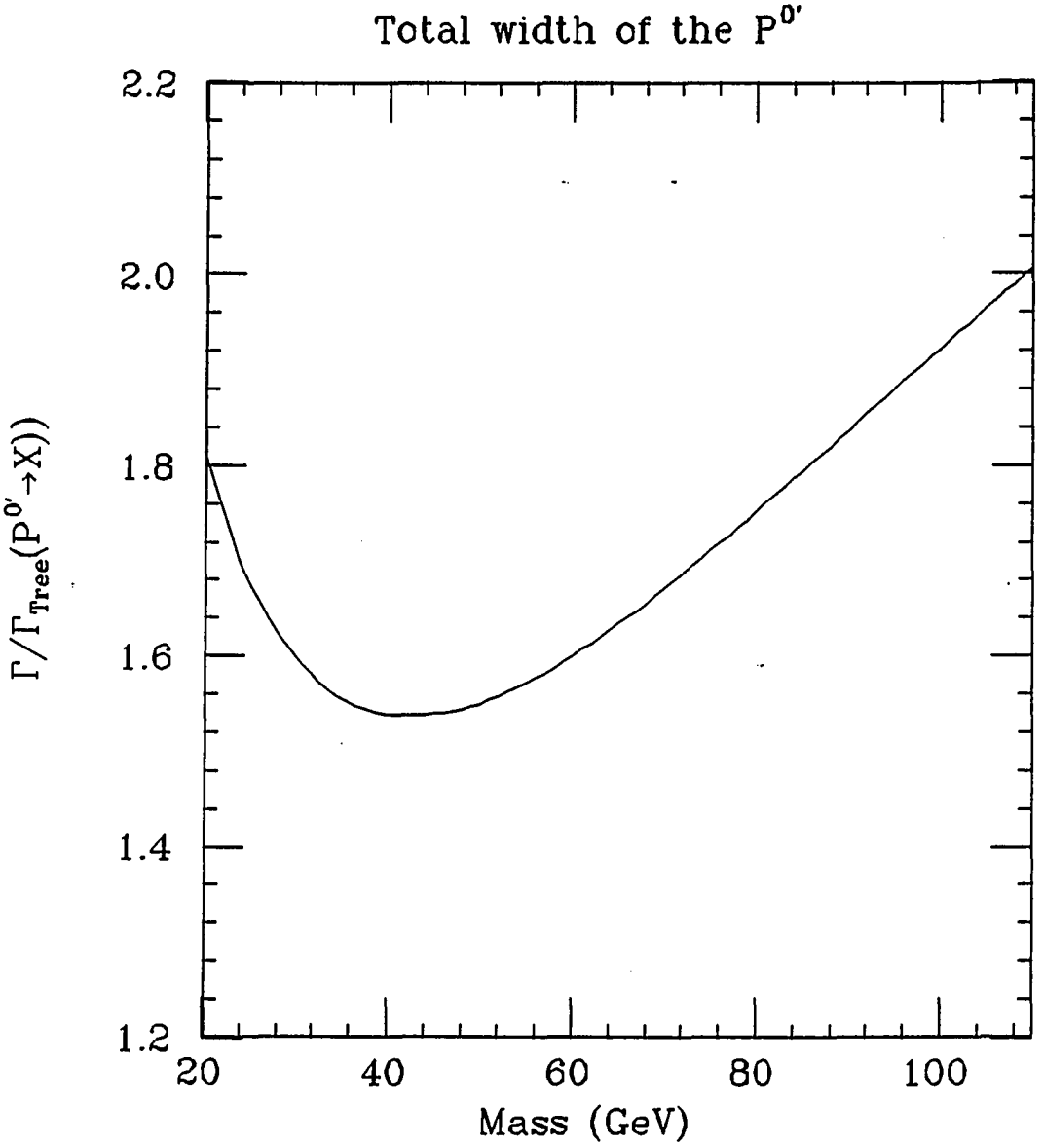

Figure 7.9. The decay width of the $P^{0'}$ in units of the tree level decay width

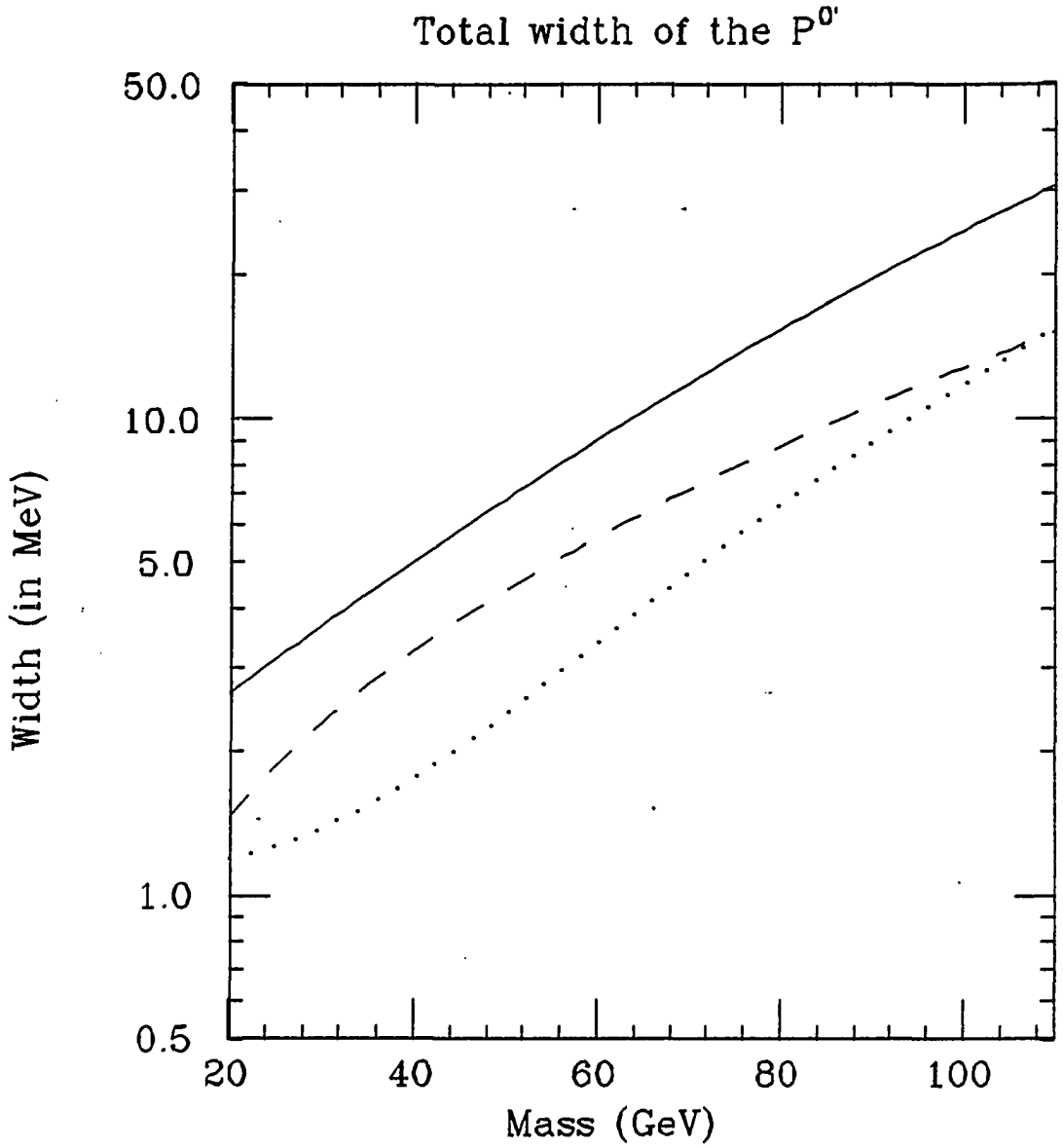

Figure 7.10. Total decay width of the $P^{0'}$ (solid curve) broken down into the corrections (dotted curve) and the tree level decay width (dashed curve)

the tree level $\bar{b}b$ decay with these means dividing the corrections by a larger number, giving a smaller final result than in Figure 7.6. The other feature is the upward slope of the curve after about 35 GeV. This is also attributable to the tree level decay to $\bar{b}b$, which does not climb nearly as quickly as the decays involving the $P^{0\prime}gg$ coupling. For higher $P^{0\prime}$ mass, this decay ceases to dominate, and the corrections, which are dominated by the $P^{0\prime}gg$ coupling, increase relative to the tree level decays.

In Figure 7.10, we have plotted both the tree level decay width and the corrections to that width, in units of MeV. We see again that the tree level dominates at low mass, but loses its dominance for higher mass $P^{0\prime}$. We also see how rapidly the absolute decay width rises as a function of the $P^{0\prime}$ mass, increasing by roughly a full order of magnitude over the range considered.

Of course, these curves are not to be taken as a perfect description of the behavior of the $P^{0\prime}$. There are too many uncertainties for that. We will sum them up here. First of all, the number of technicolors enters into the constant Γ in the $P^{0\prime}gg(g)$ coupling. Second, there is the parameter a in $G_f = am_f/F_\pi$, which describes the $P^{0\prime}\bar{f}f$ coupling. This uncertainty includes not only the magnitude of a, but the sign as well, since the quark triangle correction to the two gluon decay can contribute either constructively or destructively, depending on this sign. Next there is our choice of convention for the Levi-Civita tensor and γ_5. Then there is our choice of 125 GeV for both the t quark mass and the mass scale μ that we introduced in dimensional regularization. Finally, there are, of course, higher order corrections. Since the corrections we've calculated are sizable, we suspect that higher order corrections will make a significant, though hopefully not overwhelming contribution to the $P^{0\prime}$ decay width.

The question then, is what features of our results survive these uncertainties. If a one family technicolor model is the next correct theory of particle physics then we can expect to see a $P^{0\prime}$ with these characteristics:

- The decay width will rise monotonically with the mass of the $P^{0\prime}$. The rate of this rise will become very rapid as the decay becomes dominated by the $P^{0\prime}gg(g)$ couplings.

- QCD corrections will be important in a perturbative approach to $P^{0\prime}$ decays. This will be especially true for a heavy $P^{0\prime}$, since the tree level $\bar{b}b$ decay will be less important.

- Corrections involving $P^{0\prime}\bar{q}q$ couplings will be better behaved (i.e., smaller) than corrections involving $P^{0\prime}gg(g)$ couplings. This is apparently due to the proliferation of diagrams involving the $P^{0\prime}gg(g)$ couplings, occurring because of the non-Abelian nature of QCD, and perhaps due to the momentum dependence of the $P^{0\prime}gg(g)$ coupling. This momentum dependence may allow for a significant contribution from higher momenta in the loop integrations.

- If still higher order corrections contribute constructively to the decay width, as the next to lowest order corrections have, then we can expect the curve of Figure 7.10 to serve as a lower bound on the total decay width of the $P^{0\prime}$.

- For a heavy $P^{0\prime}$, the extended technicolor contribution (responsible for the $P^{0\prime}\bar{q}q$ coupling) will become dominated by the Wess–Zumino–Witten contribution (which gives the $P^{0\prime}gg$ couplings). In this case, then, we are free from the uncertainties in the extended technicolor sector. This will not be the case,

however, in the unlikely event that the $P^{0\prime}$ will be able to decay into $\bar{t}t$.

These are the most important results we've obtained from our calculation.

8. CONCLUSIONS

Our goal in this work has been twofold. First, past phenomonological works in technicolor have considered only the lowest order decays of technipions. We wanted to learn whether the assumption that one can ignore higher order decays is valid by calculating these corrections in order to better understand how technipions, and in particular the $P^{0'}$, decay. Our approach to this problem was to use an effective Lagrangian for technicolor, similar to effective Lagrangians which have been very successful in low energy QCD. Contained within this first goal was our secondary goal, which was simply to prove that such a calculation could be done. Although this sounds nearly trivial, it is far from simple. Our first obstacle was the non-renormalizability of the effective theory, and the ultraviolet divergences which could have prevented us from calculating anything. The second problem we had to confront (which is intertwined with the first) was the question of the regularization of divergences. Finally, we had to eliminate the infrared divergences which arise in a theory with massless particles such as gluons (and quarks in our approximation).

These obstacles have been overcome, and we were able to perform the calculation. First of all, the ultraviolet divergences were eliminated (except for one). We did this by using dimensional regularization, and by realizing that the fields and couplings in the effective Lagrangian must be treated as bare quantities, not as renormalized

quantities. With this understanding, we were able to eliminate all of the ultraviolet divergences but one in the decays of both the $P^{0\prime}$ and the $P_8^{0\prime}$. We regularized the last divergence using an ultraviolet cutoff at the scale at which techniquarks should become apparent.

Next, we had the decision of how to dimensionally regularize the quantities which are specifically four dimensional: $\epsilon^{\mu\nu\alpha\beta}$ and γ_5. Research by Bos [46] related to our model indicated to us that the most appropriate path in this matter was in fact the most difficult one, that is, a Lorentz non-covariant prescription.

Our choice was necessarily tempered by our greatest constraint, which was that the infrared divergences had to cancel when all degenerate final states were taken into account. This constraint was instrumental not only in choosing our regularization scheme for us, but also in choosing our renormalization scheme. We discovered that on shell renormalization was inappropriate for our purpose due to infrared divergences in the renormalization constants. $\overline{\text{MS}}$ renormalization, on the other hand, worked quite well. With all these considerations and constraints, we were able to obtain a result.

We found in the end that ignoring higher order decays and corrections to low order decays is erroneous. We found, first of all, that the total of all the corrections is in fact comparable to the lowest order decay width. Second, we found that separating the two body decays from the three body decays is a hopeless task due to the infrared divergences, and ultimately to the strength of the coupling, α_s. The final picture we obtained of the $P^{0\prime}$ is described in the preceding chapter. We are, unfortunately, left without very precise results. This is due partly to the model dependence of the calculation. We tried to be very general, specifying only that we were dealing with a one family technicolor model. A second source of imprecision is our uncertainty in

regularization. Two different prescriptions for the d-dimensional extensions of $\epsilon^{\mu\nu\alpha\beta}$ and γ_5 yield somewhat different final answers. We are also hampered by our ignorance of the t quark mass, which is an important quantity in the quark triangle diagrams in $P^{0\prime} \to gg$. In the same corrections, we find there is no way to determine the relative signs of two of our constants, and so we are left with interference terms which may be positive or negative. Yet in spite of all these difficulties, we were able to extract some useful results. These are contained in Chapter 7.

Finally, a look to the future. Since the QCD corrections are large, we can virtually ignore the decay of the $P^{0\prime}$ to $\bar{\tau}\tau$. This was the only non-hadronic decay which had any realistic chance of being seen, and with its absence we can simply say that the $P^{0\prime}$ will decay to jets. We are, unfortunately, unable to say how many jets, as we saw in Chapter 7. In an actual search for the $P^{0\prime}$, one is armed only with the knowledge that one should expect jets, the lower limit given in Figure 7.10 for the width, and perhaps the production cross sections. (See Chapter 5, for example.) The prospects for detection in hadron colliders are rather bleak. (See, however, reference [39].) A more hopeful place to look for the $P^{0\prime}$ may be in rare Z^0 decays at LEP. The Wess–Zumino–Witten Lagrangian which we have been using for $P^{0\prime}gg$ couplings also contains couplings of the form $P^{0\prime}Z^0\gamma$. These direct couplings to gauge bosons are one way in which the $P^{0\prime}$ differs from the ordinary Higgs. If the $P^{0\prime}$ is less massive than the Z^0, then the Z^0 can decay into a $P^{0\prime}$ and a photon. Although this decay would be rare ($\mathcal{O}(\alpha^2)$) the single photon coming off at fixed energy could be a distinctive signal. But that is another story.

9. BIBLIOGRAPHY

[1] There are many reviews of the standard model. See for example, T.-P. Cheng and L.-F. Li, *Gauge Theory of Elementary Particle Physics* (Oxford University Press, New York, 1984); C. Quigg, *Gauge Theories of the Strong, Weak, and Electromagnetic Interactions* (Benjamin/Cummings, Menlo Park, CA, 1983); K. Huang, *Quarks, Leptons, and Gauge Fields* (World Scientific, Singapore, 1982).

[2] C.N. Yang and R.L. Mills, *Phys. Rev.* **96**, 191 (1954).

[3] L. Fadeev and V.N. Popov, *Phys. Lett.* **25B**, 29 (1967).

[4] S. Weinberg, *Phys. Rev. Lett.* **19**, 1264 (1967); A. Salam, in *Elementary Particle Theory*: Relativistic Groups and Analyticity (Nobel Symposium No. 8), edited by N. Svartholm (Almqvist and Wiksell, Stockholm, 1968), p. 367.

[5] P. Higgs, *Phys. Rev. Lett.* **12**, 132 (1964); **13**, 509 (1964); *Phys. Rev.* **145**, 1156 (1966).

[6] M. Kobayashi and K. Maskawa, *Prog. Theo. Phys.* **49**, 652 (1973).

[7] S.L. Glashow, J. Iliopoulos, and L. Maiani, *Phys. Rev.* **D2**, 1285 (1970).

[8] *Beyond the Standard Model*, edited by K. Whisnant and B.-L. Young (World Scientific, Singapore, 1989).

[9] H. Georgi and S.L. Glashow, *Phys. Rev. Lett.* **32**, 438 (1974).

[10] L. Susskind, *Phys. Rev.* **D20**, 2619 (1979); S. Weinberg, Phys. Rev. **D19**, 1277 (1979).

[11] The best review of technicolor is still E. Farhi and L. Susskind, *Phys. Rep.* **74**, No. 3, 277 (1981).

[12] D. Gross and F. Wilczek, *Phys. Rev. Lett.* **30**, 1343 (1973); H.D. Politzer, *Phys. Rev. Lett.* **30**, 1346 (1973).

[13] See for example M. Peskin, in *Recent Advances in Field Theory and Statistical Mechanics*, edited by J.B. Zuber and R. Stora (North Holland, Amsterdam, 1984), p. 217.

[14] Y. Nambu, *Phys. Rev. Lett.* **4**, 380 (1960); Y. Nambu and G. Jona-Lasinio, *Phys. Rev.* **122**, 345 (1961); J. Goldstone, *Nuovo Cimento* **19**, 154 (1961); J. Goldstone, A. Salam, and S. Weinberg, *Phys. Rev.* **127**, 965 (1962).

[15] S. Dimopoulos and L. Susskind, *Nucl. Phys.* **B155**, 237 (1979); E. Eichten and K. Lane, *Phys. Lett.* **90B**, 125 (1980).

[16] S. Dimopoulos and J. Ellis, *Nucl. Phys.* **B182**, 321 (1981); J. Ellis, M.K. Gaillard, D.V. Nanopoulos, and P. Sikivie, *Nucl. Phys.* **B182**, 529 (1981).

[17] S. Dimopoulos, H. Georgi, and S. Raby, *Phys. Lett.* **127B**, 101 (1983); S.-C. Chao and K. Lane, *Phys. Lett.* **159B**, 135 (1985).

[18] R. Chivukula and H. Georgi, *Phys. Lett.* **188B**, 99 (1987); R. Chivukula, H. Georgi, and L. Randall, *Nucl. Phys.* **B292**, 93 (1987).

[19] T. Appelquist and L.C.R. Wijewardhana, *Phys. Rev.* **D36**, 568 (1987).

[20] B. Holdom, *Phys. Rev.* **D24**, 1441 (1981); K. Yamawaki, M. Bando, and K. Matumoto, *Phys. Rev. Lett.* **56**, 1335 (1986).

[21] T. Appelquist, M. Einhorn, T. Takeuchi, and L.C.R. Wijewardhana, *Phys. Lett.* **220B**, 223 (1989).

[22] J. Wess and B. Zumino, *Phys. Lett.* **37B**, 95 (1971).

[23] E. Witten, *Nucl. Phys.* **B223**, 422 (1983).

[24] S. Adler, *Phys. Rev.* **177**, 2426 (1969); J.S. Bell and R. Jackiw, *Nuovo Cim.* **60A**, 47 (1969).

[25] J.C. Ward, *Phys. Rev.* **78**, 1824 (1950); Y. Takahashi, *Nuovo Cim.* **6**, 370 (1957).

[26] Ö. Kaymakcalan, S. Rajeev, and J. Schechter, *Phys. Rev.* **D30**, 594 (1984).

[27] R. Dashen, *Phys. Rev.* **183**, 1245 (1969).

[28] M. Peskin, *Nucl. Phys.* **B175**, 245 (1980); J. Preskill, *Nucl. Phys.* **B177**, 282 (1981).

[29] J. Ellis, M.K. Gaillard, D.V. Nanopoulos, and P. Sikivie, *Nucl. Phys.* **B182**, 529 (1981).

[30] E. Eichten, I. Hinchliffe, K. Lane, and C. Quigg, *Phys. Rev.* **D34**, 1547 (1986).

[31] H. Georgi, S. Glashow, M. Machacek, and D. Nanopoulos, *Ann. Phys.* (N.Y.) **114**, 273 (1978).

[32] W.-C. Kuo, D. Slaven, and B.-L. Young, *Phys. Rev.* **D37**, 233 (1988).

[33] J.C. Taylor, *Nucl. Phys.* **B33**, 436 (1971); A. A. Slavnov, *Theor. Math. Phys.* **10**, 99 (1972).

[34] F.A. Berends et al., *Phys. Lett.* **103B**, 124 (1981); P. de Causmaecker et al., *Nucl. Phys.* **B206**, 53 (1982); Z. Xu, D.H. Zhang, and L. Chang, *Nucl. Phys.* **B291**, 392 (1987).

[35] S.J. Parke and T.R. Taylor, *Phys. Lett.* **157B**, 81 (1985); *Phys. Rev. Lett.* **56**, 2459 (1986).

[36] D. McKay, D. Slaven, and B.-L. Young, *Phys. Rev.* **D34**, 3394 (1986).

[37] W.-C. Kuo, D. McKay, and B.-L. Young, *Phys. Rev.* **D36**, 2729 (1987).

[38] D. Duke, and J. Owens, *Phys. Rev.* **D30**, 49 (1984).

[39] W.-C. Kuo, Ph.D. thesis, Iowa State University, 1990.

[40] For a review of renormalization, see D. Bailin and A. Love, *Introduction to Gauge Field Theory* (Adam Hilger, Boston, 1986); T.-P. Cheng and L.-F. Li, *Gauge Theory of Elementary Particle Physics* (Oxford University Press, New York, 1984); B.-L. Young *Introduction to Quantum Field Theory* (Science Press, Beijing, 1987).

[41] G. 't Hooft, and M. Veltman, *Nucl. Phys.* **B44**, 189 (1972); C. Bollini and J. Giambiagi, *Phys. Lett.* **40B**, 566 (1972); J. Ashmore, *Lett. Nuovo Cim.* **4**, 289 (1972).

[42] J. Collins *Renormalization* (Cambridge University Press, Cambridge, 1984), pp. 83–87, 334–337.

[43] J.G. Körner, N. Nasrallah, and K. Schilcher, *Phys. Rev.* **D41**, 888 (1990).

[44] M. Chanowitz, M. Furman, and I. Hinchliffe, *Nucl. Phys.* **B159**, 225 (1979).

[45] P. Breitenlohner and D. Maison, *Commun. Math. Phys.* **52**, 11 (1977).

[46] M. Bos, *Annals of Phys.* **181**, 177 (1988).

[47] For a still more explicit demonstration in QED, see B.-L. Young, *Introduction to Quantum Field Theory* (Science Press, Beijing, 1987).

[48] W.A. Bardeen, A. Buras, D.W. Duke, and T. Muta, *Phys. Rev.* **D18**, 3998 (1978).

[49] G. 't Hooft, *Nucl. Phys.* **B61**, 455 (1973).

[50] G. 't Hooft, *Nucl. Phys.* **B33**, 173 (1971); **B35**, 167 (1971).

[51] Y.-P. Yao, *Phys. Rev. Lett.* **36**, 653 (1976).

[52] A. Sugamoto, *Phys. Rev.* **D16**, 1065 (1977).

[53] S. Pokorski, *Gauge Field Theories* (Cambridge University Press, Cambridge, 1987), pp. 90–94.

[54] See for example, J. Bjorken and S. Drell, *Relativistic Quantum Fields* (McGraw–Hill, New York, 1965), pp. 132–137.

[55] K.-I. Aoki et al., *Supplement of the Progress of Theoretical Physics*, No. 73, 1 (1982).

[56] R. Peccei, in *Particles, Strings, and Supernovae*: Proceedings of the Theoretical Advanced Study Institute in Elementary Particle Physics, edited by A. Jevicki and C.-I. Tan (World Scientific, New Jersey, 1989), p. 1.

[57] R. Field, *Applications of Perturbative QCD*, (Addison–Wesley, Reading, MA, 1989), pp. 42–46.

10. ACKNOWLEDGMENTS

This dissertation would not have been possible without the guidance and concern of my advisor, Bing-Lin Young. In addition, I have benefited from many afternoons of bouncing my ideas off of Wang-Chuang Kuo, and listening to his ideas as well. Finally, I would like to thank Linda Shuck, who never refused me anything.

Furthermore, this work was performed at Ames Laboratory under contract W-7405-Eng-82 with the U.S. Department of Energy. The United States government has assigned the DOE Report number IS-T 1391 to this thesis.

11. APPENDIX A: FEYNMAN RULES

We begin by listing the Feynman rules for QCD. These are shown in Figures 11.1 and 11.2.

Next we will extract the Feynman rules for the couplings of $P^{0\prime}$ and $P_8^{0\prime}$ to gluons. These come from the effective Lagrangian defined by equations (3.21), (3.29), (3.30), and (3.32). We repeat them here for easy reference:

$$\mathcal{L} = \frac{F_\pi^2}{4}\mathrm{Tr}(D_\mu U)(D^\mu U^\dagger), \tag{11.1}$$

where

$$\begin{aligned} D_\mu U &= \partial_\mu U + ig[G_\mu, U] \\ D_\mu U^\dagger &= \partial_\mu U^\dagger + ig[G_\mu, U^\dagger], \end{aligned} \tag{11.2}$$

and $G_\mu = G_\mu^a \Lambda^a$. Also,

$$\tilde{\Gamma}(U, G_\mu) = \Gamma(U) + \frac{N}{48\pi^2}\int d^4x \epsilon_{\mu\nu\alpha\beta} Z^{\mu\nu\alpha\beta}, \tag{11.3}$$

where

$$\begin{aligned} Z^{\mu\nu\alpha\beta} = &-\mathrm{Tr}\left[G^\mu U_L^\nu U_L^\alpha U_L^\beta + (L \to R)\right] \\ &+i\mathrm{Tr}\left\{\left[(\partial^\mu G^\nu G^\alpha + G^\mu \partial^\nu G^\alpha)\right] U_L^\beta + (L \to R)\right\} \\ &-i\mathrm{Tr}\left[(\partial^\mu G^\nu)(\partial^\alpha U) G^\beta U^\dagger - (\partial^\mu G^\nu)(\partial^\alpha U^\dagger) G^\beta U\right] \\ &-i\mathrm{Tr}\left[G^\mu U^\dagger G^\nu U U_R^\alpha U_R^\beta - G^\mu U G^\nu U^\dagger U_L^\alpha U_L^\beta\right] \end{aligned}$$

$$
\begin{aligned}
&-\frac{i}{2}\mathrm{Tr}\left[G^\mu U_L^\nu G^\alpha U_L^\beta - (L \to R)\right] \\
&-\mathrm{Tr}\left[G^\mu G^\nu G^\alpha U_L^\beta + (L \to R)\right] \\
&-\mathrm{Tr}\left\{\left[(\partial^\mu G^\nu)G^\alpha + G^\mu(\partial^\nu G^\alpha)\right] U^\dagger G^\beta U\right. \\
&\qquad \left. - \left[(\partial^\mu G^\nu)G^\alpha + G^\mu(\partial^\nu G^\alpha)\right] U G^\beta U^\dagger\right\} \\
&-\mathrm{Tr}\left(G^\mu U G^\nu U^\dagger G^\alpha U_L^\beta + G^\mu U^\dagger G^\nu U G^\alpha U_R^\beta\right) \\
&-i\mathrm{Tr}\left(G^\mu G^\nu G^\alpha U^\dagger G^\beta U - G^\mu G^\nu G^\alpha U G^\beta U^\dagger\right. \\
&\qquad \left. -\frac{1}{2}G^\mu G^\nu U G^\alpha G^\beta U^\dagger + \frac{1}{2}G^\mu U^\dagger G^\nu U G^\alpha U^\dagger G^\beta U\right),
\end{aligned}
\tag{11.4}
$$

and $U_L^\mu = (\partial^\mu U)U^\dagger$, and $U_R^\mu = U^\dagger(\partial^\mu U)$.

The generators, Λ^a in G_μ are

$$
\Lambda^a = \begin{pmatrix} T^a & 0 \\ 0 & T^a \end{pmatrix}. \tag{11.5}
$$

We don't need to consider all the $SU(8)$ generators in the expansion of U, since we are only interested in $P_8^{0'}$ and $P_8^{0'}$. The generators for $P_8^{0'}$ are $1/\sqrt{2}$ times those

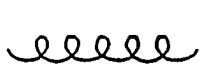

$$\frac{i\delta_{ab}}{k^2}\left[-g_{\mu\nu}+(1-\xi)\frac{k_\mu k_\nu}{k^2}\right]$$

$$\frac{i(\not{p}+m)}{p^2-m^2}$$

$$\frac{i\delta_{ab}}{k^2}$$

$$\frac{i}{k^2-m^2}$$

Figure 11.1. Propagators for a gluon, fermion, Fadeev–Popov ghost, and scalar particle

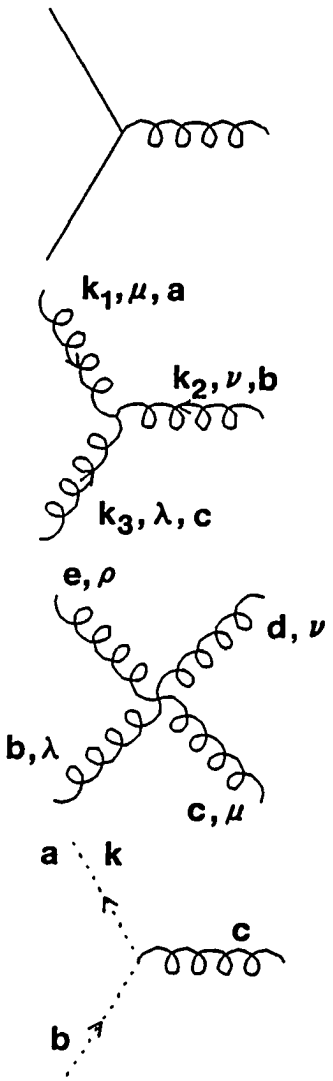

$$-ig\gamma_\mu T^a$$

$$gf^{abc}[(k_2-k_1)_\lambda g_{\mu\nu}+(k_3-k_2)_\mu g_{\nu\lambda}+(k_1-k_3)_\nu g_{\lambda\mu}]$$

$$\begin{aligned}-ig^2[&f^{abc}f^{ade}(g_{\lambda\nu}g_{\mu\rho}-g_{\mu\nu}g_{\lambda\rho})\\&+f^{adc}f^{abe}(g_{\lambda\nu}g_{\mu\rho}-g_{\mu\lambda}g_{\nu\rho})\\&+f^{abd}f^{ace}(g_{\lambda\mu}g_{\nu\rho}-g_{\mu\nu}g_{\lambda\rho})]\end{aligned}$$

$$-gf^{abc}k_\mu$$

Figure 11.2. Feynman rules for vertices in QCD

in (11.5), while the generator for $P^{0'}$ is

$$\Lambda^0 = \frac{1}{4\sqrt{3}} \left(\begin{array}{cccc|cccc} 1 & & & & & & & \\ & 1 & & & & & 0 & \\ & & 1 & & & & & \\ & & & -3 & & & & \\ \hline & & & & 1 & & & \\ & & & & & 1 & & \\ & & 0 & & & & 1 & \\ & & & & & & & -3 \end{array} \right). \tag{11.6}$$

These can be seen from Table (3.1) which displays the technipion spectrum and the techniquark content of each technipion. Note that

$$[\Lambda^0, \Lambda^a] = 0 \tag{11.7}$$

and

$$[\Lambda^a, \Lambda^b] = i f^{abc} \Lambda^c.$$

Now we can discover the relevant terms in our Lagrangian. We do this by expanding U to lowest order in the technipions and keeping only those terms containing ϕ_0 and ϕ_8 (the fields corresponding to $P^{0'}$ and $P_8^{0'}$). In the ordinary (non-anomalous) part of the Lagrangian, there is no coupling between $P^{0'}$ and gluons, since Λ^0 commutes with all the Λ^a (cf. equation 11.2, the covariant derivative). This leaves us with couplings between gluons and the $P_8^{0'}$ of the form

$$2ig\mathrm{Tr}\left(G_\mu[\phi_8, \partial^\mu \phi_8] + igG_\mu \phi_8 [G^\mu, \phi_8]\right) \tag{11.8}$$

which can be rewritten (after taking the traces)

$$\frac{1}{2}(D_\mu \phi_8^a)^2 \tag{11.9}$$

where the covariant derivative operating on ϕ_8^a is defined as

$$D_\mu \phi_8^a - \frac{1}{2} g f^{abc} G_\mu^b \phi_8^c. \tag{11.10}$$

Finding the terms we're looking for amidst the anomalous Lagrangian appears to be a somewhat daunting assignment. However, we know a few things about the terms we're looking for, so it isn't so bad. First of all, since the gluons are all Lorentz vectors and $\epsilon^{\mu\nu\alpha\beta}$ is a pseudotensor, we know we only need to look for terms with one pseudoscalar, since the Lagrangian as a whole is parity invariant. Second, since any term in the derivative of U must contain at least one pseudoscalar, we can ignore any term in (11.4) which contains more than one derivative of U such as the first term containing $U_L^\nu U_L^\alpha U_L^\beta$. This simplifies the job.

The end result is

$$\begin{aligned} &\frac{-N_{TC} g^2}{4\pi^2 F_\pi} \epsilon^{\mu\nu\alpha\beta} \mathrm{Tr} \Big\{ (\phi_0 + \phi_8)(\partial_\mu G_\nu)(\partial_\alpha G_\beta) \\ &\quad + ig(\phi_0 + \phi_8)[(\partial_\mu G_\nu) G_\alpha G_\beta + G_\mu G_\nu (\partial_\alpha G_\beta)] \\ &\quad - g^2 (\phi_0 + \phi_8) G_\mu G_\nu G_\alpha G_\beta \Big\} \\ = \; &\frac{-N_{TC} g^2}{16\pi^2 F_\pi} \left\{ \frac{1}{4\sqrt{3}} \phi_0 G_{\mu\nu}^a \tilde{G}^{a\mu\nu} + \frac{1}{2\sqrt{2}} d^{abc} \phi_8^a G_{\mu\nu}^b \tilde{G}^{c\mu\nu} \right\} \end{aligned} \tag{11.11}$$

where we have taken the trace to obtain the latter expression, and $G_{\mu\nu}^b$ is $\partial_\mu G_\nu^a - \partial_\nu G_\mu^a - g f^{abc} G_\mu^b G_\nu^c$, same as always. d^{abc} are the symmetric structure constants for $SU(3)$ defined by

$$\{T^a, T^b\} = \frac{1}{N} \delta^{ab} + d^{abc} T^c \tag{11.12}$$

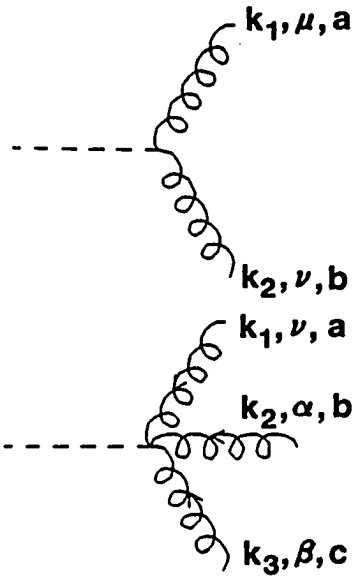

$$2i\Gamma\epsilon^{\mu\nu\alpha\beta}\delta^{ab}k_{1\alpha}k_{2\beta}$$

$$-2g\Gamma\epsilon_{\mu\nu\alpha\beta}f^{abc}(k_1+k_2+k_3)_\mu$$

Figure 11.3. Feynman rules for couplings between the $P^{0'}$ and gluons from the anomalous Lagrangian

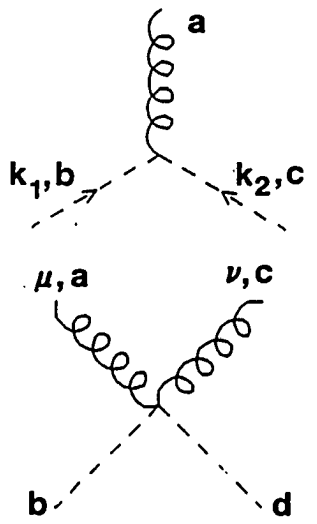

$$-gf^{abc}(k_2-k_1)_\mu$$

$$ig^2g_{\mu\nu}(f^{abe}f^{cde}+f^{ade}f^{cbe})$$

Figure 11.4. Feynman rules for couplings between the $P_8^{0'}$ and gluons from the ordinary Lagrangian

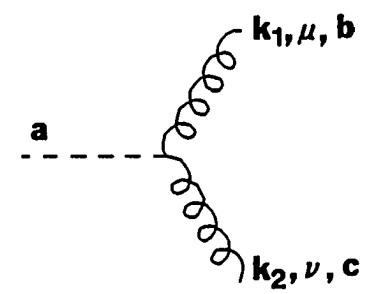

$$2i\Gamma' \epsilon^{\mu\nu\alpha\beta} d^{abc} k_{1\alpha} k_{2\beta}$$

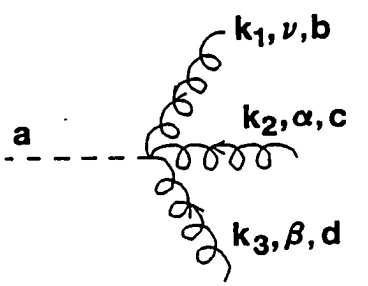

$$-2g\Gamma' \epsilon^{\mu\nu\alpha\beta} (d^{abe} f^{cde} k_{1\mu} + d^{ace} f^{dbe} k_{2\mu} + d^{ade} f^{bce} k_{3\mu})$$

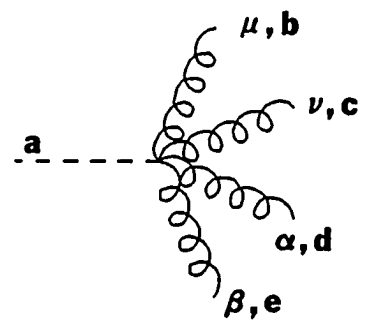

$$2ig^2\Gamma' \epsilon^{\mu\nu\alpha\beta} d^{afg} (f^{bcf} f^{deg} + f^{bdf} f^{ecg} + f^{bef} f^{cdg})$$

Figure 11.5. Feynman rules for couplings between the $P_8^{0'}$ and gluons from the anomalous Lagrangian

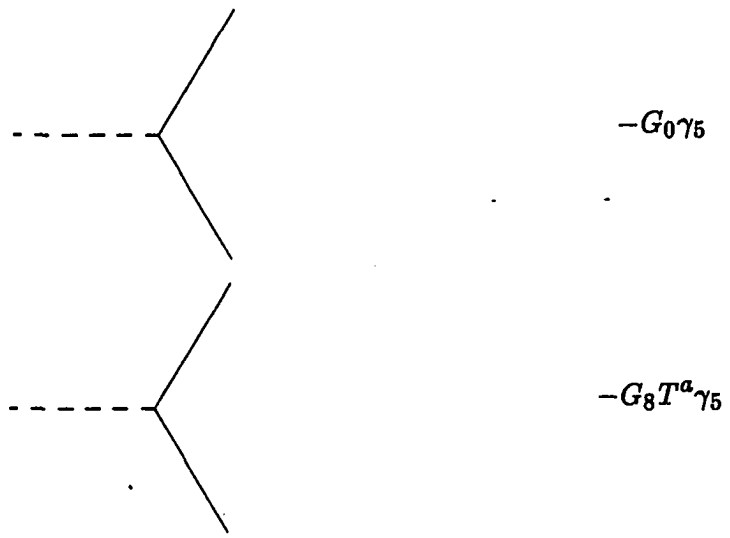

Figure 11.6. Feynman rules for technipion–fermion couplings arising from extended technicolor

for $SU(N)$ where the braces denote anti-commutation.

Finally, the Lagrangians of equations (11.9) and (11.11) yield the Feynman rules of Figures 11.3, 11.4, and 11.5, where

$$\Gamma = -\frac{N_{TC}g^2}{16\sqrt{3}\pi^2 F_\pi} \tag{11.13}$$

and

$$\Gamma' = -\frac{N_{TC}g^2}{8\sqrt{2}\pi^2 F_\pi}. \tag{11.14}$$

This leaves us with the couplings of the technipions to fermions from extended technicolor. The rules for these vertices are given in Figure 11.6 where both G_0 and G_8 are assumed to be of $\mathcal{O}(m_f/F_\pi)$. Remember that the $P_8^{0'}$ couples only to quarks, while the $P^{0'}$ couples to leptons as well. These Feynman rules, along with those for the counterterms given in chapters 6 and 7, are all the ones that we'll need.

12. APPENDIX B: INTEGRATIONS OVER PHASE SPACE

12.1. Two Body Phase Space in Four Dimensions

In four dimensions, two body Lorentz invariant phase space is just

$$\frac{d^4k_1}{(2\pi)^3}\frac{d^4k_2}{(2\pi)^3}\delta(k_1^2-m_1^2)\delta(k_2^2-m_2^2)(2\pi)^4\delta^4(P-k_1-k_2), \tag{12.1}$$

where the first two δ functions put the particles on mass shell, the last δ function provides 4-momentum conservation, and P is the total 4-momentum of the system. It is important to note that (12.1) is a Lorentz invariant. If the square of the amplitude of the process in question is rotationally invariant, we can completely integrate this. This will be the case for decay processes, since even for decays of particles with spin, we generally average over the initial spin state, washing out the directional dependence. Then we get

$$\frac{1}{8\pi}\left[1-2\frac{m_1^2+m_2^2}{s}+\frac{(m_1^2-m_2^2)^2}{s^2}\right]^{1/2}, \tag{12.2}$$

where s is the square of the center of mass energy ($s=P^2$). For massless particles, this is just $1/8\pi$.

12.2. Three Body Phase Space in Four Dimensions

In Chapter 5, we examined three body decays of $P^{0\prime}$. Here we'll focus on just the decay $P^{0\prime}\rightarrow ggg$, but the discussion is easily generalized. In order to arrive at

the decay width for this decay mode, it was necessary to integrate over three body phase space,

$$\frac{d^4k_1}{(2\pi)^3}\frac{d^4k_2}{(2\pi)^3}\frac{d^4k_3}{(2\pi)^3}(2\pi)^4\delta^4(P-k_1-k_2-k_3)\delta(k_1^2)\delta(k_2^2)\delta(k_3^2). \tag{12.3}$$

In phase space integrals, the expressions

$$\frac{d^3k}{2E} \rightleftharpoons d^4k\,\delta(k^2) \tag{12.4}$$

are interchangeable, the former derived from the latter by integrating dk^0 with the δ function. We have adopted the four-dimensional form, since we usually wish at some point to integrate a d^4k with $\delta^4(P-k_1-k_2-k_3)$.

In the three body phase space, we have the problem of the infrared divergences to deal with. In Chapter 5, we said that we would regulate the infrared by using a cutoff in the invariant mass of any two gluon system. We can accomplish this by inserting factors such as

$$1 = \int dM_{12}^2\,\delta[(k_1+k_2)^2 - M_{12}^2], \tag{12.5}$$

where M_{12} is defined by the δ function as the invariant mass of the two gluons, 1 and 2. The regularization is achieved by imposing limits on these invariant mass integrals that do not include all of phase space. Actual choices for these limits are discussed in Chapter 5.

How we make these insertions depends on the divergence of the particular term we're integrating. For example, if we're integrating a term with a denominator $(k_1+k_2)^2$, we can regularize this infrared divergence by inserting the factor shown in (12.5), and controlling the limits of the M_{12}^2 integration. On the other hand, if

the denominator looks like $(k_1+k_2)^2(k_2+k_3)^2$, then we must insert

$$\int dM_{12}^2\,\delta[(k_1+k_2)^2-M_{12}^2]\int dM_{23}^2\,\delta[(k_2+k_3)^2-M_{23}^2], \tag{12.6}$$

and cutoff the integration of both M_{12}^2 and M_{23}^2.

Other than this, the integration is rather tedious, but straightforward. Most of it can be done analytically, while a few terms involving Spence functions were done numerically. The results are given in Chapter 5.

12.3. Phase Space in d Dimensions

In order to cancel the infrared divergences, we chose the gauge invariant method of dimensional regularization. As a result, when we are calculating the full $\mathcal{O}(\alpha_s)$ corrections to technipion decay processes, we must perform phase space integration in d dimensions. This is not difficult in the case of massless particles in the final state and a Lorentz covariant integrand [57]. It becomes much more difficult if the integrand is not covariant.

12.3.1. Two Body Phase Space

In d dimensions, two body phase space takes on the form

$$(\mu^2)^{2-d/2}\frac{d^{d-1}k_1}{(2\pi)^{d-1}2E_1}\frac{d^{d-1}k_2}{(2\pi)^{d-1}2E_2}(2\pi)^d\delta^d(P-k_1-k_2), \tag{12.7}$$

where again we can substitute at will

$$\frac{d^{d-1}k}{2E}\rightleftharpoons d^dk\,\delta(k^2), \tag{12.8}$$

and we've assumed that the particles are massless. We see the same parameter, μ^2, that we saw in Chapter 6, and it serves the same purpose here: to keep the coupling constant dimensionless.

Angular integration in d dimensions is different from that in four dimensions. In d-dimensional space-time,

$$d^{d-2}\Omega = \sin^{d-3}\theta_1 \sin^{d-4}\theta_2 \ldots \sin\theta_{d-3} d\theta_1\, d\theta_2 \ldots d\theta_{d-2}. \tag{12.9}$$

(We work in more than four dimensions for convenience. The final result will be continued to arbitrary, including non-integer, dimensions.) The ranges of the angles in (12.9) are from 0 to π except for θ_{d-2} which runs from 0 to 2π. The integration can be performed with the help of the identity

$$\int_0^{\frac{\pi}{2}} \cos^m \sin^n \theta d\theta = \frac{1}{2} B\left(\frac{m+1}{2}, \frac{n+1}{2}\right), \tag{12.10}$$

where $B(a,b)$ is the beta function

$$B(a,b) = \frac{\Gamma(a)\Gamma(b)}{\Gamma(a+b)}. \tag{12.11}$$

In addition, we can use the identity

$$\Gamma\left(a+\frac{1}{2}\right) = \frac{\sqrt{\pi}\Gamma(2a)}{2^{2a-1}\Gamma(a)} \tag{12.12}$$

to express gamma functions with half-integer arguments in terms of gamma functions with integer arguments.

If there is no dependence on the angles $\theta_1, \ldots, \theta_{d-2}$, then we can integrate this immediately. We get

$$\int d^{d-2}\Omega = (4\pi)^{1-\epsilon} \frac{\Gamma(1-\epsilon)}{\Gamma(2-2\epsilon)}, \tag{12.13}$$

where again $\epsilon = 2 - d/2$. In both (12.9) and (12.13) we can see that the four-dimensional result is recovered as $\epsilon \to 0$. We can, in fact, finish the phase space integral if there is no angular dependence. The result of this is

$$\frac{1}{8\pi}\left(\frac{4\pi\mu^2}{P^2}\right)^{\epsilon} \frac{\Gamma(1-\epsilon)}{\Gamma(2-2\epsilon)}. \tag{12.14}$$

Again we see the four-dimensional result reproduced as $\epsilon \to 0$.

In the case of a spinless particle decay in which the integrand is Lorentz covariant, there is no angular dependence and we can simply use (12.14) as our result. We are especially interested, however, in the case where the integrand is *not* Lorentz covariant. The non-covariant prescription for the dimensional regularization of $\epsilon^{\mu\nu\alpha\beta}$ leads to terms in the integrand such as $\underline{k}_1^2$ and $\underline{k}_1 \cdot \underline{k}_2$, which are the products of d-dimensional vectors truncated to four dimensions.

To handle this case, we start by integrating k_2. We integrate $d^d k_2$ with the δ function, and use the substitution (12.8) with the momentum k_1. This gives us

$$\frac{d^{d-1}k_1}{(2\pi)^{d-2}2E_1}\delta[(P-k_1)^2]. \tag{12.15}$$

For convenience, we will work in the center of mass, and in units where $P^2 = 1$, so that $P = (1,0,0,\ldots)$. The non-covariant quantities that we'll have to worry about are just $\underline{k}_1^2$, $\underline{P}^2$, and $\underline{P} \cdot \underline{k}_1$. (Remember, we've integrated k_2 already.) But in the center of mass, the last two quantities are just $P_0^2 = 1$ and $P_0 E_1 = E_1$. Hence the only non-covariant quantity in our integrand will be $\underline{k}_1^2$. Phase space has now become

$$\frac{d^{d-1}k_1}{(2\pi)^{d-2}2E_1}\delta(1-2E_1)|\mathcal{M}|^2, \tag{12.16}$$

where we have now included the square of the amplitude.

In order to make the integral easy, we choose a parametrization for k_1 which will make $\underline{k}_1^2$ take on a simple form. First we separate the real four dimensions of k_1 from the extra dimensions, and put each set of dimensions into polar coordinates.

$$\begin{aligned} k_1 \;=\; (E_1, &\underline{K}\cos\theta_1, \underline{K}\sin\theta_1\cos\theta_2, \underline{K}\sin\theta_1\sin\theta_2, \\ &\underline{K}\cos\phi_1, \underline{K}\sin\phi_1\cos\phi_2, \ldots, \underline{K}\sin\phi_1\ldots\sin\phi_{d-5}), \end{aligned} \tag{12.17}$$

where $E_1^2 = \underline{K}^2 + \underline{\underline{K}}^2$. Then we make the change

$$\begin{aligned} \underline{K} &= E_1 \cos\alpha \\ \underline{\underline{K}} &= E_1 \sin\alpha. \end{aligned} \tag{12.18}$$

Then the integration measure for k_1 is

$$\begin{aligned} d^{d-1}k_1 \;=\; & E_1^{d-2} dE_1 \cos^2\alpha \sin^{d-5}\alpha d\alpha \sin\theta_1 d\theta_1 d\theta_2 \\ & \sin^{d-6}\phi_1 \sin^{d-7}\phi_2 \ldots \sin\phi_{d-6} d\phi_1 \ldots d\phi_{d-5}. \end{aligned} \tag{12.19}$$

In this parametrization,

$$\underline{k}_1^2 = E_1^2(1-\cos^2\alpha) = E_1^2 \sin^2\alpha. \tag{12.20}$$

Hence we can integrate all of the θ and ϕ variables immediately using the identity (12.10), because the integrand depends only on E_1 and α. The α integral is done using (12.10) as well, and the E_1 integral is done with the δ function.

12.3.2. Three Body Phase Space, Lorentz Invariant Integrand

Three body phase space in d dimensions requires a few more tricks. We'll assume a Lorentz invariant integrand for now. We start with

$$(\mu^2)^{2\epsilon} \frac{d^{d-1}k_1}{(2\pi)^{d-1}2E_1} \frac{d^{d-1}k_2}{(2\pi)^{d-1}2E_2} \frac{d^d k_3}{(2\pi)^{d-1}} \delta(k_3^2)(2\pi)^d \delta^d(P-k_1-k_2-k_3)|\mathcal{M}|^2. \tag{12.21}$$

Integrating k_3, we get

$$(\mu^2)^{2\epsilon} \frac{d^{d-1}k_1 d^{d-1}k_2}{(2\pi)^{2d-3}2E_1 2E_2} \delta\left[(P-k_1-k_2)^2\right] |\mathcal{M}|^2. \tag{12.22}$$

Again, we work in the center of mass, and take $P^2 = 1$. Also, we define

$$x_i = 2P \cdot k_i, \tag{12.23}$$

where i can be 1, 2, or 3. Then $E_i = x_i/2$ in the center of mass. This gives us

$$(\mu^2)^{2\epsilon}\frac{d^{d-1}k_1 d^{d-1}k_2}{(2\pi)^{2d-3}x_1x_2}\delta[(1-x_1-x_2)+2k_1\cdot k_2]|\mathcal{M}|^2. \tag{12.24}$$

Next, we switch to polar coordinates. We will use θ_i to denote angles in k_1 and ψ_i to denote angles in k_2. We also "rotate" our k_2 coordinate system[1] so that k_1 is along the 1-axis. Then $k_1\cdot k_2 = E_1E_2(1-\cos\psi_1) = \frac{1}{4}x_1x_2(1-\cos\psi_1)$.

The integrand will depend only on the invariants x_1, x_2, and $k_1\cdot k_2$, and therefore we can immediately integrate $\theta_1,\ldots,\theta_{d-2}$ and $\psi_2,\ldots,\psi_{d-2}$. When we do this, we get

$$\begin{aligned}(\mu^2)^{2\epsilon}&\frac{x_1^{1-2\epsilon}x_2^{1-2\epsilon}dx_1dx_2}{(2\pi)^{3-2\epsilon}2^{5-4\epsilon}\Gamma(2-2\epsilon)}\sin^{-2\epsilon}\psi_1 d\cos\psi_1\\ &\cdot\delta\left[(1-x_1-x_2)+\tfrac{1}{2}x_1x_2(1-\cos\psi_1)\right]|\mathcal{M}|^2.\end{aligned} \tag{12.25}$$

Next we use the δ function to integrate ψ_1. This gives us

$$(\mu^2)^{2\epsilon}\int_0^1 dx_1\int_{1-x_1}^1 dx_2\frac{x_1^{-2\epsilon}x_2^{-2\epsilon}}{(2\pi)^{3-2\epsilon}2^{4-4\epsilon}\Gamma(2-2\epsilon)}\sin^{-2\epsilon}\psi_1|\mathcal{M}|^2, \tag{12.26}$$

where we have left a ψ_1 in the expression for brevity, but it is, in fact, a function of x_1 and x_2.

This still looks rather complicated to integrate, but there is one more trick we can use that will make the whole thing quite simple. We exchange the variable x_2 for the new variable v defined by

$$x_2 = 1 - vx_1. \tag{12.27}$$

Let's see what this does for us.

---

[1] Later, when we discuss three body phase space with a non-covariant integrand, it will be better not to think of this as a rotation.

First of all, we can show that

$$\sin^{-2\varepsilon}\psi_1 = 2^{-2\varepsilon}v^{-\varepsilon}(1-v)^{-\varepsilon}(1-x_1)^{-\varepsilon}x_2^{2\varepsilon}. \tag{12.28}$$

The $x_2^{2\varepsilon}$ here cancels the $x_2^{-2\varepsilon}$ we already have in (12.26). Next, the limits of integration are now from 0 to 1 for *both* integrals. We also replace dx_1dx_2 with x_1dx_1dv.

So now we have

$$\frac{(4\pi\mu^2)^{2\varepsilon}}{16(2\pi)^3\Gamma(2-2\varepsilon)}\int_0^1 dx_1\int_0^1 dv x_1^{1-2\varepsilon}(1-x_1)^{-\varepsilon}v^{-\varepsilon}(1-v)^{-\varepsilon}|\mathcal{M}|^2. \tag{12.29}$$

All the kinematic factors we might find in $|\mathcal{M}|^2$ can be simply expressed in terms of x_1 and v:

$$\begin{aligned} 2k_1\cdot k_2 &= x_1(1-v)\\ 2k_2\cdot k_3 &= 1-x_1\\ 2k_3\cdot k_1 &= vx_1. \end{aligned} \tag{12.30}$$

Every integral that we need to do is now of the form

$$\int_0^1 daa^m(1-a)^n = B(m+1,n+1), \tag{12.31}$$

and we are done.

12.3.3. Three Body Phase Space, Non-covariant Integrand

Now things get more complicated. When we performed the phase space integration with a covariant integrand, we rotated to a coordinate system in which k_1 was along the 1-axis in the space of k_2, and this simplified the dot product $k_1\cdot k_2$. In the case of a non-covariant integrand, in which we have factors such as $\underline{k}_2^2$ and $\underline{k}_1\cdot\underline{k}_2$, we no longer have rotational symmetry. It is still desirable to make the transformation to a system in which $k_1\cdot k_2 = E_1E_2(1-\cos\psi_1)$, so that we can use the same δ

function as before to integrate ψ_1 without muddying up the limits of integration. If we want to do this, however, we must study the effects of such a transformation on the quantities $\underline{k}_1^2$, $\underline{k}_1^2$, and $\underline{k}_1 \cdot \underline{k}_2$. In order to do this, we must take a closer look at the process by which we work $k_1 \cdot k_2$ into the form $E_1 E_2(1 - \cos\psi_1)$.

We'll start with a simpler example. Consider the integral

$$\int d^3x d^3y f(x,y), \tag{12.32}$$

where $x = (x_1, x_2, x_3)$, $y = (y_1, y_2, y_3)$, and f is a function of x^2, y^2, and $x \cdot y$. Let's say we want to put this in a form where

$$x \cdot y = |x||y| \cos\theta_y, \tag{12.33}$$

where θ_y is the polar angle of y. We start by making a change in variables in the y coordinate:

$$\begin{aligned} y_1 &= y_1' \\ \begin{pmatrix} y_2 \\ y_3 \end{pmatrix} &= \frac{1}{\sqrt{x_2^2+x_3^2}} \begin{pmatrix} x_2 & -x_3 \\ x_3 & x_2 \end{pmatrix} \begin{pmatrix} y_2' \\ y_3' \end{pmatrix}. \end{aligned} \tag{12.34}$$

Although this looks very much like a rotation, it is probably best not to think of it thus. In a true rotation, x would also change, and $x \cdot y$ would be invariant. One should think of this merely as a change of variables, with Jacobian 1.

When we express $x \cdot y$ in terms of the new variables, y', we get

$$x \cdot y = x_1 y_1' + y_2' \sqrt{x_2^2 + x_3^2}. \tag{12.35}$$

We see that $x \cdot y$ now has no y_3' dependence. One more such transformation will give

us what we want.

$$\begin{pmatrix} y_1' \\ y_2' \end{pmatrix} = \frac{1}{|x|} \begin{pmatrix} x_1 & -\sqrt{x_2^2+x_3^2} \\ \sqrt{x_2^2+x_3^2} & x_1 \end{pmatrix} \begin{pmatrix} y_1'' \\ y_2'' \end{pmatrix} \tag{12.36}$$
$$y_3' = y_3''.$$

This now gives us

$$x \cdot y = |x| y_1'', \tag{12.37}$$

and when we go to polar coordinates, we get

$$x \cdot y = |x||y| \cos\theta_{y''}. \tag{12.38}$$

This is exactly the form we want. As for the other invariants, x^2 is unchanged, since we've made no transformation on x. Also, $y^2 = y_1''^2 + y_2''^2 + y_3''^2$, since the transformations on y were both orthogonal. Now that we've seen the nature and effects of the transformation that we wish to make, we can move on to the more complicated case that we're really interested in.

When we integrate three body phase space with a non-covariant integrand, we start exactly as before, and integrate k_3 with the δ function, leaving us with (12.24) again. Now we start making transformations on the components of k_2 similar to those we made on y above. In particular, we first transform k_2 until

$$k_1 \cdot k_2 = E_1 E_2 - \underline{K} k_{21} - \underset{\sim}{K} k_{24}, \tag{12.39}$$

where k_{ij} is the jth spacial component of k_i. Also, $\underline{K}^2 = k_{11}^2 + k_{12}^2 + k_{13}^2$ and $\underset{\sim}{K}^2 = k_{14}^2 + k_{15}^2 + \ldots$, so that $E_1^2 = \underline{K}^2 + \underset{\sim}{K}^2$. The other kinematic factors we'll have

to deal with are

$$\begin{aligned} \underline{k}_1 \cdot \underline{k}_2 &= E_1 E_2 - \underline{K}_1 k_{21} \\ \underline{k}_1^2 &= E_1^2 - \underline{K}^2 \\ \underline{k}_2^2 &= E_2^2 - \underline{K}_2^2. \end{aligned} \tag{12.40}$$

The last transformation we make is

$$\begin{pmatrix} k_{21} \\ k_{24} \end{pmatrix} = \frac{1}{E_1} \begin{pmatrix} \underline{K} & \underline{K} \\ -\underline{K} & \underline{K} \end{pmatrix} \begin{pmatrix} k'_{21} \\ k'_{24} \end{pmatrix}. \tag{12.41}$$

Finally, we switch to polar coordinates in k_2 and we treat k_1 just as we did in the two body case, going to polar coordinates separately in the first three spacial components and the last $d-4$ components. Then the kinematic factors in the integrand have become

$$k_1 \cdot k_2 = E_1 E_2 (1 - \cos\psi_1) \tag{12.42}$$

$$\begin{aligned} \underline{k}_1 \cdot \underline{k}_2 = E_1 E_2 (1 &- \cos^2\alpha \cos\psi_1 \\ &- \cos\alpha \sin\alpha \sin\psi_1 \sin\psi_2 \sin\psi_3 \cos\psi_4) \end{aligned} \tag{12.43}$$

$$\underline{k}_1^2 = E_1^2 \sin^2\alpha \tag{12.44}$$

$$\begin{aligned} \underline{k}_2^2 = E_2^2 (&\sin^2\psi_1 \sin^2\psi_2 \sin^2\psi_3 + \sin^2\alpha \cos^2\psi_1 \\ &+ 2\cos\alpha \sin\alpha \cos\psi_1 \sin\psi_1 \sin\psi_2 \sin\psi_3 \cos\psi_4 \\ &- \sin^2\alpha \sin^2\psi_1 \sin^2\psi_2 \sin^2\psi_3 \cos^2\psi_4). \end{aligned} \tag{12.45}$$

Recall that ψ_i is the ith angle describing k_2 and that $\cos\alpha$ describes that fraction of $\vec{k}_1$ which lies in the three physical spacial dimensions.

Any angle not appearing in (12.42-12.45) can be integrated immediately. We can also replace E's with $\frac{1}{2}x$'s. We integrate ψ_1 with the δ function left over from the k_3

integration. Finally, we get

$$\frac{2^{2\epsilon}}{64\pi^{9/2}}(4\pi\mu^2)^{2\epsilon}\frac{1}{\Gamma(-\epsilon)\Gamma(-\frac{1}{2}-\epsilon)}x_1^{1-2\epsilon}(1-x_1)^{-\epsilon}v^{-\epsilon}(1-v)^{-\epsilon}dx_1dv\cos^2\alpha\sin^{d-5}\alpha d\alpha$$
$$\sin^{d-4}\psi_2\sin^{d-5}\psi_3\sin^{d-6}\psi_4 d\theta_2 d\theta_3 d\theta_4. \tag{12.46}$$

The integrand will be independent of all other variables. Finally, we display the expressions for all the kinematic factors that we might have in terms of the remaining variables:

$$\begin{aligned}
2k_1\cdot k_2 &= x_1(1-v)\\
2k_2\cdot k_3 &= 1-x_1\\
2k_3\cdot k_1 &= x_1v\\
\underline{k}_1^2 &= \tfrac{1}{4}x_1^2\sin^2\alpha\\
\underline{k}_2^2 &= v(1-v)(1-x_1\sin^2\psi_2\sin^2\psi_3+\tfrac{1}{4}\sin^2\alpha[v(1-x_1)-(1-v)]^2\\
&\quad+\cos\alpha\sin\alpha[v(1-x_1)-(1-v)][v(1-v)(1-x_1)]^{1/2}\\
&\quad\cdot\sin\psi_2\sin\psi_3\cos\psi_4\\
2\underline{k}_1\cdot\underline{k}_2 &= x_1(1-v)+\tfrac{1}{2}\sin^2\alpha x_1[v(1-x_1)-(1-v)]\\
&\quad-\cos\alpha\sin\alpha x_1[v(1-v)(1-x_1)]^{1/2}\sin\psi_2\sin\psi_3\cos\psi_4\\
\underline{k}_3 &= \underline{P}-\underline{k}_1-\underline{k}_2\\
\underline{P}^2 &= 1\\
2\underline{P}\cdot\underline{k}_1 &= x_1\\
2\underline{P}\cdot\underline{k}_2 &= 1-vx_1.
\end{aligned} \tag{12.47}$$

The x_1 and v integrals can be performed using (12.31), and the angular integrals can be done with (12.10) and (12.12). We have now covered everything we need to know to do the phase space integrals for the processes in this work.